THE UNIVERSITY OF MICHIGAN

COLLEGE OF LITERATURE, SCIENCE, AND THE ARTS
Department of Chemistry

Progress Report

A STUDY OF "INDUCED" ABSORPTION IN URANYL SOLUTIONS AND GLASS

Thomas M. Dunn
Lee A. Cross

under contract with:

U. S. AIR FORCE
AIR FORCE OFFICE OF SCIENTIFIC RESEARCH
OFFICE OF AEROSPACE RESEARCH
GRANT NO. AF-AFOSR-865-65
WASHINGTON, D.C.

administered through:

OFFICE OF RESEARCH ADMINISTRATION ANN ARBOR

February 1966

enS11

UMR6912

ABSTRACT

An analysis of the absorption induced by an intense xenon light flash in several media containing fluorescent uranyl ions has been accomplished. Spectrographic studies on uranyl glass (Canary glass) and a solution of uranyl sulfate in concentrated sulphuric acid have shown the induced absorption to be a broad band extending from 4600 Å to 7000 Å with a maximum in the neighborhood of 5800 Å. Spectrophotometric studies on the same systems have shown that the lifetime for this absorption is the same as for the normal fluorescence and that the transition being observed via the absorption measurements is from the initial state of the fluorescence to a still more highly excited state. The failure of uranyl salts to exhibit the induced absorption in solutions in which they are only faintly fluorescent (for example, in water or alcohol) confirms the assignment of the initial state of this transition. The absorption induced in a solution of uranyl phosphate in 80% phosphoric acid has been shown by spectrophotometric means to be nearly indistinguishable from that induced in the sulfate solution. Ultraviolet absorption measurements of the spectra of the sulfate and phosphate solutions have shown that the absorption which normally appears as a high frequency continuum beginning at 3500 Å in samples which are concentrated enough to show the visible absorption system in the region from 4900 Å to 3500 Å has its peak at 2200 Å (or perhaps to shorter wavelengths in the phosphate) and is detectable at 3500 Å only because of its moderately high molar extinction coefficient which is much larger than that of the visible system. In the sulfate solution, the band at 2200 Å has two longer wavelength shoulders at 2600 Å and 2830 Å and it is possible to show, by assuming that the initial state of the induced absorption is also the initial state of the ordinary fluorescence, that the final state of the induced absorption must be the same as the terminal level of the 2600 Å shoulder. The oscillator strengths for the three transitions considered are: (1) from the vibrationless ground state to the vibrationless first excited electronic state (the resonance line): 1.28×10^{-6}, (2) from the vibrationless ground state to the central UV level: 2.29×10^{-3}, and (3) from the vibrationless first excited electronic state to the central UV level (the induced absorption): 6.54×10^{-5}.

ACKNOWLEDGMENTS

I would like to acknowledge Professor Thomas M. Dunn for his continuing interest and support of this work, for many invaluable discussions regarding the interpretation of molecular spectra, and for his assistance in making the following pages more intelligible.

To Professors Chihiro Kikuchi and Edgar F. Westrum goes my appreciation for their valuable suggestions concerning this manuscript.

The cooperation and skill of Mr. Norman G. Johnston and Mr. Ernest Metzner of the chemistry machine shop who constructed the flash tube heads is gratefully recognized.

The construction of the power supplies and mechanical timing equipment by Mr. Victor Podolak of the chemistry electronics shop was of considerable assistance.

The support of this research by the United States Air Force under Grant No. AF-AFOSR-865-65 is thankfully acknowledged.

TABLE OF CONTENTS

	Page
ABSTRACT	iii
ACKNOWLEDGMENTS	v
LIST OF TABLES	ix
LIST OF FIGURES	xi
LIST OF APPENDICES	xv
I. STATEMENT OF THE PROBLEM	1
II. EXPERIMENTAL	2
A. Ordinary Absorption Spectra of Uranyl Glass and Uranyl Sulfate and Phosphate Solutions	2
B. Ordinary Fluorescence Spectra of Uranyl Glass, Uranyl Sulfate Solution, and Polycrystalline Uranyl Sulfate Trihydrate	9
C. Induced Absorption Spectra	19
D. Time-Resolved Induced Absorption in Uranyl Glass and Uranyl Sulfate and Phosphate Solutions	27
E. Time-Resolved Fluorescence in Uranyl Glass and Uranyl Sulfate Solution; Comparison of DC- and Flash-Excited Fluorescence Spectra of Uranyl Sulfate Trihydrate	42
F. Ultraviolet Absorption Spectra of Uranyl Sulfate Solution and Uranyl Phosphate Solution	50
III. DISCUSSION OF RESULTS AND SUMMARY	57
BIBLIOGRAPHY	91

LIST OF TABLES

Table		Page
I	Absorption Bands of Uranyl Glass	2
II	Absorption Bands of Uranyl Sulfate Solution	6
III	Absorption Bands of Uranyl Phosphate Solution	7
IV	Molar Extinction Coefficients of Uranyl Sulfate Solution	7
V	Fluorescence Bands of Uranyl Glass	9
VI	Fluorescence Bands of Uranyl Sulfate Solution	16
VII	Fluorescence Bands of Uranyl Sulfate, Polycrystalline, 300°K	17
VIII	Changes in Ordinary Absorption Peaks of Sulfate Solution Upon Optical Pumping	25
IX	Ultraviolet Absorption Bands of Uranyl Sulfate and Phosphate Solutions	55
X	The Character Table for $D_{\infty h}$	62
XI	Assignment of Terms for a Molecule of Symmetry $D_{\infty h}$	63
XII	Assignment of the Uranium and Oxygen Orbitals to the Representations of the $D_{\infty h}$ Group	64
XIII	Assignment of the Oxygen Linear Combinations to the Representations of the $D_{\infty h}$ Group	65
XIV	The Character Table for the $D_{\infty h}$ Double Group	70
XV	Assignment of Terms for a Molecule of the $D_{\infty h}$ Double Group	71
XVI	Resolution, Dispersion, and Wavelength Ranges for the 31,000 Å Blaze Side of 3.4 Meter Ebert Spectrograph	87
XVII	Resolution, Dispersion, and Wavelength Ranges for the 59,000 Å Blaze Side of the 3.4 Meter Ebert Spectrograph	87

LIST OF FIGURES

Figure		Page
1.	Visible Absorption Spectrum of Uranyl Glass.	3
2.	Visible Absorption Spectrum of Uranyl Sulfate in Sulphuric Acid Solution.	4
3.	Visible Absorption Spectrum of Uranyl Phosphate in Phosphoric Acid Solution.	5
4.	Fluorescence Spectrum of Uranyl Glass, 300°K.	10
5.	Fluorescence Spectrum of Uranyl Glass, 77°K.	11
6.	Fluorescence Spectrum of Uranyl Sulfate in Sulphuric Acid Solution, 300°K.	12
7.	Fluorescence Spectrum of Uranyl Sulfate in Sulphuric Acid Solution, 77°K.	13
8.	Fluorescence Spectrum of $UO_2SO_4 \cdot 3H_2O$, 300°K.	14
9.	Fluorescence Spectrum of $UO_2SO_4 \cdot 3H_2O$, 77°K.	15
10.	Energy Level Diagram for Uranyl Solutions, the Glass, and Uranyl Sulfate.	18
11.	Photographically Recorded Transmission Spectra of Optically Pumped and Unpumped Uranyl Glass.	20
12.	Induced Absorption Cross-Section of Uranyl Glass.	21
13.	Photographically Recorded Transmission Spectra of Optically Pumped and Unpumped Uranyl Sulfate Solution.	22
14.	Induced Absorption Cross-Section of Uranyl Sulfate Solution.	23
15.	Time-Resolved Induced Absorption in Uranyl Glass.	28
16.	Induced Absorption Cross-Section for Uranyl Glass as Deduced from Photoelectric Measurements (versus wavelength).	29

LIST OF FIGURES (Continued)

Figure		Page
17.	Induced Absorption Cross-Section for Uranyl Glass as Deduced from Photoelectric Measurements (versus energy).	30
18.	Time-Resolved Induced Absorption in Uranyl Sulfate Solution.	31
19.	Induced Absorption Cross-Section for Uranyl Sulfate Solution as Deduced from Photoelectric Measurements (versus wavelength.	33
20.	Induced Absorption Cross-Section for Uranyl Phosphate Solution as Deduced from Photoelectric Measurements (versus wavelength).	34
21.	Theoretical Time-Profile for the Excited State Population Assuming Square-Wave Pumping.	37
22.	Induced Absorption Decay Measurement for Uranyl Glass.	38
23.	Induced Absorption Decay Measurement for Uranyl Sulfate Solution.	39
24.	Induced Absorption Decay for Uranyl Glass.	41
25.	Time-Resolved Fluorescence for Uranyl Glass.	43
26.	Time-Resolved Fluorescence for UO_2SO_4 in H_2SO_4 Solution.	44
27.	Fluorescence Decay Measurements for UO_2SO_4 in H_2SO_4 Solution.	45
28.	Fluorescence Decay for Uranyl Glass.	46
29.	Fluorescence Decay for UO_2SO_4 in H_2SO_4 Solution.	47
30.	DC- and Flash-Excited Fluorescence of $UO_2SO_4 \cdot 3H_2O$ at 77°K.	49
31.	Ultraviolet Absorption Spectrum of UO_2SO_4 in H_2SO_4 Solution (versus wavelength).	51
32.	Ultraviolet Absorption Spectrum of UO_2SO_4 in H_2SO_4 Solution (versus energy).	52
33.	Resolution of the Ultraviolet Absorption Spectrum of UO_2SO_4 in H_2SO_4 Solution by Subtraction of the Induced Absorption Contour.	53

LIST OF FIGURES (Concluded)

Figure		Page
34.	Ultraviolet Absorption Spectrum of UO_2HPO_4 in H_3PO_4 Solution Showing the Relationship Between the Long Wavelength Shoulder and the Induced Absorption Maximum.	54
35.	Principle Transitions Observed for the Uranyl Ion.	60
36.	Flash Head and Arc Lamp Arrangement.	73
37.	Optical Bench Arrangement for the Recording of Induced Absorption Spectra.	75
38.	Camera Shutter, Mirror, and Trigger Photocell Arrangement.	76
39.	Oscilloscope and Delay Network Arrangement.	78
40.	Induced Absorption Tracings for UO_2SO_4 in H_2SO_4 Solution Illustrating Film Error.	82
41.	Intensity "Amplification" by Film H & D Curve.	83
42.	H & D Curve for Kodak Pan-X Film.	85
43.	Order-Sorter for 3.4 Meter Jarrell-Ash Spectrograph.	88
44.	An Attempt to Observe Quenching of the Induced Absorption in Uranyl Sulfate Solution.	90

LIST OF APPENDICES

Appendix		Page
I.	DISCUSSION OF THE MOLECULAR ORBITAL REPRESENTATIONS FOR THE URANYL ION AND THE ASSIGNMENT OF TERM LEVEL DESIGNATIONS TO THE LOWER URANYL ION LEVELS	62
II.	THE EXPERIMENTAL ARRANGEMENT AND ITS OPERATION	72
III.	ATTEMPTS AT CRYSTAL GROWTH AND REMARKS ON SIZE AND CLARITY REQUIREMENTS	79
IV.	FILM ERRORS, THEIR EFFECTS ON THE SPECTRA, AND THEIR CORRECTION	81
V.	A DESCRIPTION OF THE SPECTROGRAPHS	86
VI.	AN ATTEMPT TO OBSERVE "BLEACHING" OF THE INDUCED ABSORPTION	89

SECTION I

STATEMENT OF THE PROBLEM

In connection with work concerning the construction of high power lasers, this author and a co-worker[1] reported the observation of an absorption "induced" in Corning No. 3-79 filter glass (a glass whose coloring constituent is the uranyl ion) by the light flash from a high-intensity xenon flash lamp. These authors noted that this absorption was quite broad, extending from 5460 Å to at least 7000 Å and decayed at the same rate as the fluorescence of the glass. By the construction of a laser cavity incorporating this glass as a saturable filter, they were able to demonstrate that the absorption could be wiped out by the application of an intense "depumping" light provided by the laser.[2] Because of experimental limitations, this induced absorption could only be monitored photoelectrically and then at only a few wavelengths so that the shape of the absorption remained unknown, as did the exact nature of the levels taking part in the absorption.

As it seemed likely that the induced absorption was in fact a transition from the initial state of the normally observed fluorescence to some higher excited state, it was decided that a series of experiments could be set up to establish whether or not this was the case. One alternate proposal for the appearance of this absorption would be that some sort of photodecomposition product is formed in the glass which happens to have the same recombination rate as the normal fluorescence decay rate and that it is this product which gives rise to the absorption. If the previous hypothesis concerning the nature of the initial level is correct, then those systems which contain uranyl ions but the mechanics of which are such that no fluorescence occurs, the induced absorption should not be observable and all uranyl systems which are fluorescent should exhibit it.

The terminal level of the transition also must be established, i.e., the higher excited state which is the upper state for the induced absorption process. Assuming that the transition being observed is in fact between states of the uranyl ion, the possibility exists that the transition from the ground state to this excited state is forbidden and therefore the presence of this state could not be detected by ordinary absorption spectroscopy.

SECTION II

EXPERIMENTAL

A. ORDINARY ABSORPTION SPECTRA OF URANYL GLASS AND URANYL SULFATE AND PHOSPHATE SOLUTIONS

Using a Cary Model 11 spectrophotometer, whose resolution is approximately 10 cm^{-1}, the absorption spectra in the region from 3500 to 5500 Å of the following materials were run at 300 °K: (1) a 5 mm thick sample of Corning No. 3-79 filter glass (uranyl glass); (2) a 10 mm path length sample of a solution of uranyl sulfate ($UO_2SO_4 \cdot 3H_2O$) in concentrated sulphuric acid (4.7×10^{-2} gm/ml); and (3) a 10 mm path length sample of a solution of uranyl carbonate* in 80% phosphoric acid (7.0×10^{-2} gm/ml). These spectra are shown in Figures 1-3, respectively.

Table I lists the transitions which are observed for the uranyl glass.

TABLE I

ABSORPTION BANDS OF URANYL GLASS

Wavelength (Å)	Frequency (cm^{-1})	$\Delta\nu$
5130	19500	
		1070
4862	20570	
		1170
4601	21740	
		1980
4216	23720	
		400
4147	24120	
		2510
3756	26630	
		630
3668	27260	

The glass spectrum is quite diffuse but is much more detailed than the Corning

*Prepared by precipitation from a concentrated solution of uranyl nitrate with ammonium carbonate.

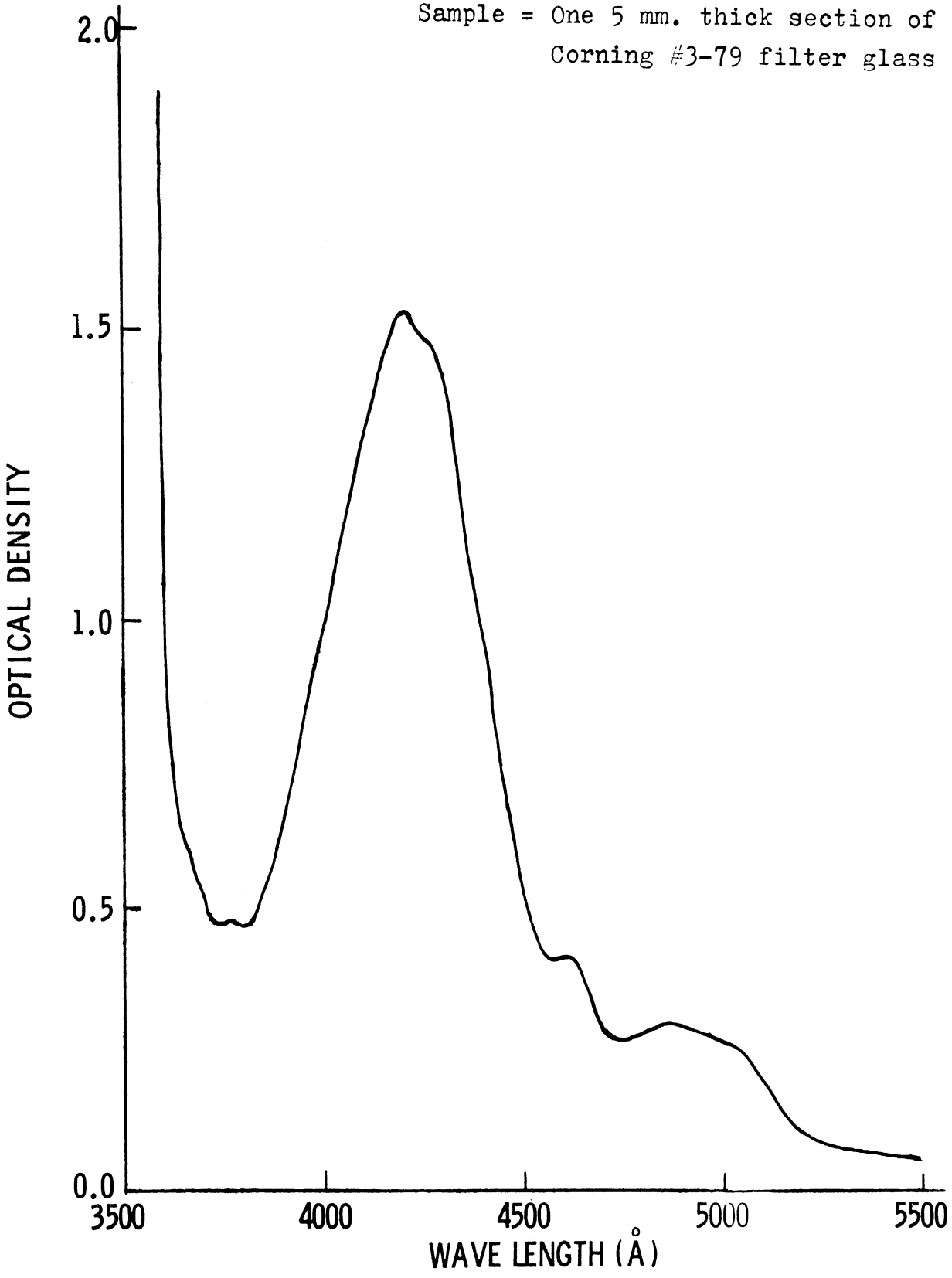

Figure 1. Visible Absorption Spectrum of Uranyl Glass, 300°K.

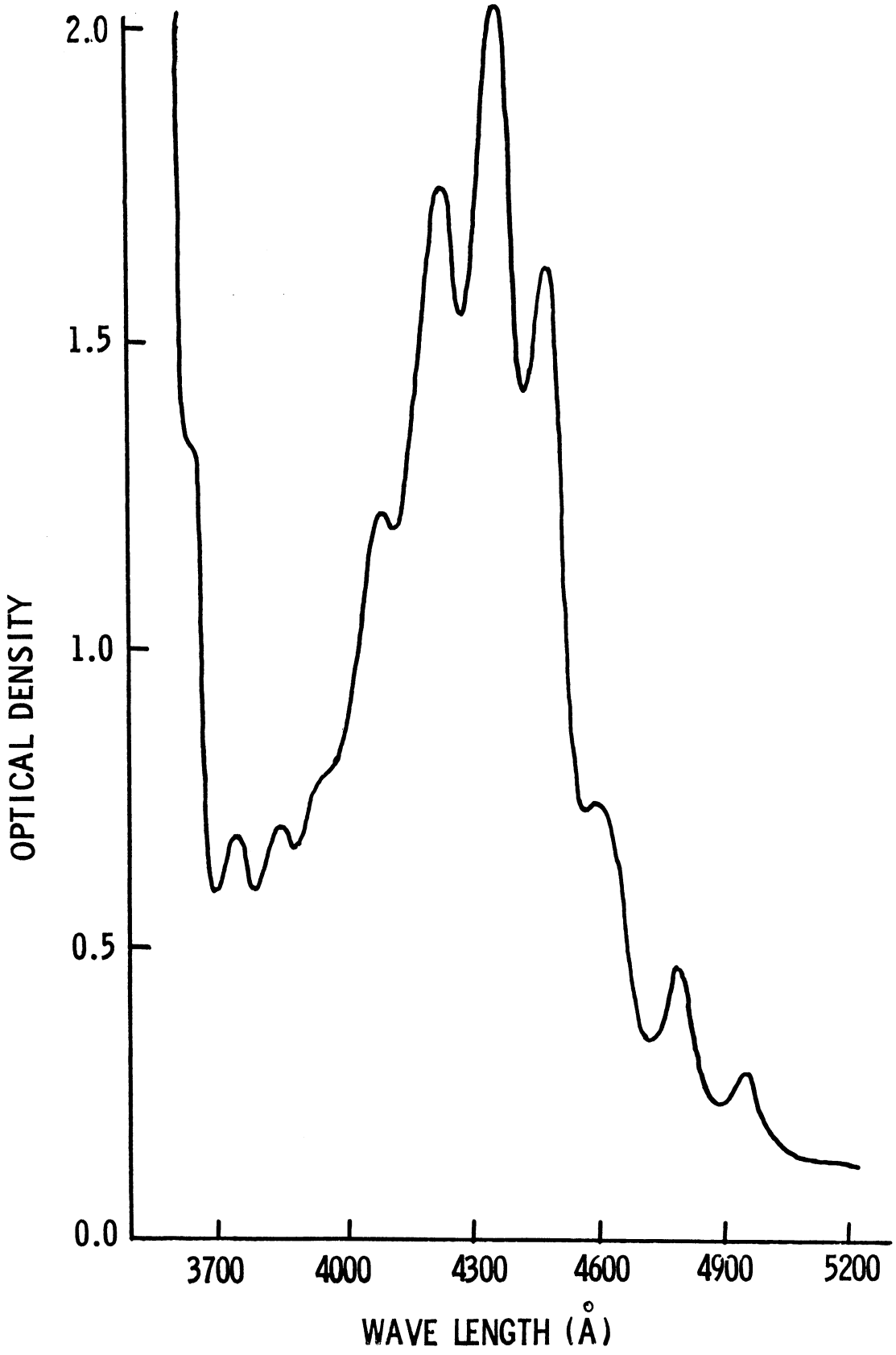

Figure 2. Visible Absorption Spectrum of Uranyl Sulfate in Sulphuric Acid Solution, 300°K.

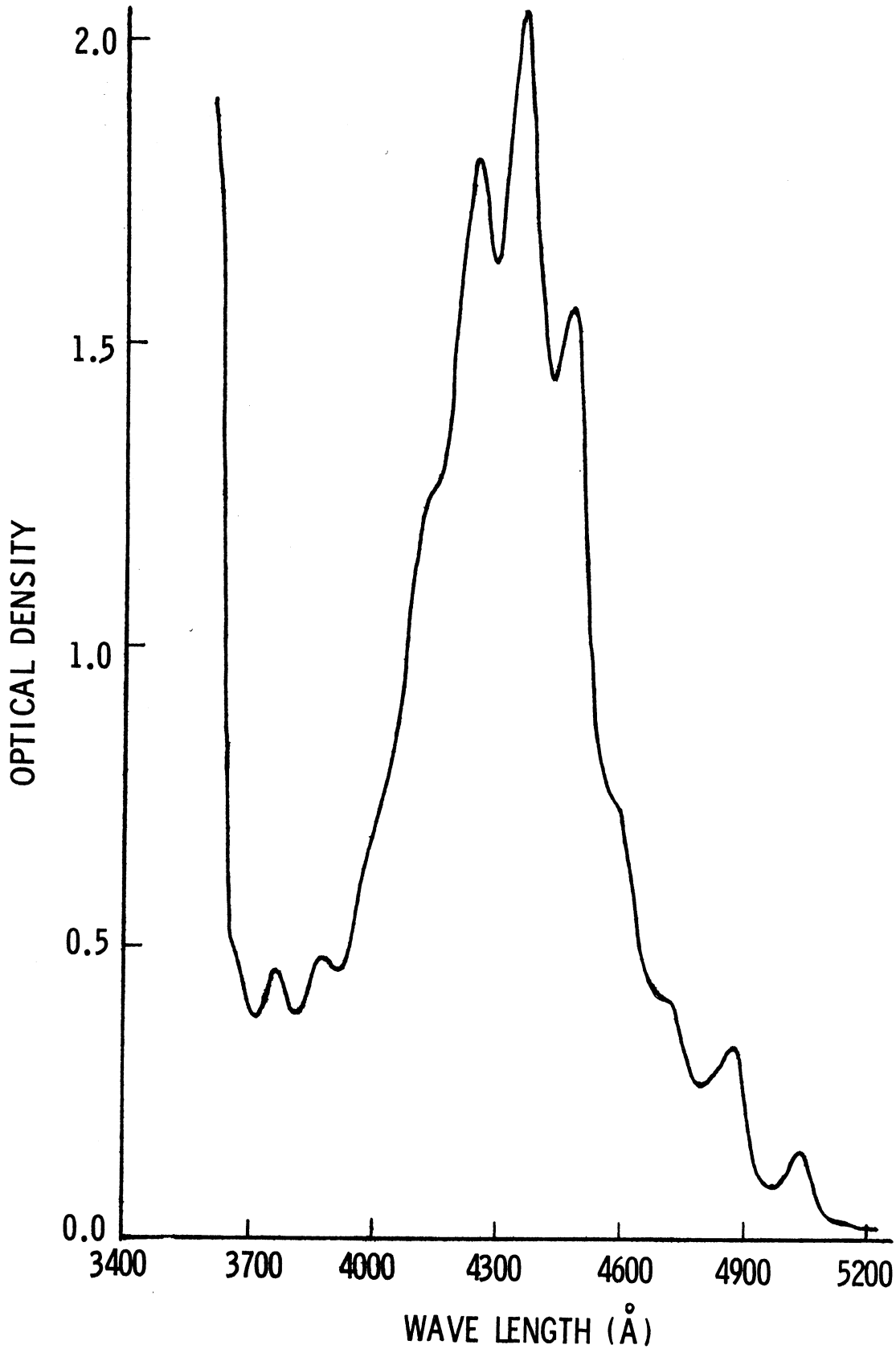

Figure 3. Visible Absorption Spectrum of Uranyl Phosphate in Phosphoric Acid Solution, 300°K.

Company's published transmission curve* and it does show some trace of the different electronic transitions of the uranyl ion to be expected in this region[3] as well as some finer structure which may either be attributed to vibrational intervals or to the presence of different uranyl ion sites in the glass.

The solution spectra, whose bands are listed in Tables II and III, respectively, have a much better resolved vibrational structure than the glass. The vibrational interval observed here is the symmetric stretching frequency. The average value of this interval is 720 cm^{-1} for the sulfate and 640 cm^{-1} for the phosphate but some large deviations are observed in the high- and low-wavelength portions of this region. These are probably due to the fact that there are at least three electronic transitions in this region and that the intervals which deviate represent the transition from the vibrational structure of one electronic state to that of another. Table II also lists for comparison the absorption bands of an aqueous solution of uranyl sulfate and Table III the absorption bands of an aqueous solution of uranyl monophosphate as measured by Morton and Bolton[4] and corrected by Kayser.[5]

TABLE II

ABSORPTION BANDS OF URANYL SULFATE SOLUTION

In Sulphuric Acid (This Study)			In Water (Morton and Bolton[4])		
λ(Å)	$\nu(cm^{-1})$	$\Delta\nu$	λ(Å)	$\nu(cm^{-1})$	$\Delta\nu$
4922	20320	730	4955	20160	850
4751	21050	940	4750	21050	850
4548	21990	800	4570	21900	650
4389	22790	740	4434	22550	620
4250	23530	700	4315	23120	640
4127	24230	700	4200	23810	700
4010	24930	750	4080	24510	
3895	25680	710			
3789	26390	740			
3686	27130	1130			
3539	28260				

*"Glass Color Filters," Corning Glass Works, Corning, New York

TABLE III

ABSORPTION BANDS OF URANYL PHOSPHATE SOLUTION

In Phosphoric Acid (This Study)			In Water (Morton and Bolton[4])		
λ(Å)	ν(cm^{-1})	$\Delta\nu$	λ(Å)	ν(cm^{-1})	$\Delta\nu$
5036	19860	710	5060	19760	1180
4862	20570	680	4775	20940	730
4706	21250	620	4615	21670	650
4572	21870	650	4480	22320	700
4444	22520	600	4345	23020	570
4325	23120	600	4240	23590	
4216	23720	670			
4100	24390	610			
4000	25000	890			
3862	25890	490			
3753	26380	930			
3662	27310				

The absorption spectrum of the sulfate is sufficiently well resolved so that the oscillator strength of the resonance line at 20,320 cm^{-1} may be calculated. Table IV lists the molar extinction coefficients for the 11 absorption peaks of

TABLE IV

MOLAR EXTINCTION COEFFICIENTS OF URANYL SULFATE SOLUTION

Band No.	ν(cm^{-1})	ϵ
1	20320	1.1
2	21050	2.2
3	21990	4.0
4	22790	9.3
5	23530	11.8
6	24230	10.0
7	24930	6.8
8	25680	4.2
9	26390	3.7
10	27130	3.6
11	28260	6.8

the uranyl sulfate solution spectrum. If a Gaussian line shape of the form

$$\epsilon(\bar{\nu}) = \epsilon_o \exp\left(-k(\bar{\nu}-\bar{\nu})^2\right)$$

is assumed for the resonance line then the oscillator strength may be directly obtained. The oscillator strength can be calculated via a formula given by Mulliken[6]:

$$f = 4.20 \times 10^{-8} \int k_\nu d\bar{\nu}$$

where $\bar{\nu}$ is the frequency in cm^{-1} and k_ν is the absorption coefficient at the frequency ν measured in $(cm\text{-}atmospheres)^{-1}$ at 0°C. This form is clearly most useful for gasses but it can be normalized to the measurement of the absorption coefficient as a molar extinction coefficient, $\epsilon(\bar{\nu})$, and in this form is given by Rabinowitch and Belford[14] as:

$$f = 4.32 \times 10^{-9} \int \epsilon(\bar{\nu}) d\bar{\nu}$$

For a Gaussian line, this reduces to

$$f = 4.32 \times 10^{-9} \epsilon_o \Delta\nu$$

The half width of the resonance line is 271 cm^{-1} and from Table IV the molar extinction coefficient at the center of the line is 1.1. This yields an oscillator strength of 1.23×10^{-6}. The absorption cross-section at line center is 3.24×10^{-23} cm^2. The oscillator strength for the entire first electronic system, assuming that the absorption profile is symmetric about the 21,990 cm^{-1} band (the 3rd vibrational quantum of the first electronic state) is 1.25×10^{-5}.

B. ORDINARY FLUORESCENCE SPECTRA OF URANYL GLASS, URANYL SULFATE SOLUTION, AND POLYCRYSTALLINE URANYL SULFATE TRIHYDRATE

The fluorescence spectra of uranyl glass, a solution of uranyl sulfate in concentrated sulphuric acid (4.7×10^{-2} gm/ml), and polycrystalline uranyl sulfate trihydrate ($UO_2SO_4 \cdot 3H_2O$) were recorded using a 1-meter Jarrell-Ash scanning spectrometer at 300°K and 77°K. This instrument had a grating ruled with 590 lines/mm and a total ruled area of 102 x 102 mm. In the first order, the dispersion is 16.4 Å/mm.

These spectra are shown in Figures 4 through 9. The room temperature spectra of the two solid samples were taken by supporting the sample directly in front of the spectrometer input slit and illuminating it from the side. The solution spectrum and all the spectra taken at 77°K were made by placing the sample in the square cross-sectioned tip of a Dewar flask and supporting this section of the flask directly in front of the slit. The exciting light was provided by a low pressure mercury-neon discharge lamp* and the fluorescent output was detected by an RCA 1P21 photomultiplier operated at 1200 VDC. The slit width employed varied from 200 to 25 microns depending on the intensity of the fluorescent output which implies a resolution of from 9 to 1.6 cm^{-1}. Fortunately, the bandwidth of the fluorescent bands was always much larger than the necessary bandwidth which was resolvable because of intensity considerations. The 77°K solution spectrum was obtained by dropping the solution into the Dewar flask filled with liquid nitrogen; the frozen globules then fell through the nitrogen to the bottom of the flask. The polycrystalline uranyl sulfate showed a considerable amount of short-lived triboluminescence as it warmed up.

TABLE V

FLUORESCENCE BANDS OF URANYL GLASS

Band No.	Temperature					
	300°K			77°K		
	λ(Å)	ν(cm^{-1})	Δν	λ(Å)	ν(cm^{-1})	Δν
1	5181	19300	530	5138	19460	780
2	5327	18770	700	5352	18680	890
3	5534	18070		5558	17790	

*"Pen-Ray" type obtained from Ultraviolet Products Co., San Gabriel, California. Operated with their Type SCT-3 power supply.

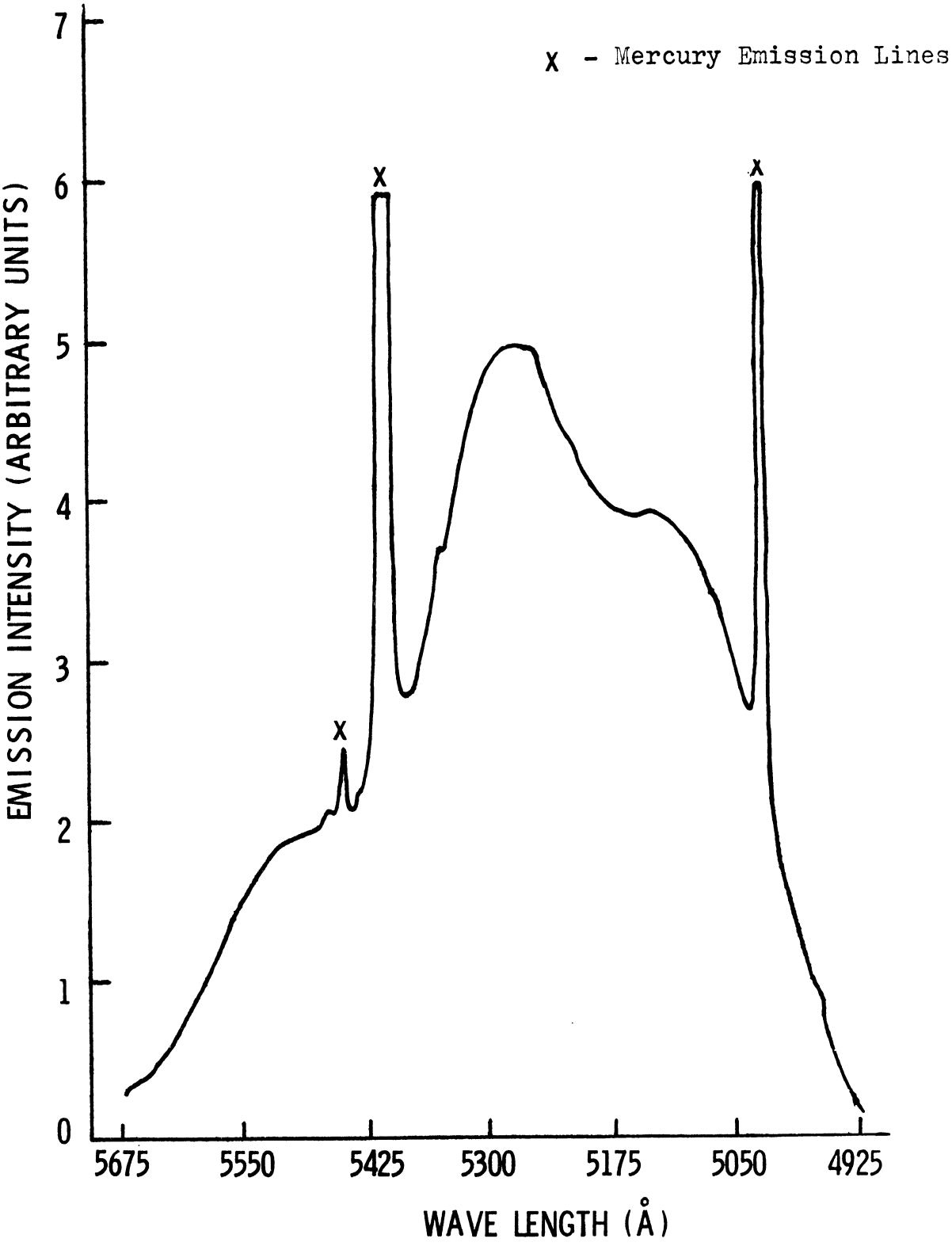

Figure 4. Fluorescence Spectrum of Uranyl Glass, 300°K.

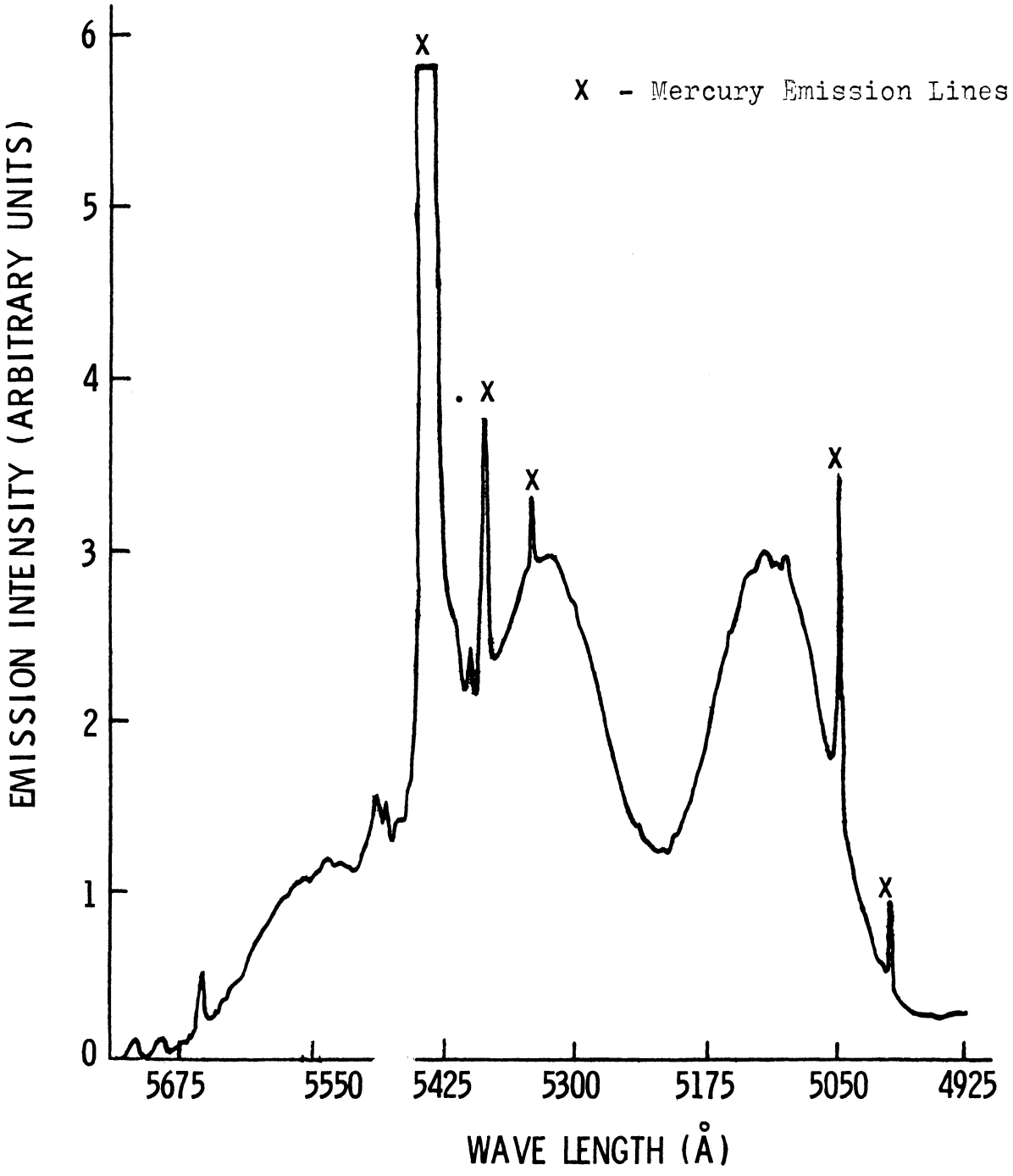

Figure 5. Fluorescence Spectrum of Uranyl Glass, 77°K.

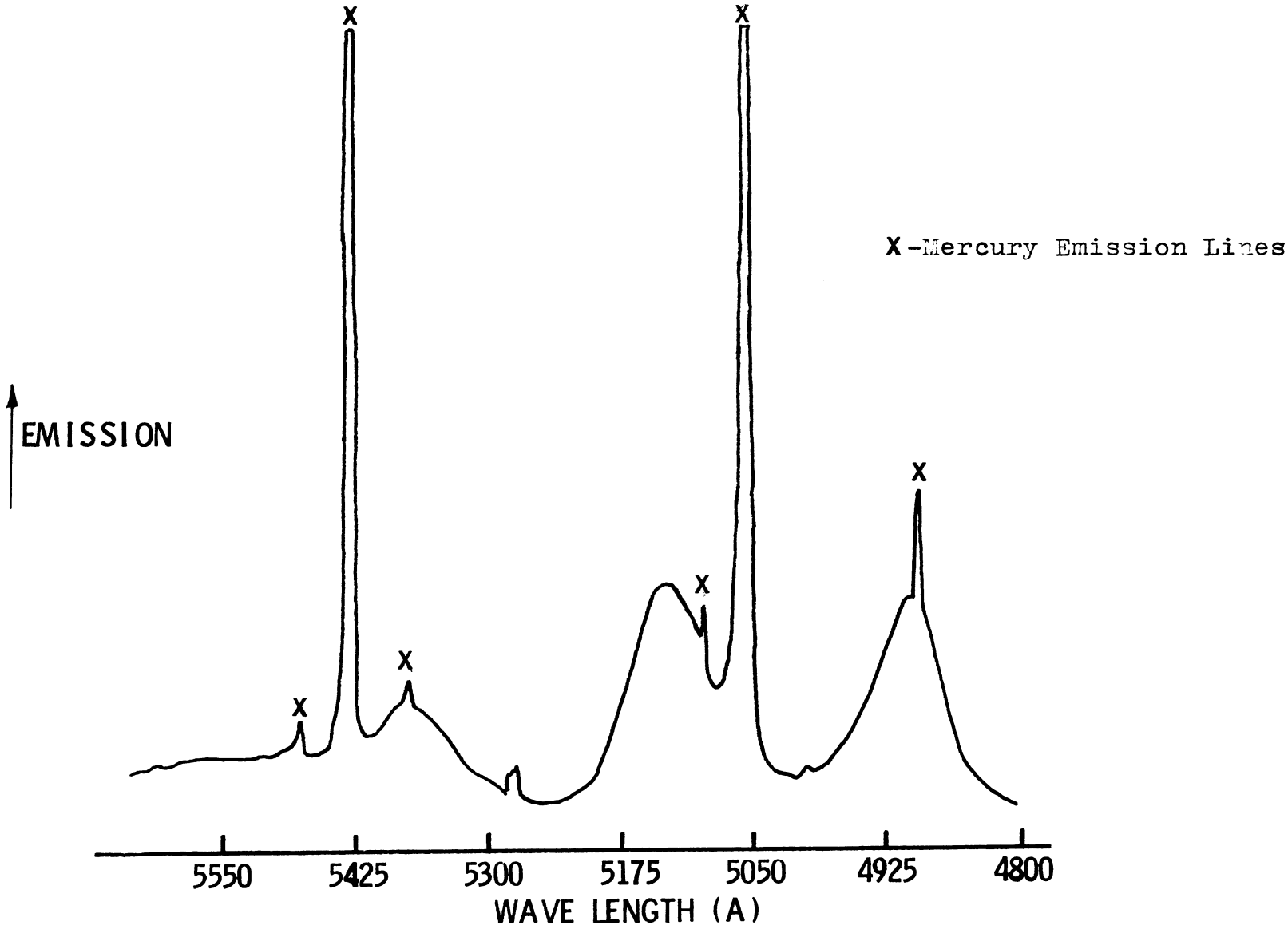

Figure 6. Fluorescence Spectrum of Uranyl Sulfate in Sulphuric Acid Solution, 300°K.

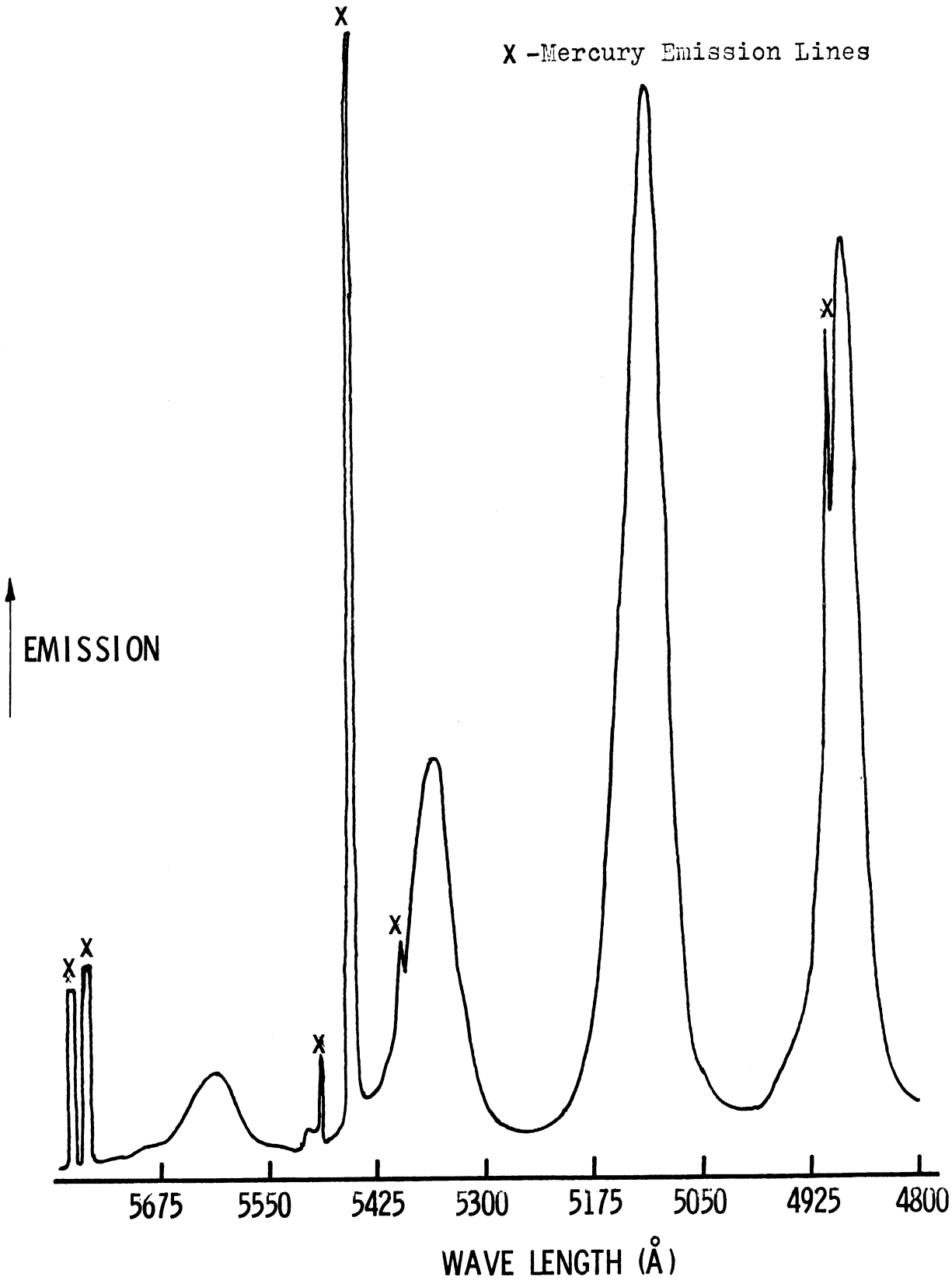

Figure 7. Fluorescence Spectrum of Uranyl Sulfate in Sulphuric Acid Solution, 77°K.

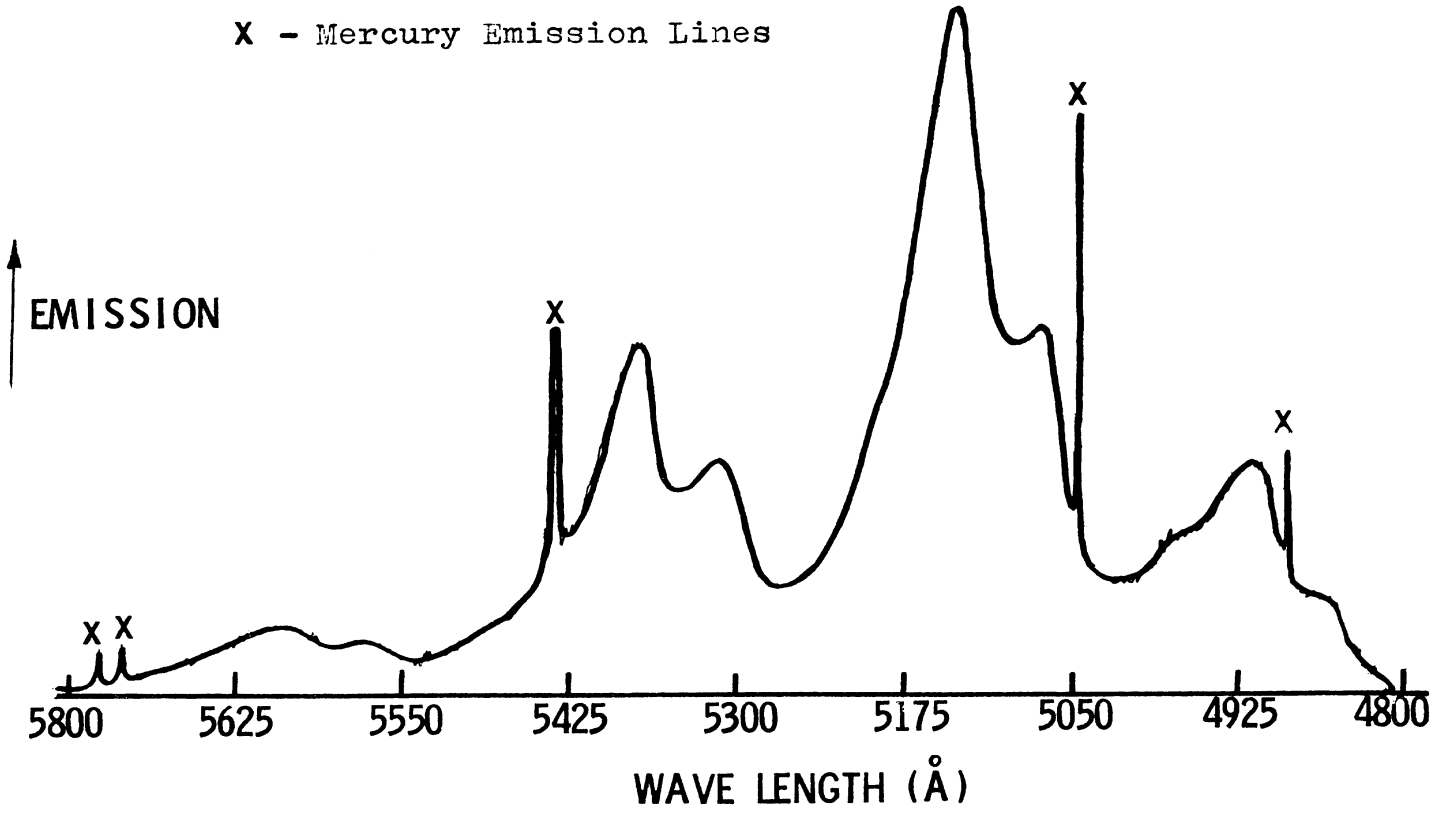

Figure 8. Fluorescence Spectrum of $UO_2SO_4 \cdot 3H_2O$, 300°K.

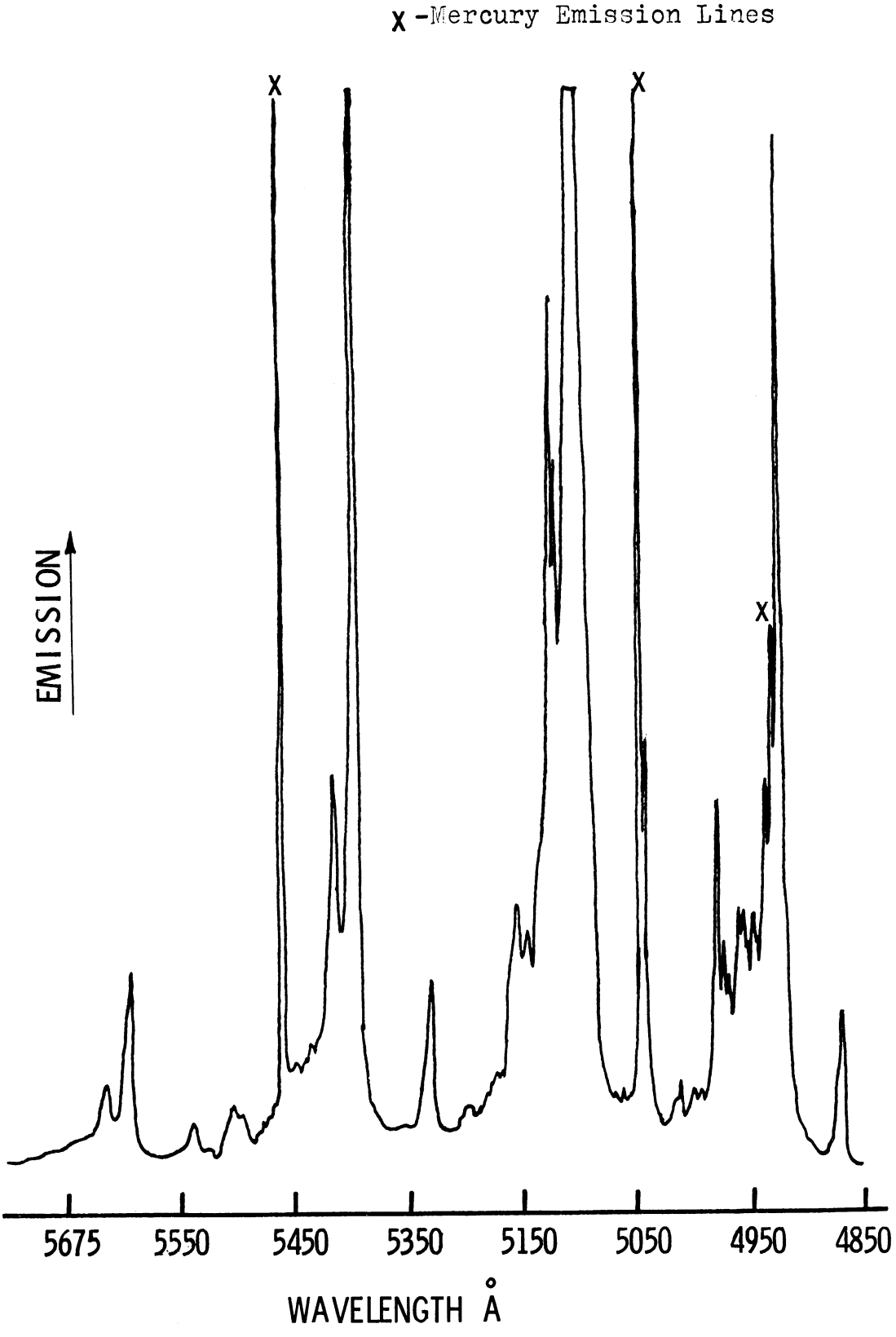

Figure 9. Fluorescence Spectrum of $UO_2SO_4 \cdot 3H_2O$, 77°K.

The spectrum of uranyl glass shows a considerable amount of sharpening as it is cooled from 300°K to 77°K as well as shifts in the positions and relative intensities of the bands. Table VI lists the positions of the bands at 300 and 77°k along with the data of Gordon[7] of the spectrum of a 3 molar frozen aqueous solution at 77°K. The sulfate solution and polycrystalline uranyl sulfate also exhibit shifts in the positions and relative intensities of the bands and the spectra of both become sharper at lower temperatures. Only in the case of the polycrystalline uranyl sulfate, however, is there any more structure to the fluorescence at 77°K than is observable at room temperature. The vibrational quantum observed in the fluorescence spectrum of the sulfate solution is that of the symmetric stretch and the bands are given in Table VI. The bands observed for crystalline uranyl sulfate at 300°K are listed in Table VII along with the same data obtained by Pant.[8] The variations between the positions of the bands as measured here and those of the other authors are not significant since they are within the experimental error. It is interesting to note that in the case of the frozen sulfate solution none of the other vibrations of the molecule are seen (as in the case of the crystals even at room temperature) even through the bandwidths of the fluorescence bands which are seen are narrow enough to prevent their masking the presence of other bands.

TABLE VI

FLUORESCENCE BANDS OF URANYL SULFATE SOLUTION

Band No.	In Sulphuric Acid (This Study)						In Water (Gordon[7])
	T = 300°K			T = 77°K			T = 77°K
	λ(Å)	ν(cm^{-1})	Δν	λ(Å)	ν(cm^{-1})	Δν	ν(cm^{-1})
1	4915	20346	926	4871	20530	950	20310
2	5150	19420	917	5106	19583	930	19460
3	5404	18503		5362	18649	870	18610
4				5625	17780		17750
5							16900

Figure 10 shows a resumé of the energy levels of the uranyl ion deduced from analysis of the absorption and fluorescence spectra in these various hosts.

TABLE VII

FLUORESCENCE BANDS OF URANYL SULFATE, POLYCRYSTALLINE, 300°K

Band No.	(This Study) λ(Å)	ν(cm^{-1})	$\Delta\nu$	(Pant[8]) ν(cm^{-1})
1	4888	20460	230	20460
2	4944	20230	210	20244
3	4994	20020	410	19976
4	5099	19610	240	19615
5	5163	19370	630	19392
6	missing			19134
7	5337	18740	210	18755
8	5398	18530	350	18560
9	5500	18180	310	18304
10	5595	17870	200	17899
11	5660	17670		17695

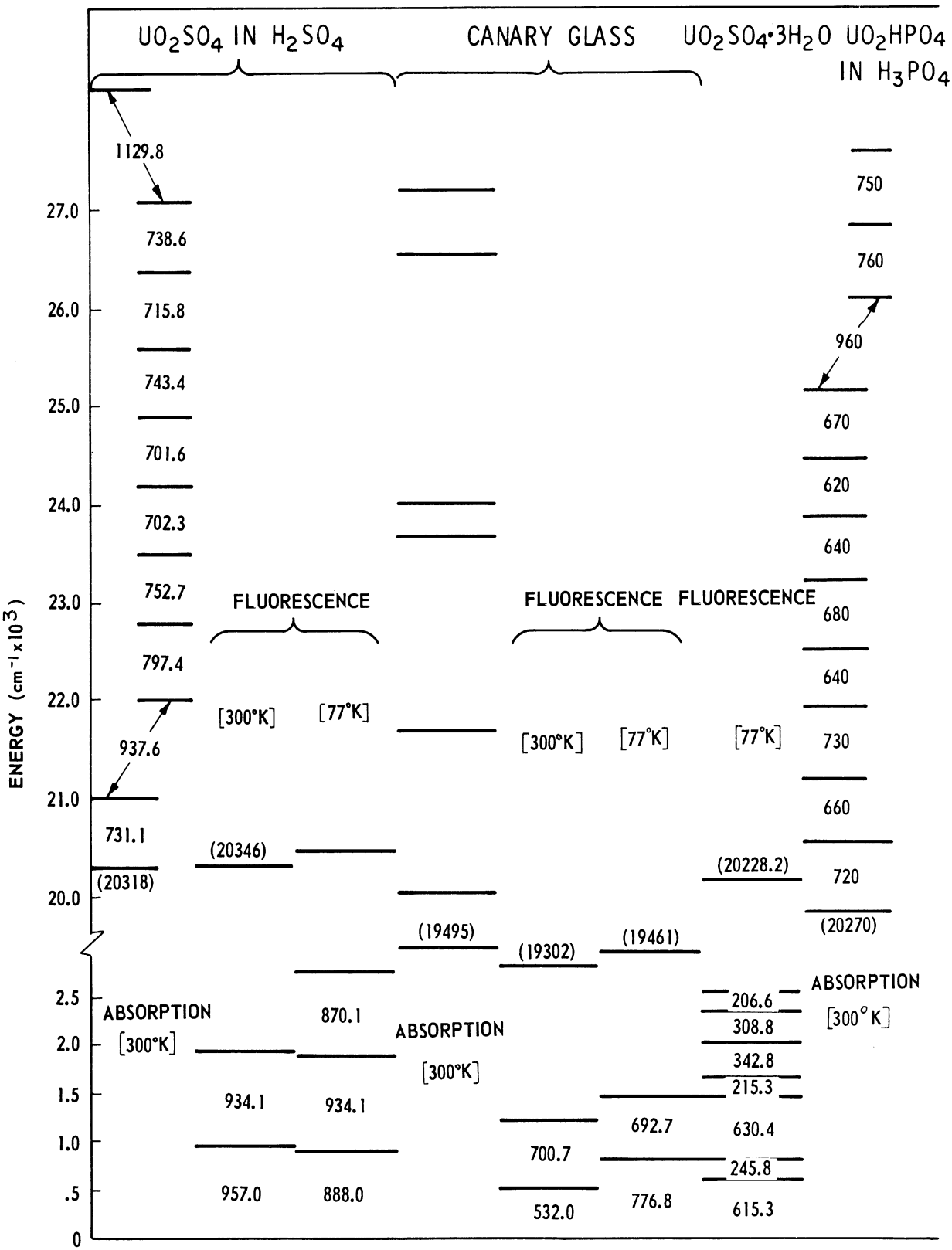

Figure 10. Energy Level Diagrams for Uranyl Solutions, the Glass, and Uranyl Sulfate.

C. INDUCED ABSORPTION SPECTRA

The spectrum of a 1600 watt compact arc lamp* transmitted through a 5-mm thick section of uranyl glass and a solution of UO_2SO_4 in H_2SO_4 (0.0466 gm/ml) contained in a 10-mm path length Beckman liquid sample cell were recorded on Kodak Pan-X film in the region from 3750 Å to 6500 Å using the first order of Al.5 meter Bausch and Lomb grating spectrograph both with and without excitation with a xenon flash lamp.** The resolution of this spectrograph is about 50,000 in the first order and the input energy to the flash tube was nominally 500 joules (2000 VDC at 250 mfd). These spectra for uranyl glass and uranyl sulfate are given in Figures 11 and 13 respectively. The details of the timing and triggering networks used to obtain the spectra only when the flash lamp is firing are discussed in Appendix II. The difficulties encountered due to the nonlinearity of the film blackening with respect to log (exposure) are discussed in Appendix IV.

If the optical density of the film versus log (exposure) curve for the film is assumed to be linear, then the difference in optical density between the pumped and unpumped tracings should be directly proportional to the induced absorption coefficient. This does, of course, ignore the spectral response of the film which will modify the constant of proportionality between the change in optical density and the absorption coefficient. The correction for this variation can be made by reference to the published spectral response curves for a given film but since it was known that spectrophotometric measurements of the absorption were also to be made, this correction was not applied as the photoelectric measurements can give a much better measure of the magnitude of the induced absorption as well as its period of induction and decay. The induced absorption cross-sections for uranyl glass and sulfate solution are given in Figures 12 and 14, respectively.

The induced absorption in the uranyl glass is quite diffuse and shows only a vague structure. The sulfate spectrum is equally diffuse and shows no sign of any separation which might be taken to be a vibrational separation. (The dips around 5275 Å were subsequently shown by photoelectric measurements to be fallacious. Their exact cause is uncertain.) Since the sulfate solution absorption and fluorescence spectra at 300°K both show considerable vibrational structure, it was concluded that only a crystal cooled to 77°K or lower could yield more information than the room temperature solution.

*Osram type XBO-1600, operated with a model MHXM 2500-2S power supply (Christie, Los Angeles 43, California).

**EG and G type FX-42.

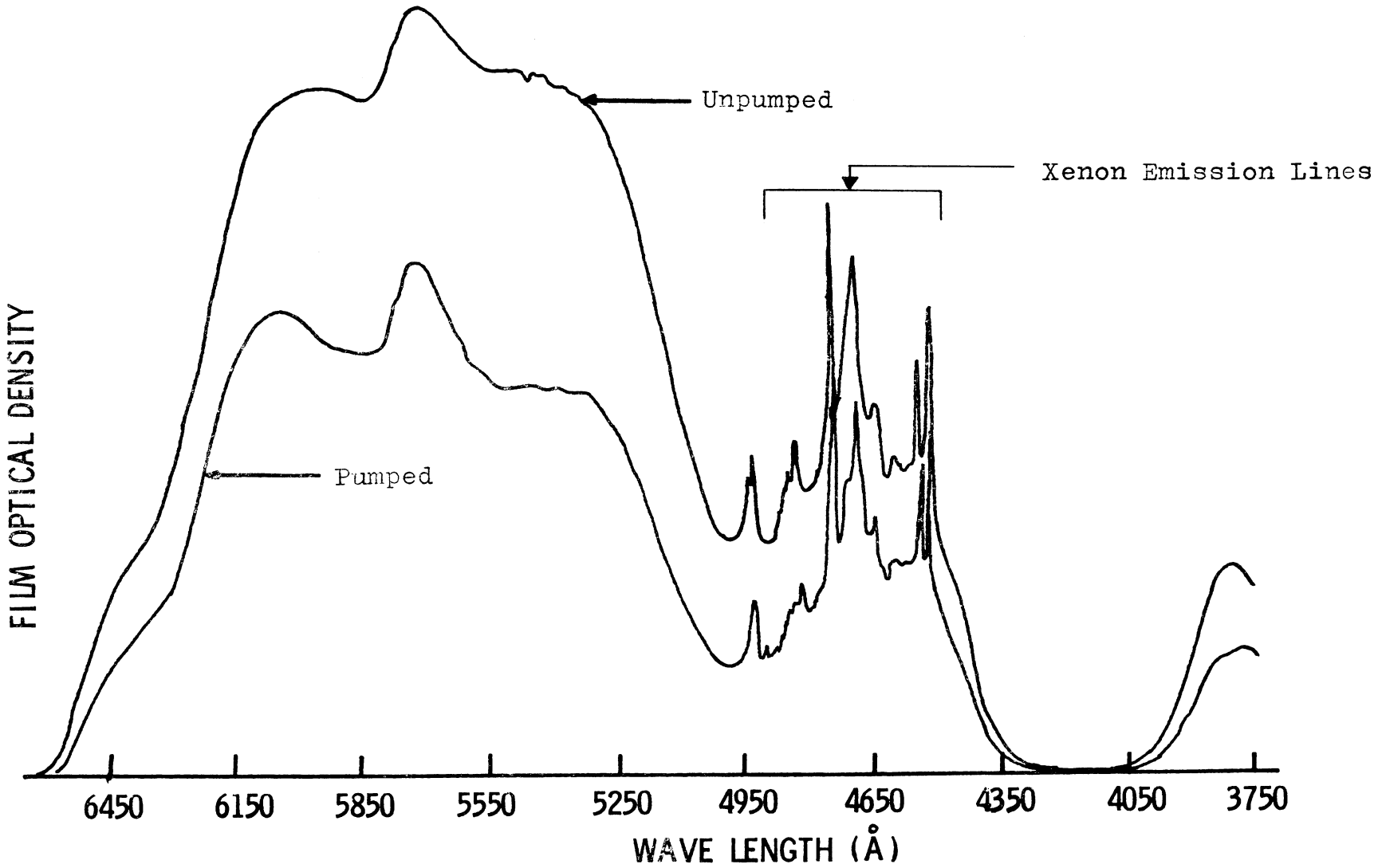

Figure 11. Photographically Recorded Transmission Spectra of Optically Pumped and Unpumped Uranyl Glass.

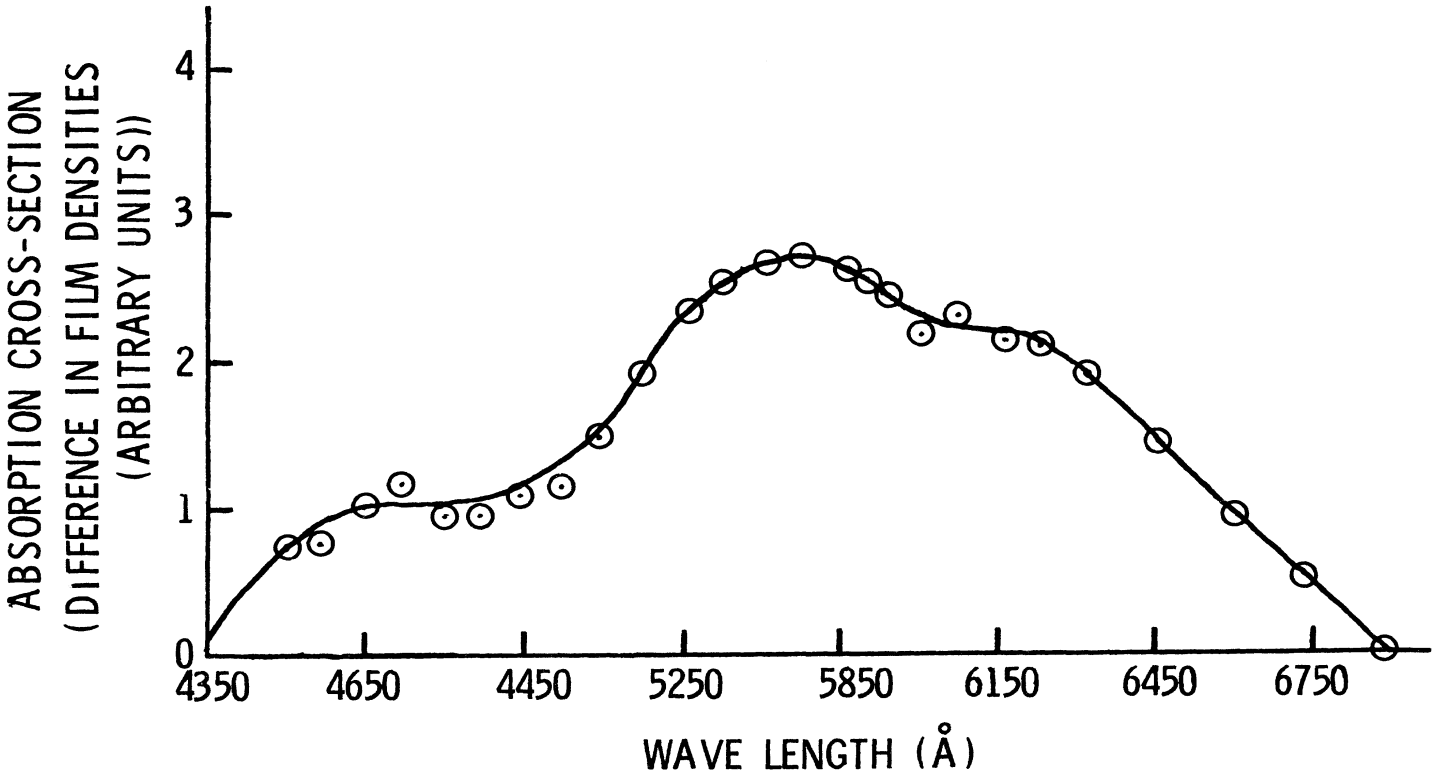

12. Induced Absorption Cross-Section of Uranyl Glass. (Note: absorption cross-section is not corrected for film response.)

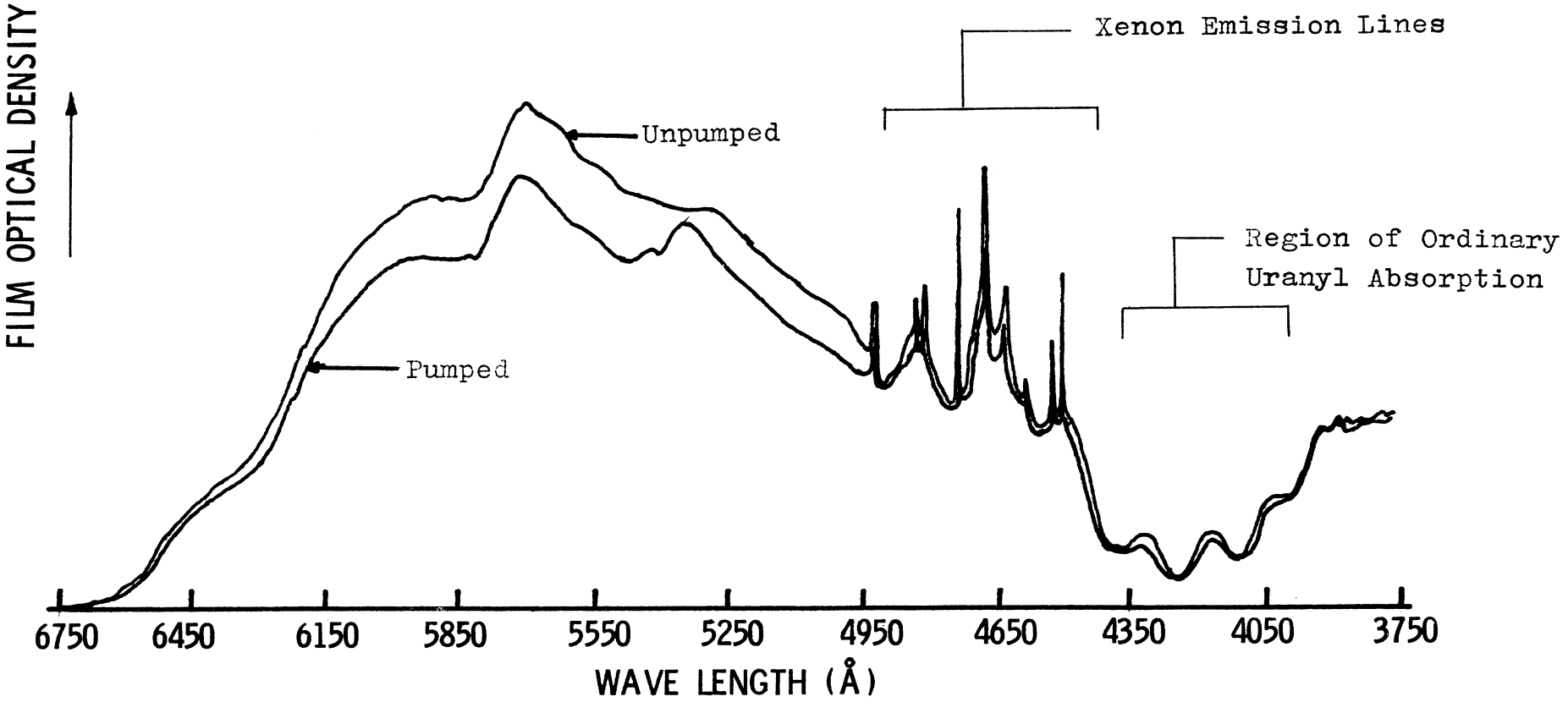

Figure 13. Photographically Recorded Transmission Spectra of Optically Pumped and Unpumped Uranyl Sulfate Solution.

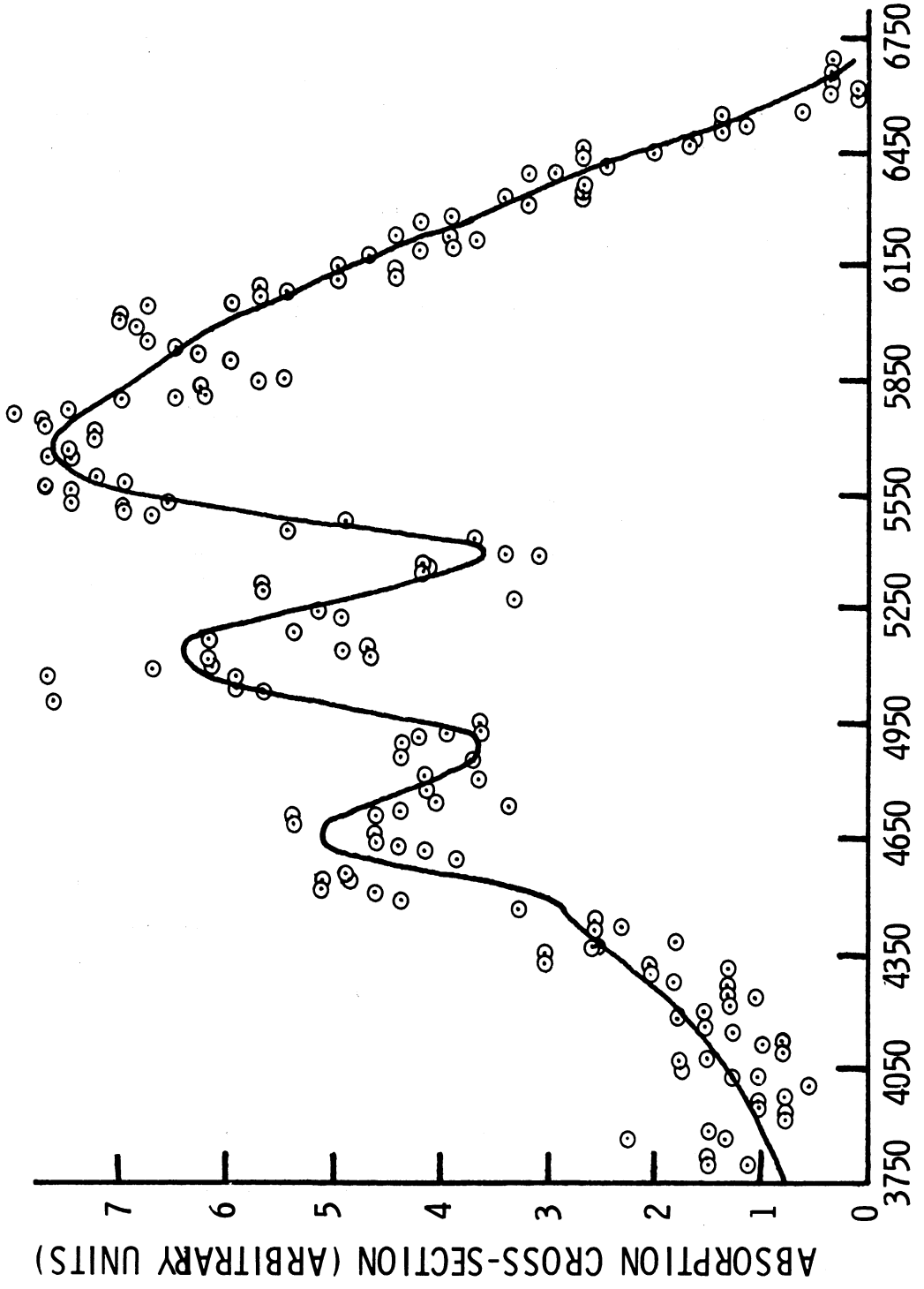

Figure 14. Induced Absorption Cross-Section of Uranyl Sulfate Solution.

An estimation of the number of ions giving rise to this absorption can be made by noticing the difference between the ordinary absorption peaks and dips in the pumped and unpumped spectra. If the average number of ions giving rise to absorptions at frequencies ν and ν' is N and the absorption cross sections at these frequencies are σ and σ', then the difference in optical density of the film at these two frequencies will simply be $N(\sigma-\sigma')\ell$, where ℓ is the path length of the sample. If the number of ions decreases, then the difference in optical density at ν and ν' will also decrease so that the new difference will be $N^*(\sigma-\sigma')\ell$. Thus, the ratio between the original population and the new (in the pumped condition) population for the ground state can be calculated by comparing the ratio between the differences in optical density between two predetermined points in the pumped and umpumped spectra:

$$N^*/N = \text{x } (OD_p(\nu) - OD_p(\nu'))/(OD_u(\nu) - OD_u(\nu')) \qquad (1)$$

where $OD_p(\nu)$ means the optical density of the film at frequency ν for the pumped spectra and $OD_u(\nu)$ means the optical density of the umpumped spectra at the same frequency.

Equation (1) holds only under the condition that the number of ions depleted from the ground state is small compared to the number originally there since the actual amount of absorption is proportional to the difference between the population of the excited state and the ground state, not just the population of the ground state alone. If the transition being considered can have an appreciable lifetime, a sufficient concentration of ions could be built up so as to invalidate this result.

It is necessary to derive a expression for the excited state population which better fits the conditions of this experiment.

There are several assumptions to be made and experimental conditions which must be taken into account: (1) Due to the fact that the flash lamp does not illuminate the sample during the entire time that the camera shutter is open, there is a period of time during the recording of the pumped spectrum in which the ion populations are the same as in the umpumped spectra. This situation arises both before and after the flash lamp fires since the shutter is open longer than the duration of the discharge and the decay of the induced absorption in the uranyl sulfate is very rapid. (See the next section.) (2) A great deal depends on the nature of the upper level involved in the absorption process. If the level has a long half-life, then the disappearance of the ordinary absorption will be proportional to the difference between the upper state and ground state populations, but if the upper state may always be regarded as being empty, the disappearance of the ordinary absorption can be ascribed to the depletion of the ground state population alone. The relaxation time from the other states to the resonance state has been measured as less than 3×10^{-6} seconds by Levshin and Sheremetjev[9] by noting the delay between the application of exciting light and the onset of fluorescence. This does not mean, however, that no population

density in any of these states can be observed because, if the exciting light is sufficiently intense, the pumping rate may be an appreciable fraction of the normal relaxation rate. (3) In accordance with the foregoing considerations, the following assumptions are made: (a) The exposures of both the pumped and unpumped spectra are made with a light pulse which has a square time profile of length $\Delta t_1 + \Delta t_2$. (b) The difference between the ground and excited state populations during the unpumped spectrum is ΔN and this persists throughout the duration of the exposure. (c) The difference between the ground and excited state populations in the pumped spectrum is broken into two time regions, each of which is square and during the time Δt_1 the difference is ΔN (the same as in the unpumped case) and during the time Δt_2 the difference is ΔN^*.

The ratio of the differences in optical densities between the pumped and unpumped spectra is then given by:

$$\frac{\Delta OD'}{\Delta OD} = \frac{\Delta t_1 \Delta N^*(\sigma-\sigma')\ell + \Delta t_2 \Delta N(\sigma-\sigma')\ell}{(\Delta t_1+\Delta t_2)\Delta N(\sigma-\sigma')} \qquad (2)$$

where $\Delta OD'$ is the difference is the pumped spectrum and ΔOD is the difference in the unpumped spectrum. Rearrangement of this equation yields:

$$\Delta N^*/\Delta N = (1/\Delta t_1)((\Delta OD^*/\Delta OD)(\Delta t_1+\Delta t_2)-\Delta t_2) \qquad (3)$$

Table VIII shows the results of the measurements of several of the absorption

TABLE VIII

CHANGES IN ORDINARY ABSORPTION PEAKS OF SULFATE SOLUTION UPON OPTICAL PUMPING

Wavelengths where Optical Densities Determined	Change in Optical Density (Arb. Units) Unpumped	Pumped	$\Delta OD_1/\Delta OD_2$
Max. of 4389 Å abs. band—Min. between 4389 and 4250 Å band.	3.8	3.0	.79
Min. between 4389 and 4250 Å band—Max. of 4250 Å band.	7.9	5.8	.74
Max. of 4250 Å band--Min. between 4250 and 4127 Å band.	7.6	5.3	.70
Min. between 4250 and 4127 Å band—Max. of 4127 Å band.	4.2	2.4	.57
Max. of 4127 Å band—Max. of 4010 Å band.	10.0	9.0	.90
Max. of 4010 Å band—Max. of 3895 Å band.	11.5	10.4	.90

peaks and dips in the pumped and unpumped spectra. We shall assume the following values for the variables appearing in Equation (3):

$$\Delta t_1 = 0.5 \text{ msec.}$$
$$\Delta t_2 = 0.5 \text{ msec.}$$
$$\Delta OD^*/\Delta OD = 0.77$$

which yields the result:

$$\Delta N^* = 0.54\ \Delta N.$$

If we further assume that there is no population in the upper states, then the population of the ground state has therefore been decreased by 46% since ΔN^* equals the ground state population. The population of excited ions (all of which have been assumed to reside in the lowest vibrational level of the lowest excited electronic state) is then in the neighborhood of 0.0565 molar.

The experimental evidence for the exact population is admittedly open to question since the range of ratios in Table VIII is quite large. Complications also arise because of the nonlinearity of the film which may be the cause of the large variation seen there. The mean deviation for the optical density ratios is 0.13 which would give the limits of the ground state depletion as 20% to 72%. This latter figure is quite high but it is certainly reasonable to suppose that the population in the resonance level is within 50% of the previously calculated value.

D. TIME-RESOLVED INDUCED ABSORPTION IN URANYL GLASS AND URANYL SULFATE AND PHOSPHATE SOLUTIONS

Using the experimental setup described in detail in Appendix II, the induced absorption spectra of a 10-mm thick section of uranyl glass, a 10-mm path length solution of uranyl sulfate in concentrated sulphuric acid (4.7×10^{-2} gm/ml) and a 10-mm path length solution of uranyl phosphate in 80% phosphoric acid (7.7×10^{-2} gm/ml) were recorded on Polaroid type 107 film using an RCA 1P21 photomultiplier as a detector and the Jarrell-Ash 3.4 meter Ebert spectrograph as a monochromator. Some of these time-resolved traces are given in Figures 15 and 18 for the uranyl glass and the sulfate solution respectively. (The results for the uranyl phosphate are very similar to those for the sulfate, so none of these are included.)

The photographs in Figure 15 were taken in the following manner. (1) The scale was put on the film with a rather low level of illumination for the grid and exposure settings of 1/10 sec and f/1.9. The grid illumination was then turned down and the rest of the photograph taken with the aperture stopped down to f/22 and the trace intensity adjusted to give a good record. The purpose of this process was to insure that the grid intensity would always be the same, regardless of the manner in which the rest of the photograph was exposed. (2) The record of the induced absorption was then made by firing the flash tube with the cammera shutter held open in the "bulb" position and the oscilloscope sweep set to trigger off an input signal taken directly from the flash tube trigger. Only one beam of the oscilloscope was used and the signal from the photomultiplier monitoring the xenon arc light and the signal from an RCA 933 photodiode monitoring the output from the flash lamp was fed into the two inputs of the dual trace plug-in amplifier which was operated in the chopped mode. The lowest trace on the photograph is the record of the light emitted by the flash lamp; an increase in light signal causing an upward deflection of the beam. The middle trace on the photograph is the xenon arc light as monitored by the photomultiplier. The sense of the beam deflection is reversed from the normal, however, since a <u>downward</u> deflection of the beam corresponds to an increase in the photomultiplier output signal. Thus, in Figure 15, all of the photographs from 4800 Å to 6400 Å show a decrease in the xenon arc light when the flash lamp is fired since the beam deflects upward. The appearance of the "increased" xenon arc light at 4400 Å is dealt with below. (3) The record of the light scattered from the sample and detected by the photomultiplier was then made by blocking the xenon arc light from passing through the sample with an opaque shutter and firing the flash lamp a second time under the same conditions as before. The flash tube capacitor bank was not always fully charged the second time so the flash light trace is sometimes slightly different in this second exposure than in the first giving the appearance of a doubling in the lowest trace. Were there no flash lamp light scattered from the sample, the uppermost trace would have been a straight horizontal line since no light would have been present. The fact that there is a downward deflection of the beam indicates that a small amount of light is being scattered from the sample.

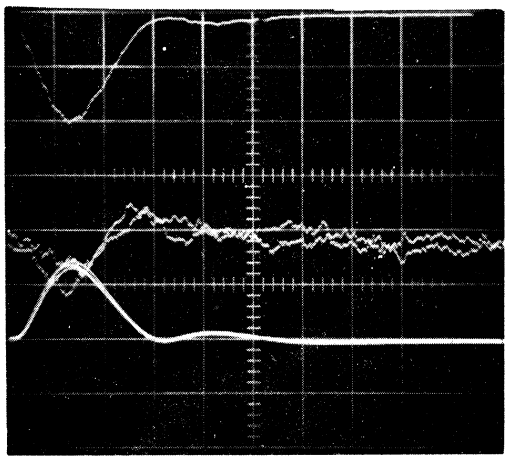

4400 A

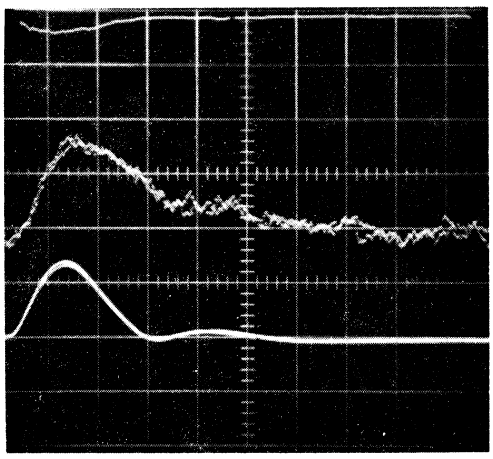

4800 A

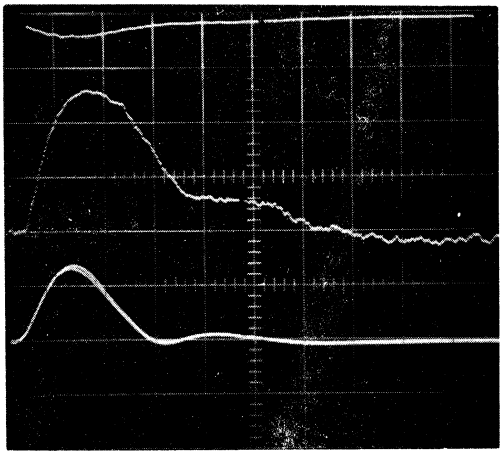

5200 A

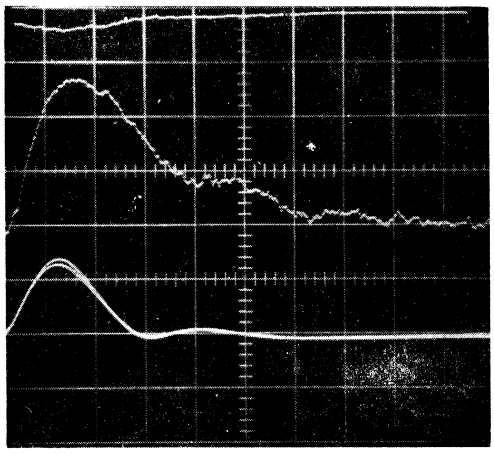

5600 A

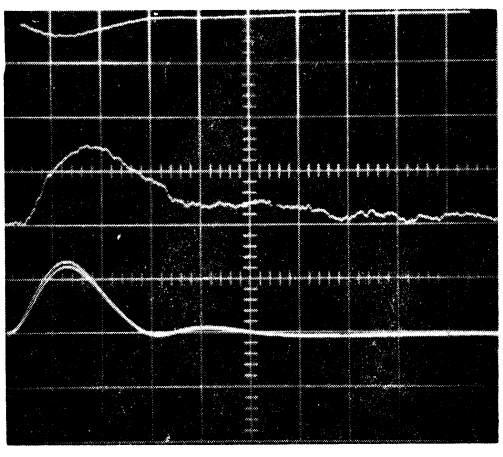

6000 A

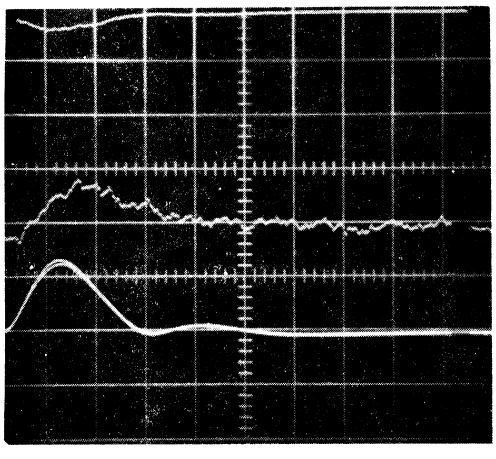

6400 A

Figure 15. Time-Resolved Induced Absorption in Uranyl Glass. (Time scale is 2 msec./div.)

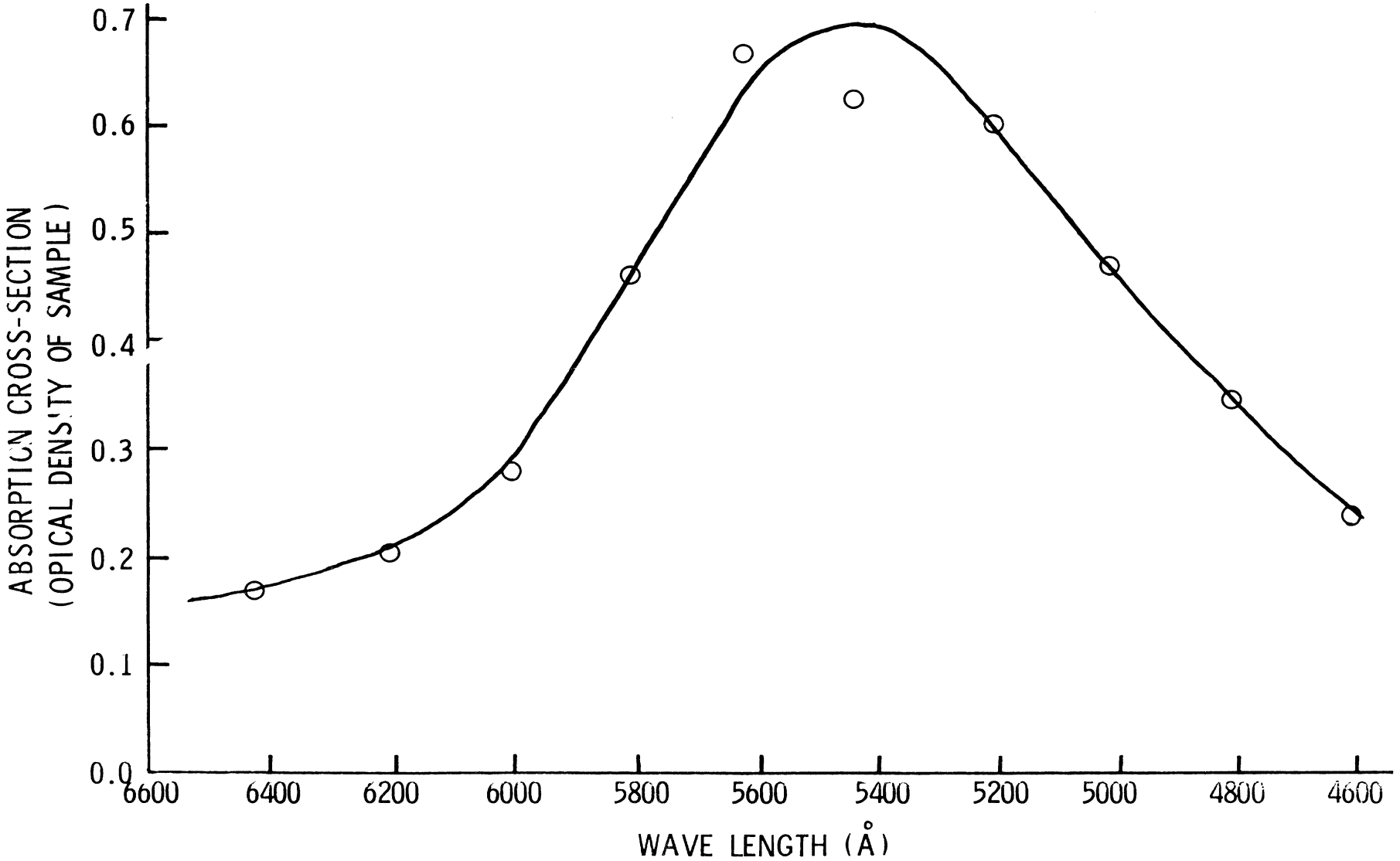

Figure 16. Induced Absorption Cross-Section for Uranyl Glass as Deduced from Photoelectric Measurements (versus wavelength).

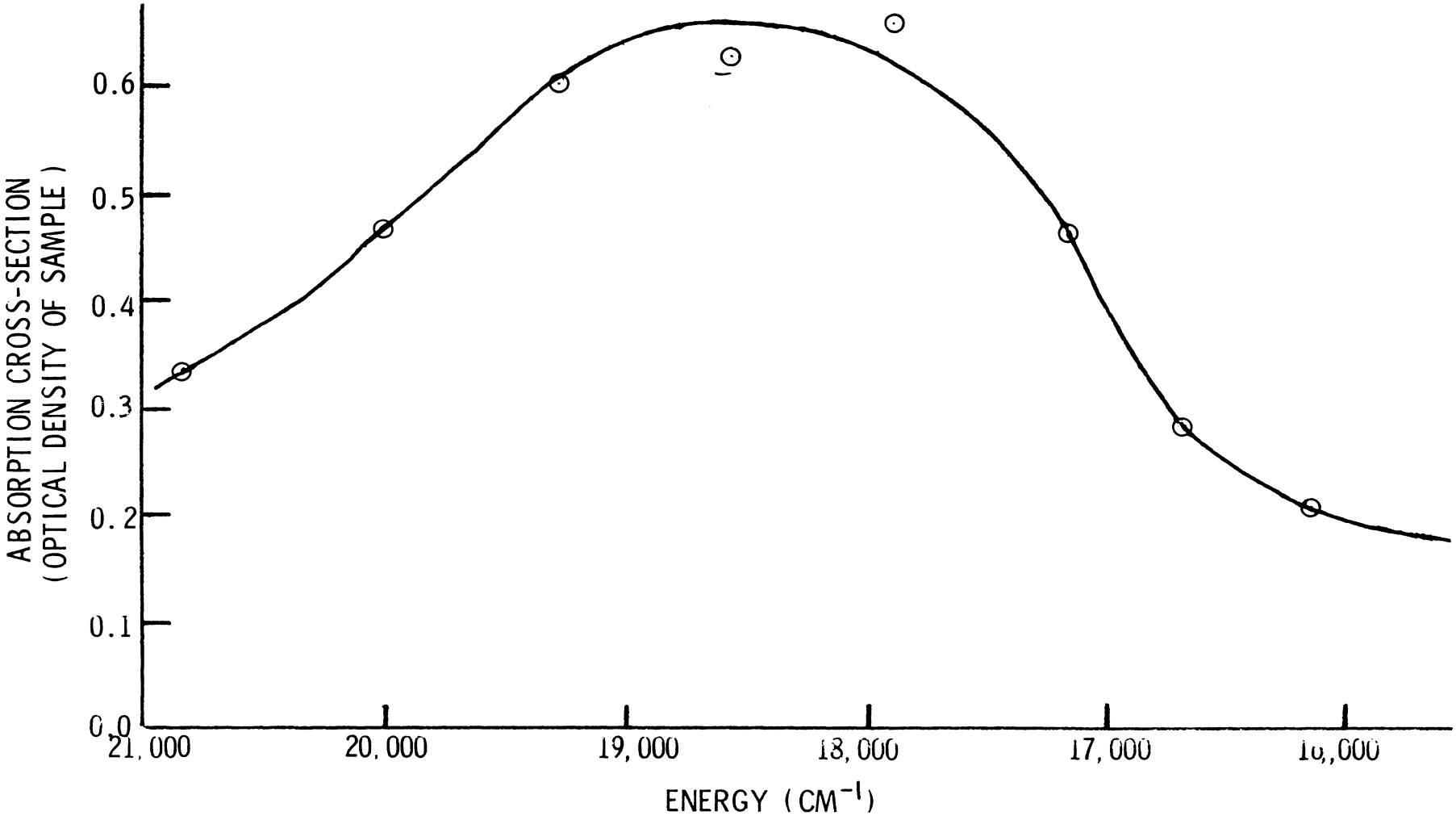

Figure 17. Induced Absorption Cross-Section for Uranyl Glass (versus energy).

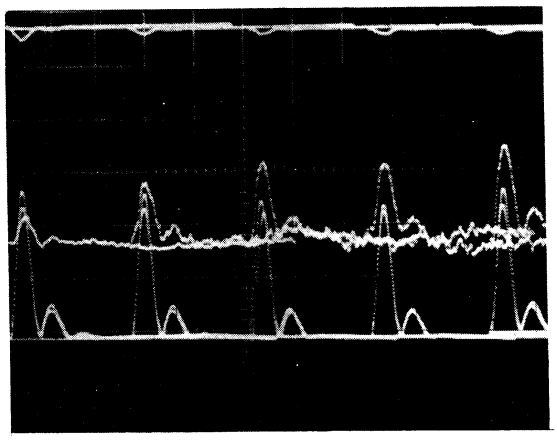

5200-5600 A

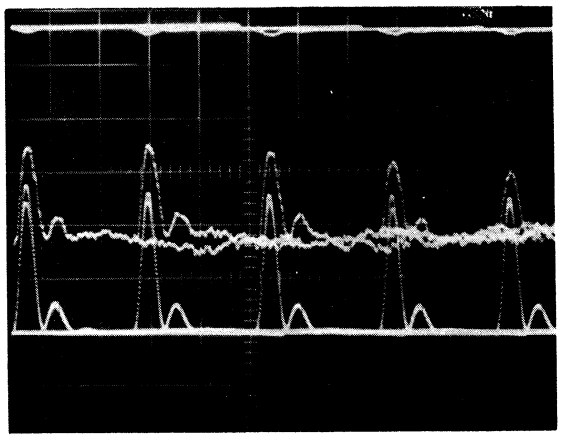

5700-6100 A

6200-6600 A

Figure 18. Time-Resolved Induced Absorption in Uranyl Sulfate Solution. (Time scale is 10 msec./div.)

The photographs for the uranyl glass were taken every 200 Å since no structure was expected to appear of a spacing closer than this and the minimum percent of transmission at each wavelength determined by measurement of the difference between the uppermost and middle tracings at the maximum of the middle trace and dividing by the spacing between them when no induced absorption or scattered light was present, i.e., at the far right of the photograph. (The gain of the oscilloscope and the aperture of the sample were adjusted to give a nearly constant signal at each of the different wavelengths.) These results were then converted to optical density and plotted versus wavelength in Figure 16 and versus energy in Figure 17. The appearance of the plateau in the decay of the induced absorption is attributable to the presence of a second hump in the flash tube light output—the circuit was "ringing." This disappeared when a second inductor which quenched the ringing was substituted. Because of the high ordinary absorption in the sample, the photograph at 4400 Å in Figure 15 had to be taken with a high gain on the oscilloscope so that the scattered light appears to be larger at this wavelength than at the others. Such is not the case, however, and this scattered light signal is more than enough to make up for the diminution of the xenon arc signal due to the induced absorption so the middle trace of this photograph deflects downwards instead of upwards as in the rest of the photographs. There is just a barely detectable induced absorption at this wavelength as can be observed by subtracting the uppermost trace from the middle one and observing that the middle trace does deflect upwards once this source of noise has been accounted for.

The photographs of the uranyl sulfate solution were taken in exactly the same manner as those of the uranyl glass with but one exception: in order to conserve film, the sweep time of the oscilloscope trace was lengthened to 10 msec/cm and the time base operated in the "strobe" mode which brightens any particular preselected portion of the trace. In this manner, all of the sweep can be eliminated from the photograph except this brightened portion since the beam intensity can be adjusted so that all the rest is too weak to record on the film. The beam was then positioned so as to start in the middle of the oscilloscope face and the camera moved between exposures. In this manner, five separate exposures can be made on each film. A survey every 100 Å was first made and then a series every 10 Å in the region from 4800 to 5270 Å and every 20 Å in the region from 5350 to 5530 Å to check for finer structure. None was detected so it was concluded that its appearance is only an artifact of the photographic film.

The profiles of the induced absorption in the sulfate and phosphate solutions were determined in the same manner as was that of the glass and these are plotted in Figures 19 and 20, respectively. The general outline of the band in all three media is basically the same but the oscilloscope photographs give more detail than just the intensity of the absorption. One immediate discernible difference between the glass and sulfate traces is the prominence of the second hump in the induced absorption decay. As stated before, this is due to the presence of a second hump in the flash tube output (more prominent because of the condensation of the time axis in Figure 18 but of equal magnitude). The decay of the absorption induced in the glass is so slow that this

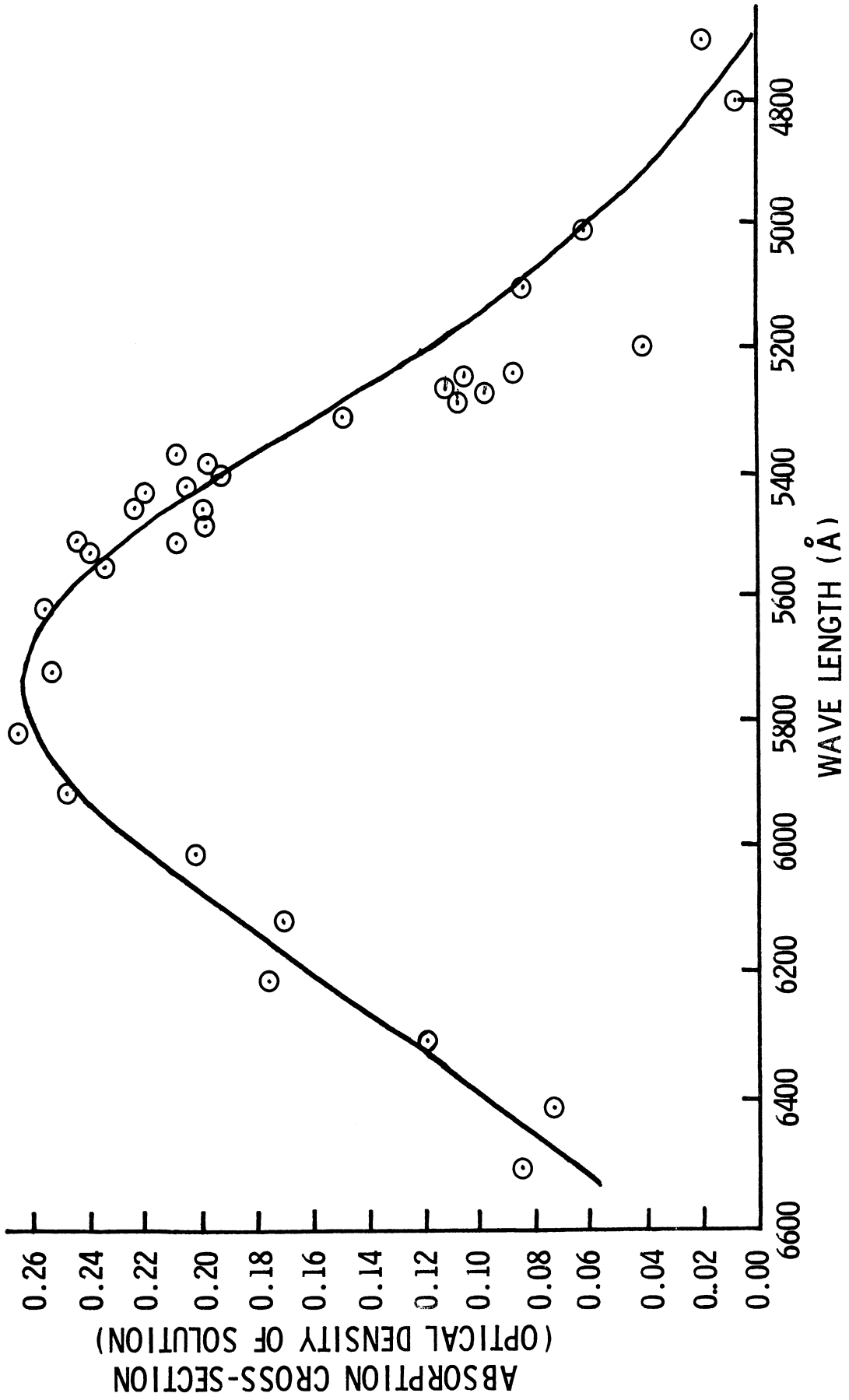

Figure 19. Induced Absorption Cross-Section for Uranyl Sulfate Solution as Deduced from Photoelectric Measurements (versus wavelength).

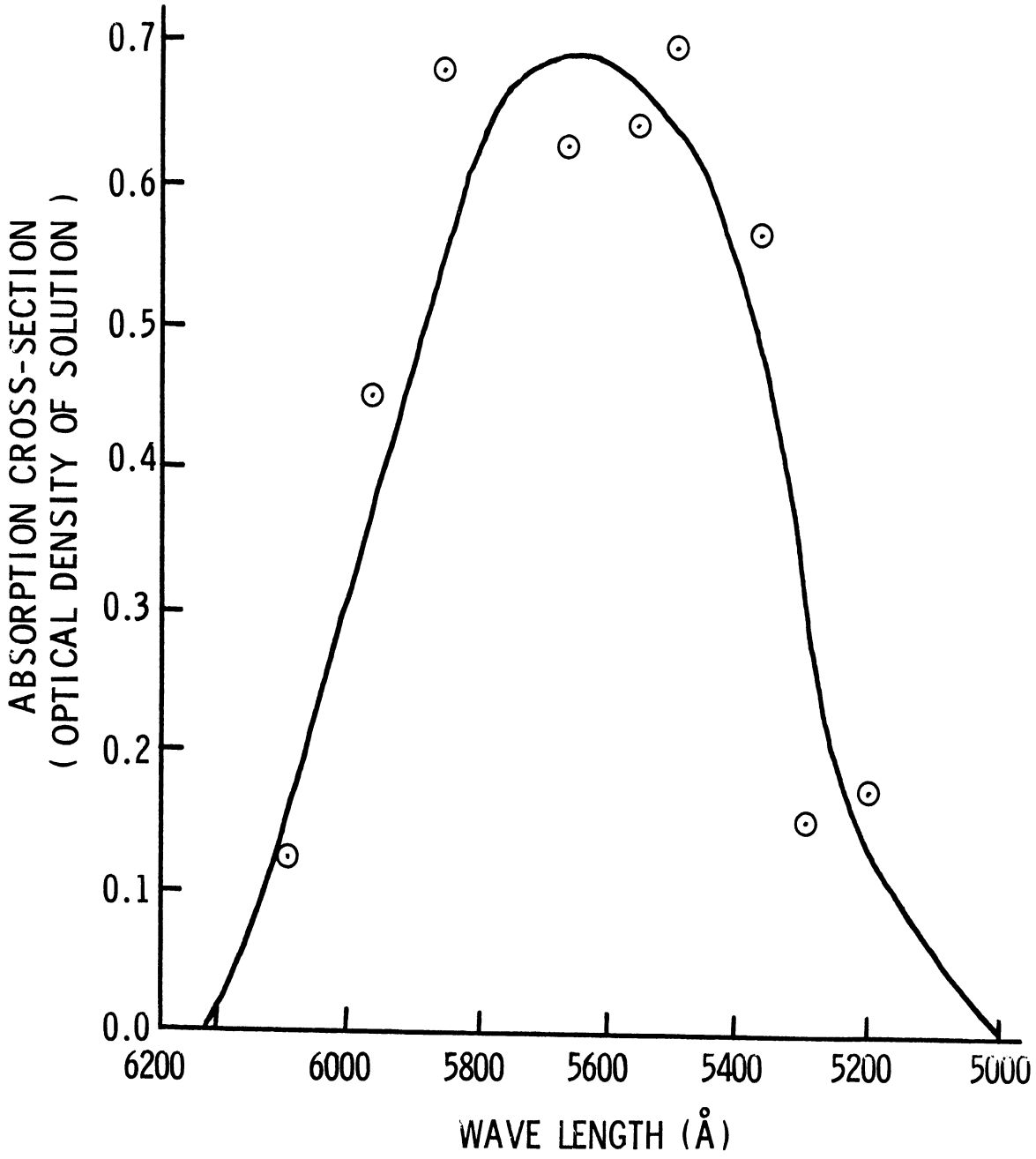

Figure 20. Induced Absorption Cross-Section for Uranyl Phosphate Solution as Deduced from Photoelectric Measurements (versus wavelength).

second pumping appears only as a plateau in the induced absorption curve while in the sulfate the relaxation is so much faster that the second hump is very prominent in the induced absorption curve. This difference in decay time evidences itself in other ways. The effect of the integration of the pumping light in the glass can be seen in the fact that the maximum of the induced absorption occurs slightly after the peak of the flash lamp while the sulfate, which apparently has a much faster relaxation time has its peak absorption at the same time as the flash lamp. The differential equation describing this process is

$$dN^*/dt = N \beta I(t) - \alpha N^* \tag{4}$$

where N^* is the concentration of excited ions, N is the concentration of ground state ions, β is a factor dependent on pumping efficiency, i.e., geometry and size of sample, flash tube, and reflector and intensity distribution of the pump lamp and absorption cross-section of the sample as a function of wavelength, etc., and α is the decay time constant. Assuming that the ground state population does not change during this process, the solution for this equation is

$$N^*(t) = N \beta e^{-dt} \int_o^t I(t')e^{\alpha t'} dt \tag{5}$$

where it is assumed that $N^*(t = 0) = 0$. The assumption that the ground state population does not change is not a particularly good one at these high pumping intensities. The solution obtained when taking this into account is

$$N^*(t) = \frac{N_o \beta}{e^{[\alpha t + \beta \int_o^t I(t')e^{\alpha t'} dt']}} \times \int_o^t I(t')e^{+\alpha t' + \beta \int_o^{t'} I(t'')e^{\alpha t''} dt''} dt' \tag{6}$$

where N_o is the total number of ions. The right hand side of (6) is seen to converge to that of (5) if the integral

$$\int_o^t I(t')e^{\alpha t'} dt$$

is small. As an example of the behavior of the function in (6), suppose the pumping intensity is assumed to be a square wave extending in time from 0 to T and is of amplitude I. Then (6) reduces to:

$$N^*(t) = \frac{N_o \beta I}{\alpha+\beta I} \frac{e^{(\alpha+\beta I)t} - 1}{e^{(2+\beta I)t}}, \quad 0 \leq t \leq T \tag{7}$$

and

$$N^*(t) = \frac{N_o \beta I}{\alpha+\beta I} \left(\frac{e^{(\alpha+\beta I)T} - 1}{e^{(\alpha+\beta I)T}} \right) e^{-\alpha(t-T)}, \quad t > T \tag{8}$$

Figure 21 illustrates the behavior of this solution. The characteristics of these curves which are of interest is that the faster the decay time of the excited state, the sooner the maximum population is reached and the smaller it is. These are exactly the phenomena observed by contrasting the induced absorption traces of the glass and sulfate solutions: (1) the maximum of the induced absorption in the sulfate solution occurs before that of the glass, and (2) the induced absorption in the sulfate is smaller (for roughly the same number of ions).

In order to determine the decay constant of the induced absorption, the same experiment was run but with an inductor which did not cause the flash tube to ring. This was an air core inductor having a calculated inductance of 700 μ-henries. (No attempt was made to optimize the discharge circuit for critical damping or to measure the inductance of the circuit.) The induced absorption traces for uranyl glass and uranyl sulfate are shown in the normal perspective in Figures 22(a) and 23(a), respectively. In order to examine that portion of the induced absorption trace which occurs after the pump lamp has cut off (and thus to see the pure exponential decay of the absorption), the same photograph was then repeated using the "strobe" mode of triggering so that only a portion of the trace has sufficient intensity to be visible on the film. Part (b) of each of these figures shows that portion of the curve which is to be expanded for better time resolution. Part (c) then shows the decay curve recorded at a higher sweep speed. The sweep speed of the fastest traces of the sulfate absorption is fast enough to show the chopping between the beams.

The intensity of the light transmitted through the sample is assumed to follow Beer's law

$$I = I_i e^{-N\sigma\ell} \tag{9}$$

where I is the transmitted intensity, I_i is the incident intensity, N is the number of active centers/cm^3, σ is the absorption cross section at a particular frequency, and ℓ is the path length. The number of active centers, however, varies as a function of time and this is assumed to be a pure exponential decay:

$$N = N_o e^{-\beta t} \tag{10}$$

Substitution from (10) into (9) yields:

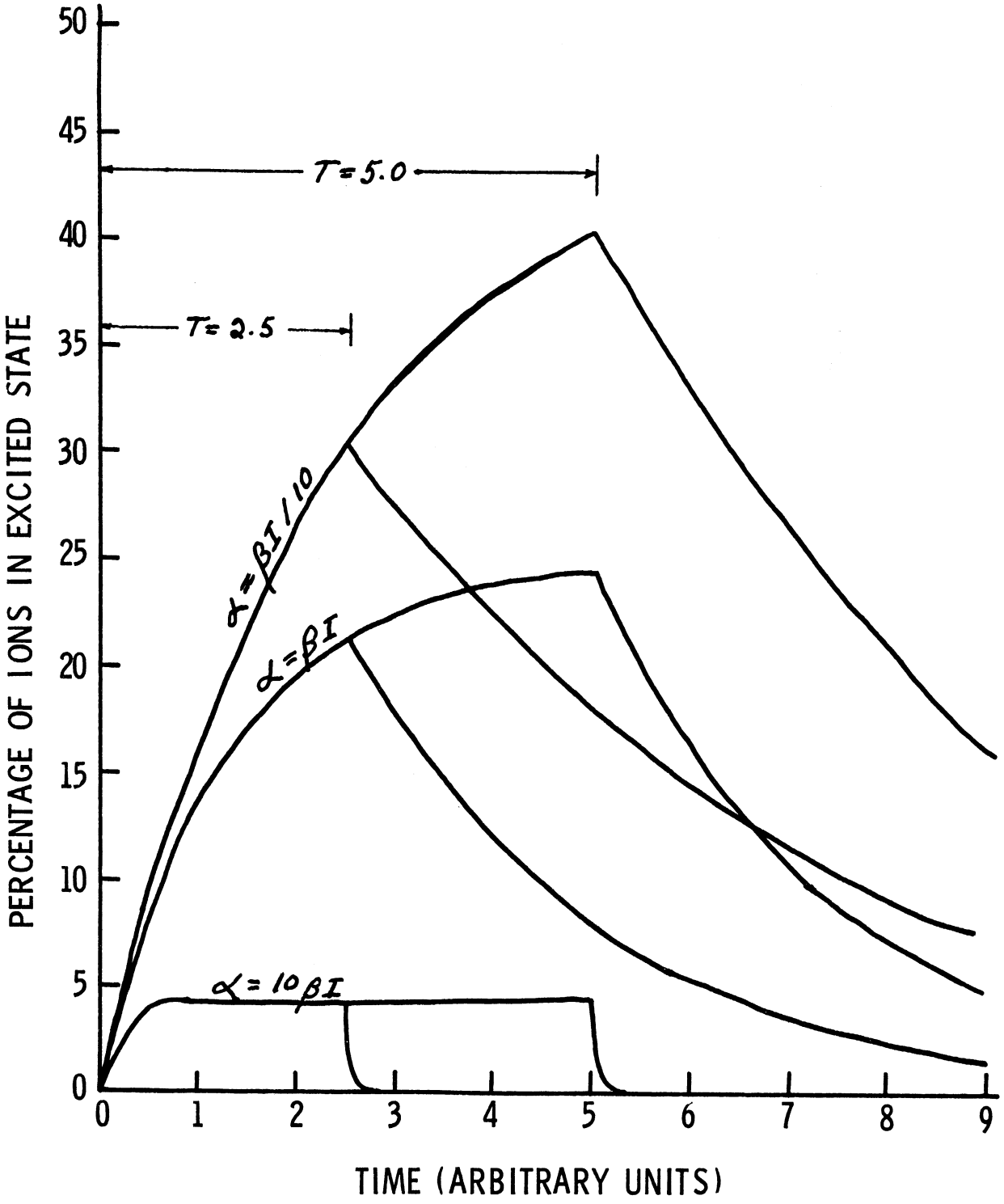

Figure 21. Theoretical Time-Profile for the Excited State Population Assuming Square-Wave Pumping.

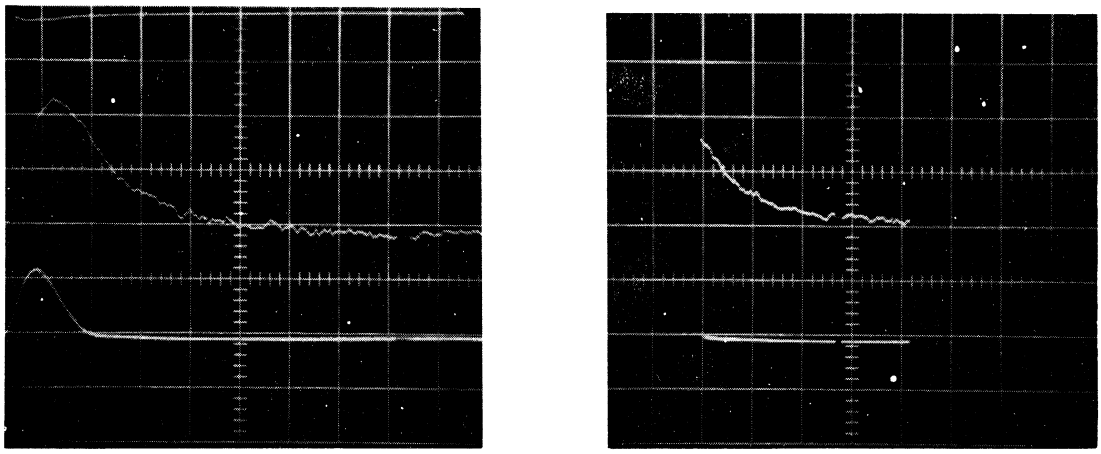

(a) (b)

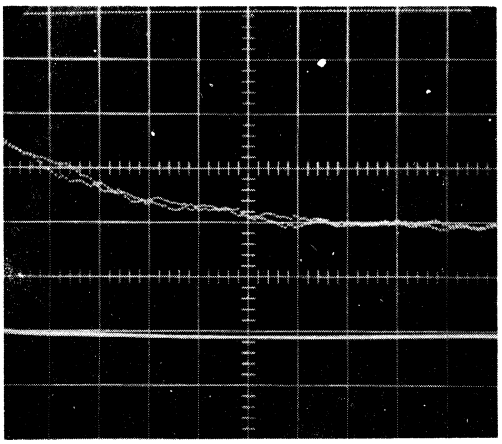

Figure 22. Induced Absorption Decay Measurement for Uranyl Glass.

(a) Normal sweep, 0.5 msec./div.
(b) Strobe sweep showing region to be expanded.
(c) Delayed sweep, 0.2 msec./div.

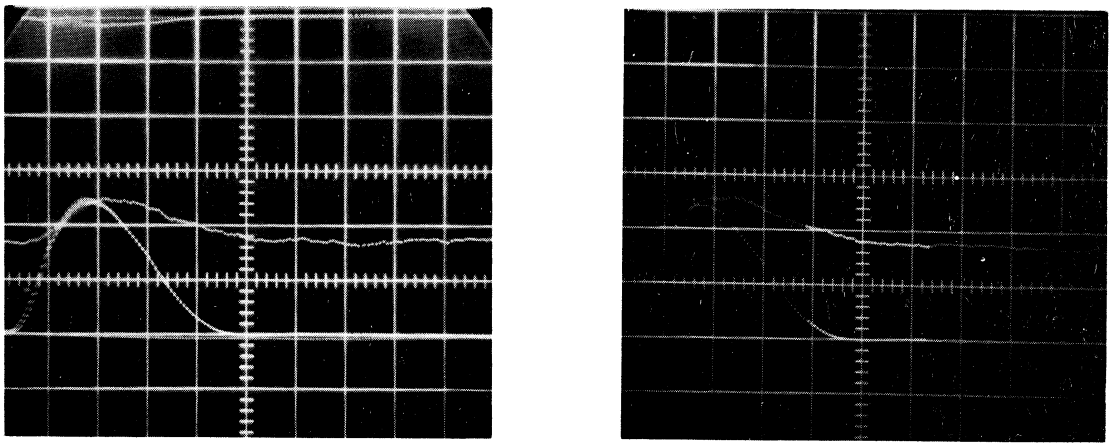

(a) (b)

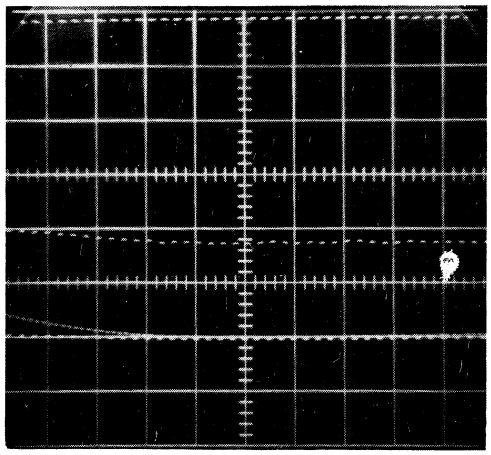

(c)

Figure 23. Induced Absorption Decay Measurement for Uranyl Sulfate Solution.

(a) Normal sweep, 0.2 msec./div.
(b) Strobe sweep showing region to be expanded.
(c) Delayed sweep, 0.05 msec./div.

$$I = I_i \exp\left(-\sigma \ell N_o \exp(-\beta t)\right) \tag{11}$$

At time t = 0, let I = I_o so that (11) becomes

$$I_o = I_i \exp(-\sigma \ell N_o)$$

or:

$$\sigma \ell N_o = -2.303 \log_{10}\left(\frac{I_o}{I_i}\right) \tag{12}$$

Equation (11) may be rearranged to:

$$-2.303 \log_{10}\frac{I}{I} = \sigma \ell N_o \exp(-\beta t) \tag{13}$$

and substitution from (12) yields:

$$\text{Exp}(-\beta t) = \log_{10}\left(\frac{I}{I_i}\right) \Big/ \log_{10}\left(\frac{I_o}{I_i}\right) \tag{14}$$

Equation (14) can also be written as:

$$\beta t = -2.303 \log_{10}\left(\log_{10}\left(\frac{I}{Ii}\right) \Big/ \log_{10}\left(\frac{I_o}{I_i}\right)\right) \tag{15}$$

i.e., the rather complicated expression on the right hand side should be a linear function of the time.

Equation (15) is plotted in Figure 24 for the data obtained from Figure 22 for the uranyl glass. The agreement is very good indicating that the decay of the induced absorption is purely exponential. The time constant is 429 μsec. The data for the sulfate solution is much poorer, however, but data from Figure 23 indicates a decay time of 52 μsec. (This figure is probably larger than the true decay time because measurement of the decay of the absorption induced in the sulfate solution must be made while the flash tube is still pumping the sample and this will give an apparent lengthening of the decay time. As can be seen from Figure 23, the induced absorption is practically zero by the time the flash tube has finished firing.)

Coupled with the result from the photographically recorded spectrum that approximately 50% of the uranyl ions participate in the induced absorption, it is possible to calculate the molar extinction coefficient and the oscillator strength for this transition in the case of the sulfate where the concentrations are known. Based on the previous calculation of the population of the resonance level, the molar extinction coefficient at the maximum of the induced absorption curve at 5700 Å is 5.65 and the calculated oscillator strength is 6.54×10^{-5}. As remarked before, these values may be as much as 50% in error.

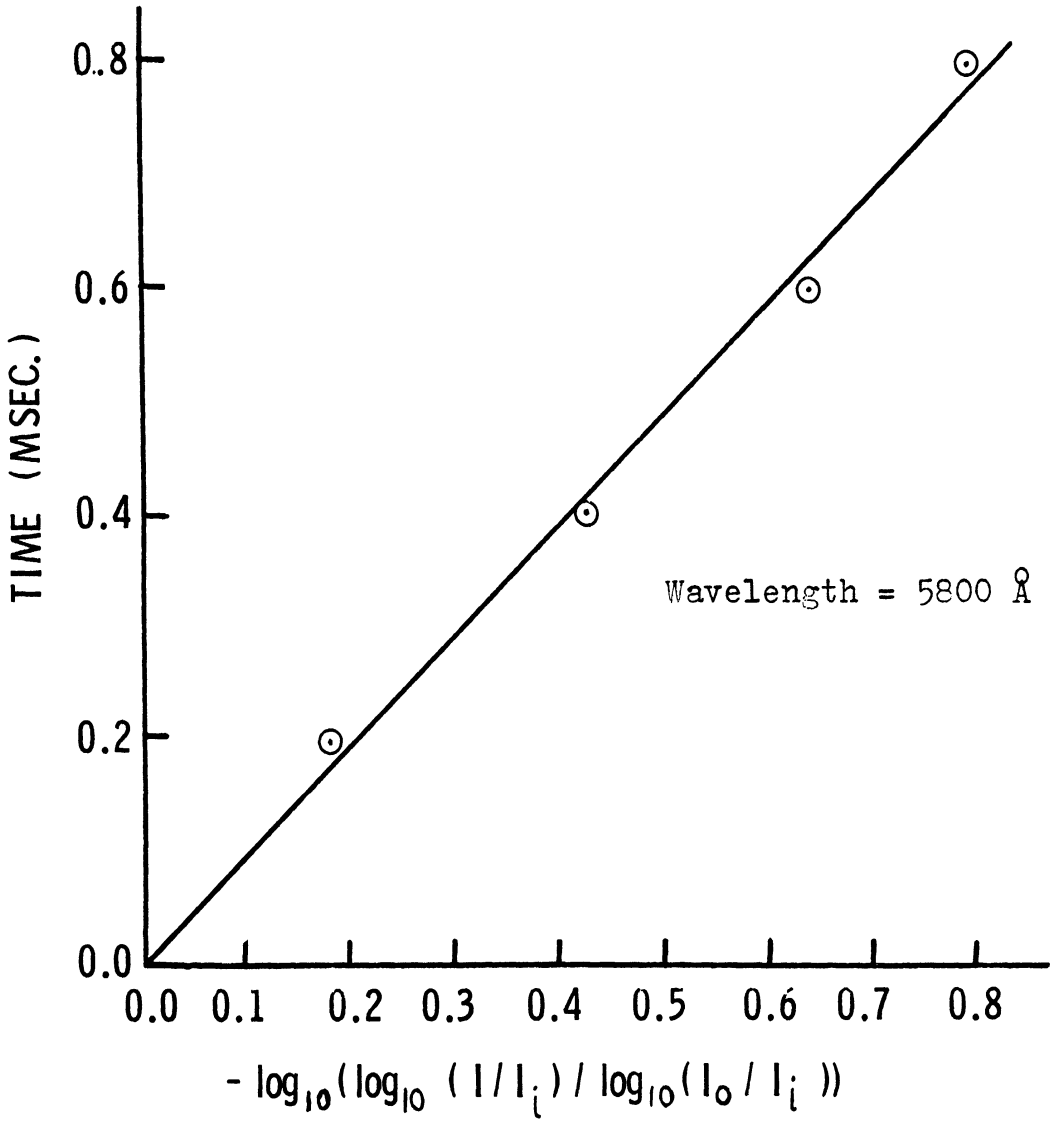

Figure 24. Induced Absorption Decay for Uranyl Glass.

E. TIME-RESOLVED FLUORESCENCE IN URANYL GLASS AND URANYL SULFATE SOLUTION; COMPARISON OF DC- AND FLASH-EXCITED FLUORESCENCE SPECTRA OF URANYL SULFATE TRIHYDRATE

The induction and decay of the fluorescence of a 5-mm thick section of uranyl glass and a 10-mm path length solution of uranyl sulfate solution in concentrated sulfuric acid (4.7×10^{-2} gm/ml) were recorded using the same apparatus as in the case of the time-resolved induced absorption measurements. The physical setup, however, was different because the flash head was positioned differently on the optical bench so that the sample was at a focus point. (Appendix II describes the optical path and how this can be accomplished.) The samples were excited with the xenon flash lamp as in the case of the induced absorption measurements but it was necessary to impose a 3-mm thick section of deep blue Corning No. 5-57 filter glass between the sample and the flash lamp to avoid picking up the flash lamp light which scatters off the sample and which is at the same frequency as the fluorescence.

The photographs of the fluorescence decay were made at the wavelengths of the peaks of the emission bands at room temperature, at 5180, 5327, and 5534 Å for the glass and at 4915, 5150, and 5405 Å for the sulfate solution. These are shown in Figures 25 and 26. These photographs are mounted upside down from the position in which they were taken so that time proceeds from right to left. The upper trace is a record of the light emitted by the flash tube with an increase in output corresponding to a downward deflection and is the result of the superposition of several traces. Several exposures were made on each photograph, the only change being made from one exposure to the next being the vertical gain of the lower beam which displays the fluorescent light signal. The gains employed for the lower beam are listed at the bottoms of the figures.

Comparing the two sets of traces makes the faster decay time of the fluorescence in the sulfate solution very evident and, in fact, while it was possible to determine the decay rate directly from these photographs for the glass, the sulfate solution required the use of the technique employed in measuring the induced absorption decay: delaying the sweep and expanding a portion of the decay curve after the pump lamp has cut off. Figure 27 illustrates this process. Since the decay rate measurements were performed an appreciable time after the pump lamp had cut off, no short-lived second component of the fluorescence decay such as that observed by Billington[10] is expected to be detectable. The decay should be a pure exponential and this was verified by plotting log (intensity) versus time. This is shown in Figure 28 for the glass and Figure 29 for the sulfate. The decay constant for the glass is 458 μsec which is in good agreement with the induced absorption decay measurement of 429 μsec. The agreement between the decay constants of the fluorescence and induced absorption in the sulfate solution is much poorer, being 13.8 and 52 μsec, respectively, but this is due to the inaccuracy of the induced absorption measurement.

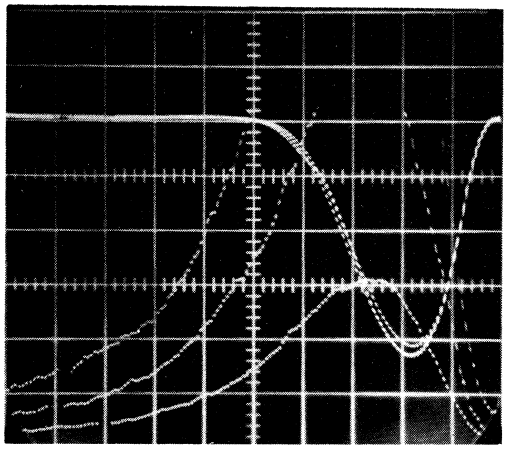

(a)

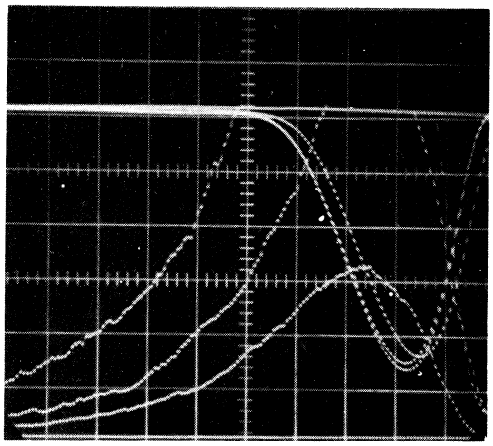

(c)

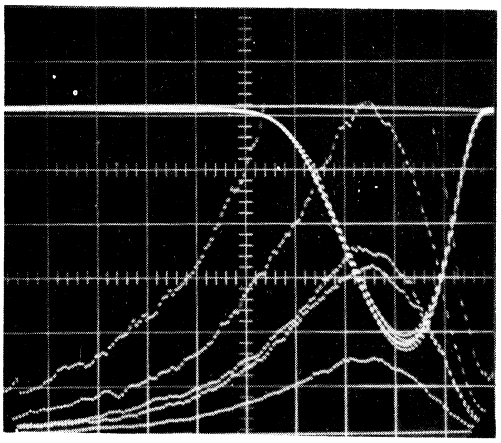

(b)

Figure 25. Time-Resolved Fluorescence for Uranyl Glass.

(a) 5180 Å, lower scales are 5, 2, 1 V/div.
(b) 5327 Å, lower scales are 5, 2, 1 V/div.
(c) 5534 Å, lower scales are 5, 2, 2, 1, 1/2 V/div.

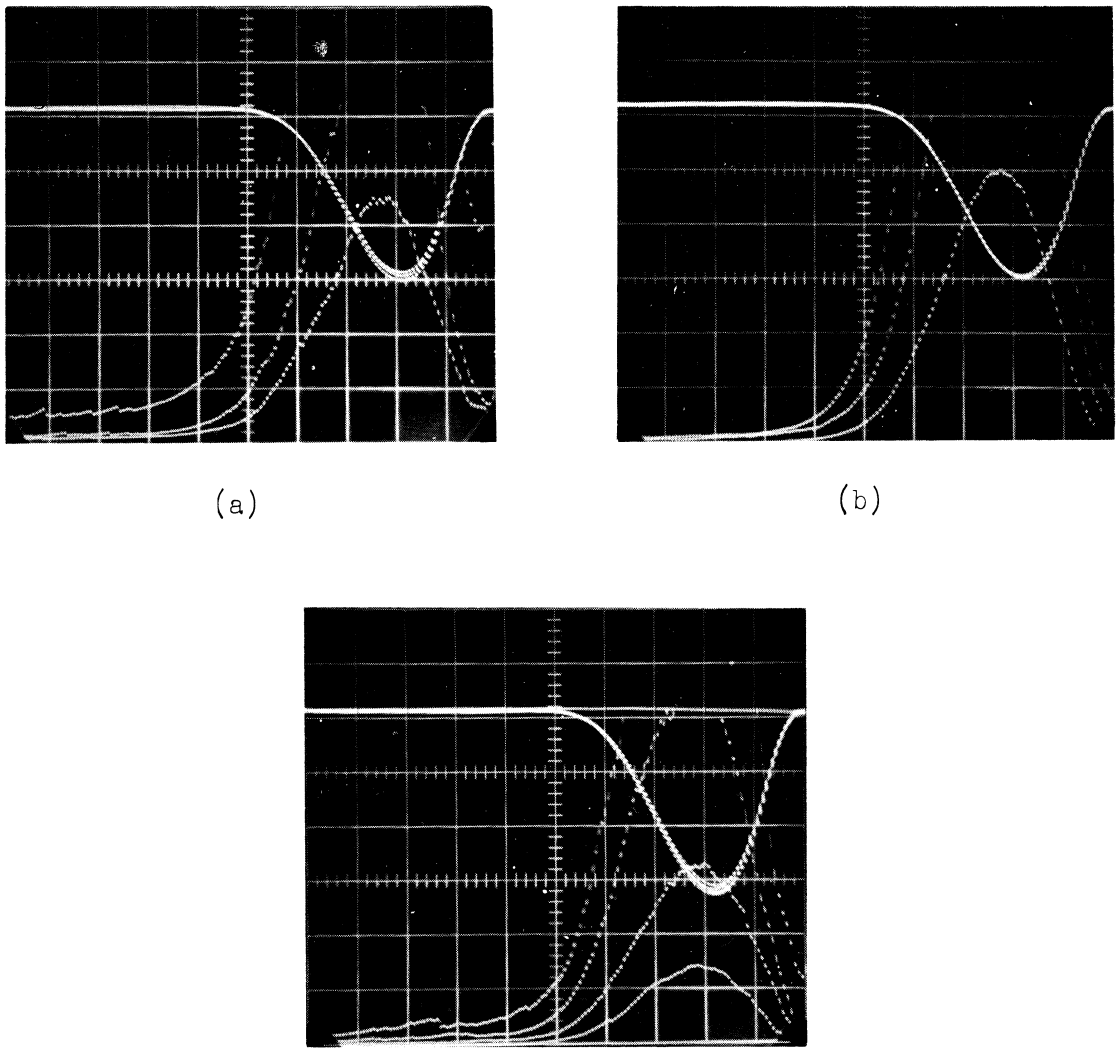

Figure 26. Time-Resolved Fluorescence for UO_2SO_4 in H_2SO_4 Solution.

(a) 4915 Å, lower scales are 5, 2, 1 V/div.
(b) 5150 Å, lower scales are 5, 2, 1 V/div.
(c) 5405 Å, lower scales are 5, 2, 1, 1/2 V/div.

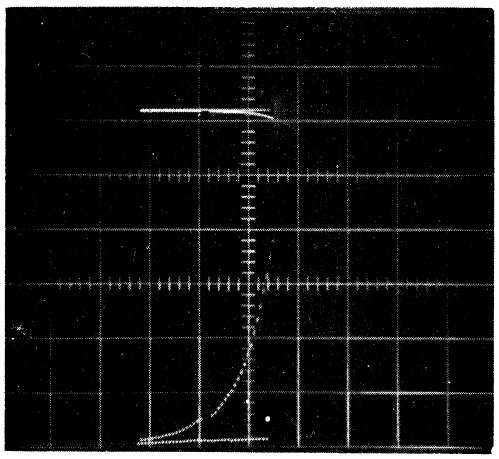

(a)

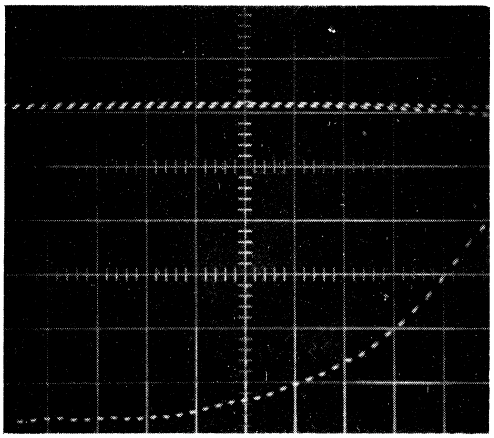

(b)

Figure 27. Fluorescence Decay Measurement for UO_2SO_4 in H_2SO_4 Solution.

(a) Strobe operation showing region to be expanded.
(b) Expanded sweep, 0.05 msec./div.

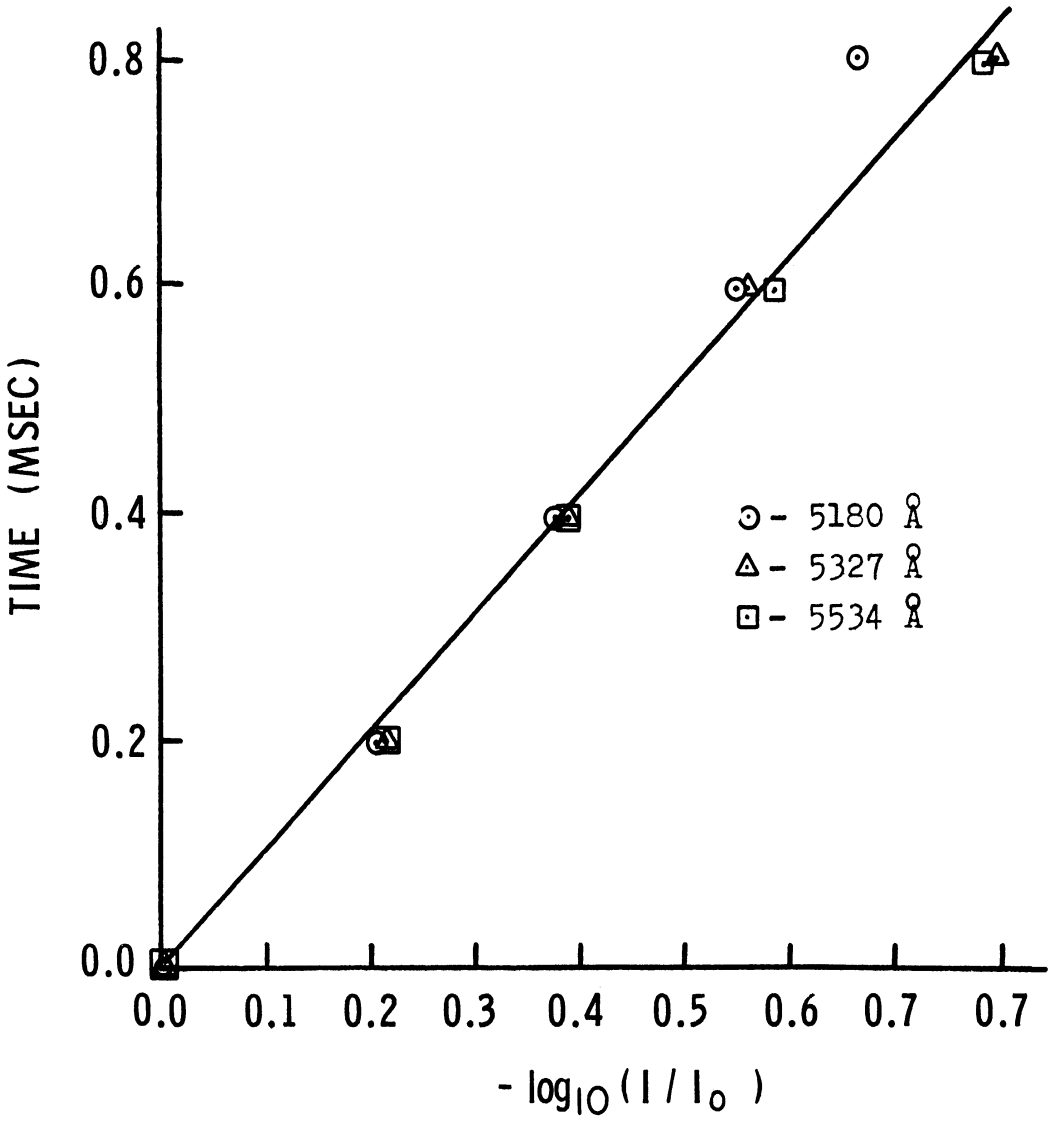

Figure 28. Fluorescence Decay for Uranyl Glass.

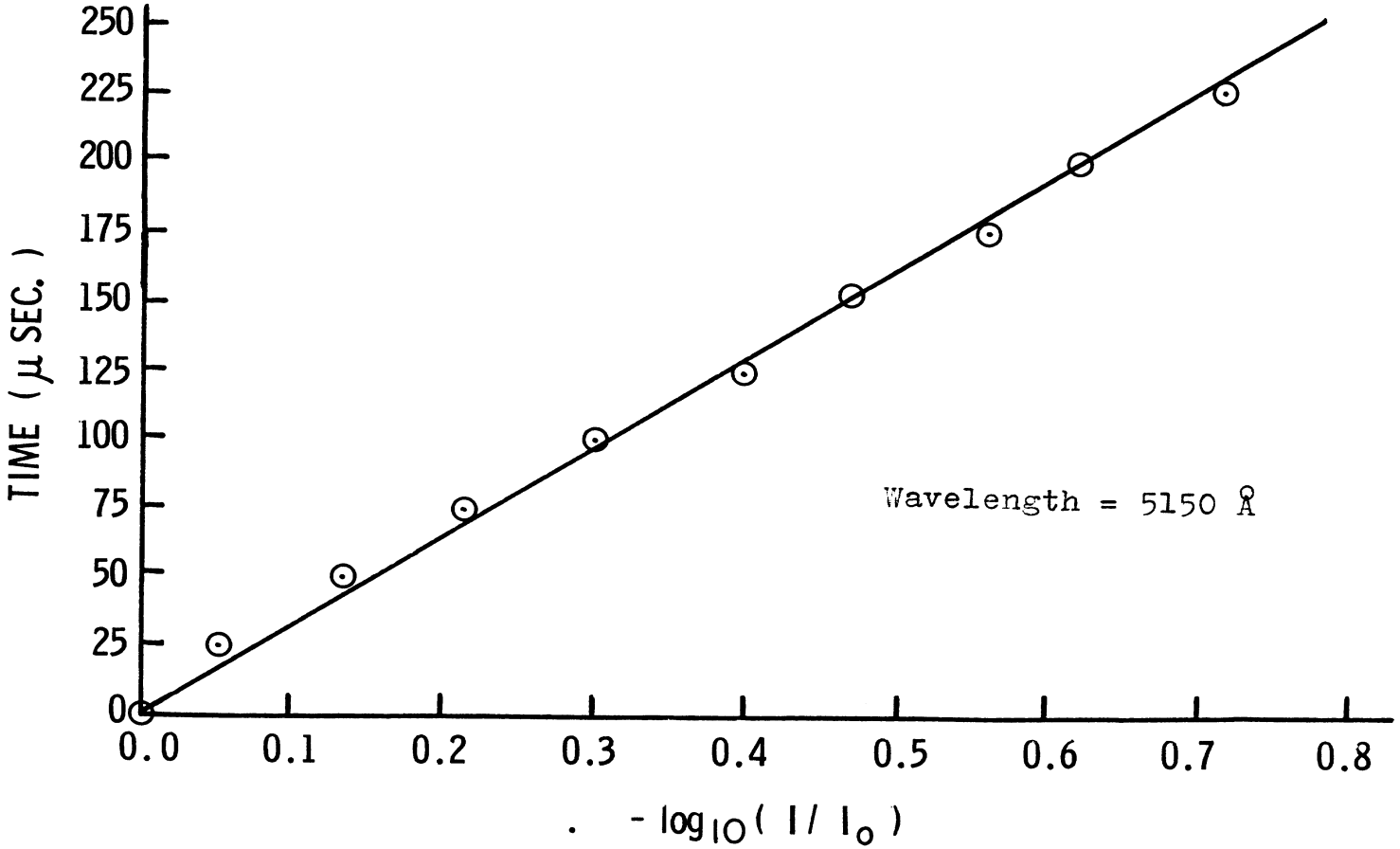

Figure 29. Fluorescence Decay for UO_2SO_4 in H_2SO_4 Solution.

In order to establish whether or not there could be any appreciable population of the uranyl ions in the excited vibrational states of the first excited electronic state, the fluorescence spectrum of polycrystalline uranyl sulfate trihydrate was recorded at 77°K on Kodak Pan-X film using the 1.5 meter B & L spectrograph. The first fluorescence spectrum was recorded using the DC xenon arc as the exciting source and the second using the xenon flash lamp. In both cases the exciting light was filtered using the Corning No. 5-57 filter. The microdensitometer tracings of these spectra are shown in Figure 30. There were, of course, no differences between the spectra which indicates that, despite the higher transition probability from the ground state to the v + 1 level of the first excited electronic level (as evidenced by the absorption spectrum), the population of this state is so low during the time the sample is pumped with the flash lamp that its fluorescence is negligible.

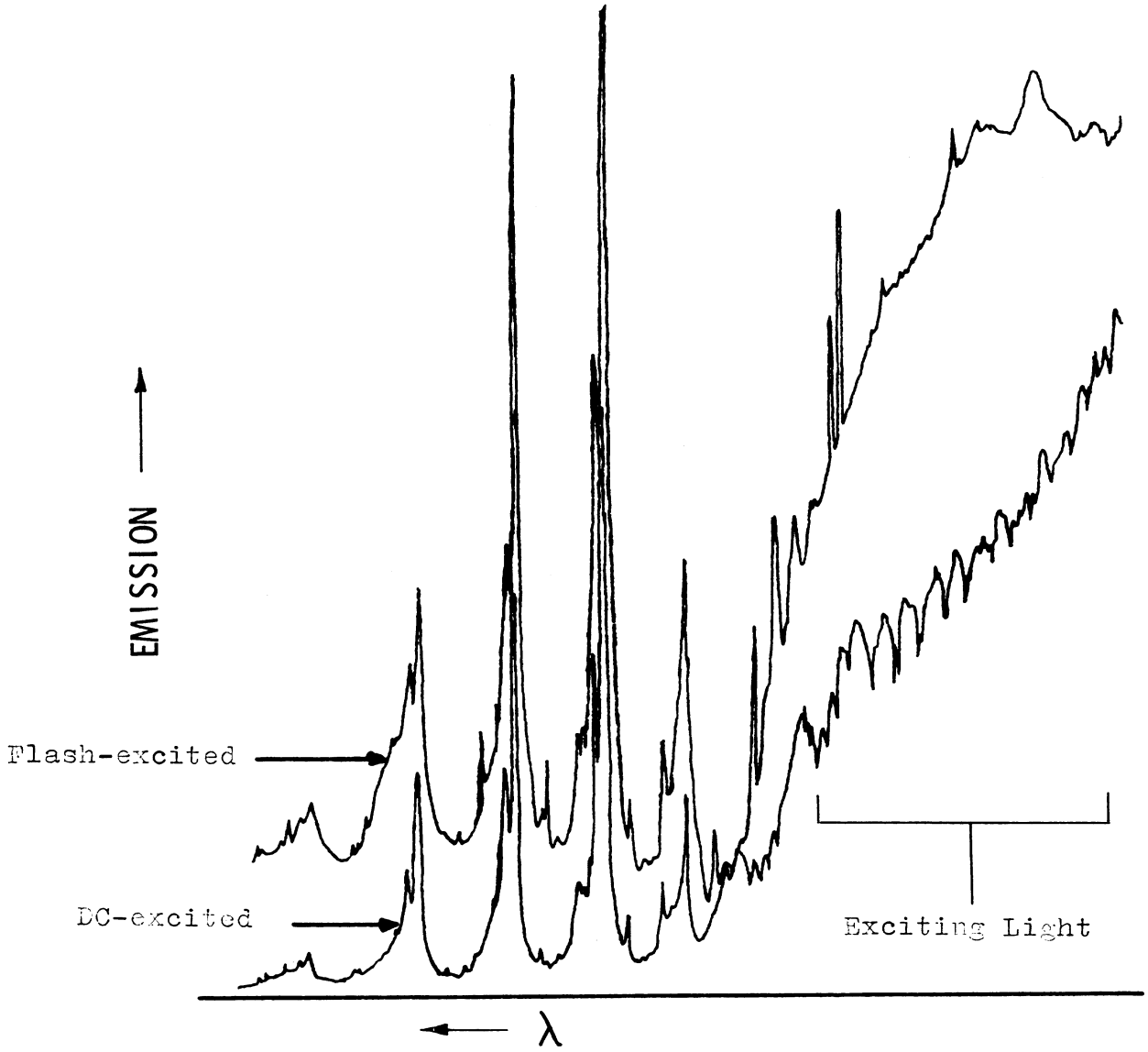

Figure 30. DC- and Flash-Excited Fluorescence of $UO_2SO_4 \cdot 3H_2O$, 77°K.

F. ULTRAVIOLET ABSORPTION SPECTRA OF URANYL SULFATE SOLUTION AND URANYL PHOSPHATE SOLUTION

The absorption spectra of a solution of uranyl sulfate in concentrated sulphuric acid (2.77×10^{-4} gm/ml) and uranyl phosphate in 80% phosphoric acid (4.66×10^{-4} gm UO_2CO_3/ml) were taken in a 10-mm path length cell on a Cary Model 15 spectrophotometer in the region from 3000 to 1900 Å using the pure acids as references. The acids themselves were also run using air as a reference to establish how good their transmission was in this region and therefore how good the resolution of the spectra would be. The sulphuric acid did not show any appreciable absorption above 1900 Å so the resolution should be near that of the manufacturers ratings (0.3 cm^{-1}). The phosphoric acid, however, is not well suited for use in cells with such a long path length since by 2300 Å it has an optical density of 0.5 and this rises to about 0.75 at 1900 Å. Unfortunately, shorter path length cells were not available so that the resolution in the phosphate solution is poor below 2400 Å. The results of these measurements are presented in Figures 31 and 32 for the sulfate and Figure 34 for the phosphate.

The results for the sulfate are different from those of previous authors, notably Henri and Landau,[11] Ahrland,[12] and McGlynn and Smith,[13] in that this ultraviolet absorption band is shown to have a definite upper limit and its peak lies at 2200 Å. There are also two longer wavelength shoulders at 2600 Å and 2830 Å which are barely discernible on the tracings and are very apparent only if the wavelength scale is greatly compressed.

The phosphate spectrum shows no such maximum and this is probably due to the poor transmission of the phosphoric acid in this region. In fact, the same behavior, i.e., the indicated absorbance of the sample monotonically becoming greater above 2200 Å was also observed in the case of the sulfate when the same experiment was run on a Cary Model 11 spectrophotometer which had a range of usefullness limited to 2300 Å. This behavior seems to be linked with the performance of the machine when the source intensity drops to too low a value so that scattered light becomes important. Instead of two longer wavelength bands as in the sulfate, only one is present at about 2500 Å but the relative intensities of the bands may be shifted sufficiently so that the longer wavelength band, which was marginal to begin with, is no longer discernible.

Table IX shows the molar extinction coefficients and absorption cross-sections of these bands for the sulfate and the phosphate. The oscillator strength of this higher system (treated as a single band) is much larger than for the visible system but is not as large as that derived by Rabinowitch and Belford.[14] The oscillator strength calculated using the data obtained here for the entire UV system obtained by Simpson's rule integration of the absorption curve is 1.77×10^{-2} in contrast to the previous authors' value of 7.89×10^{-2}. Assuming that the degeneracy of the upper state may be regarded as the

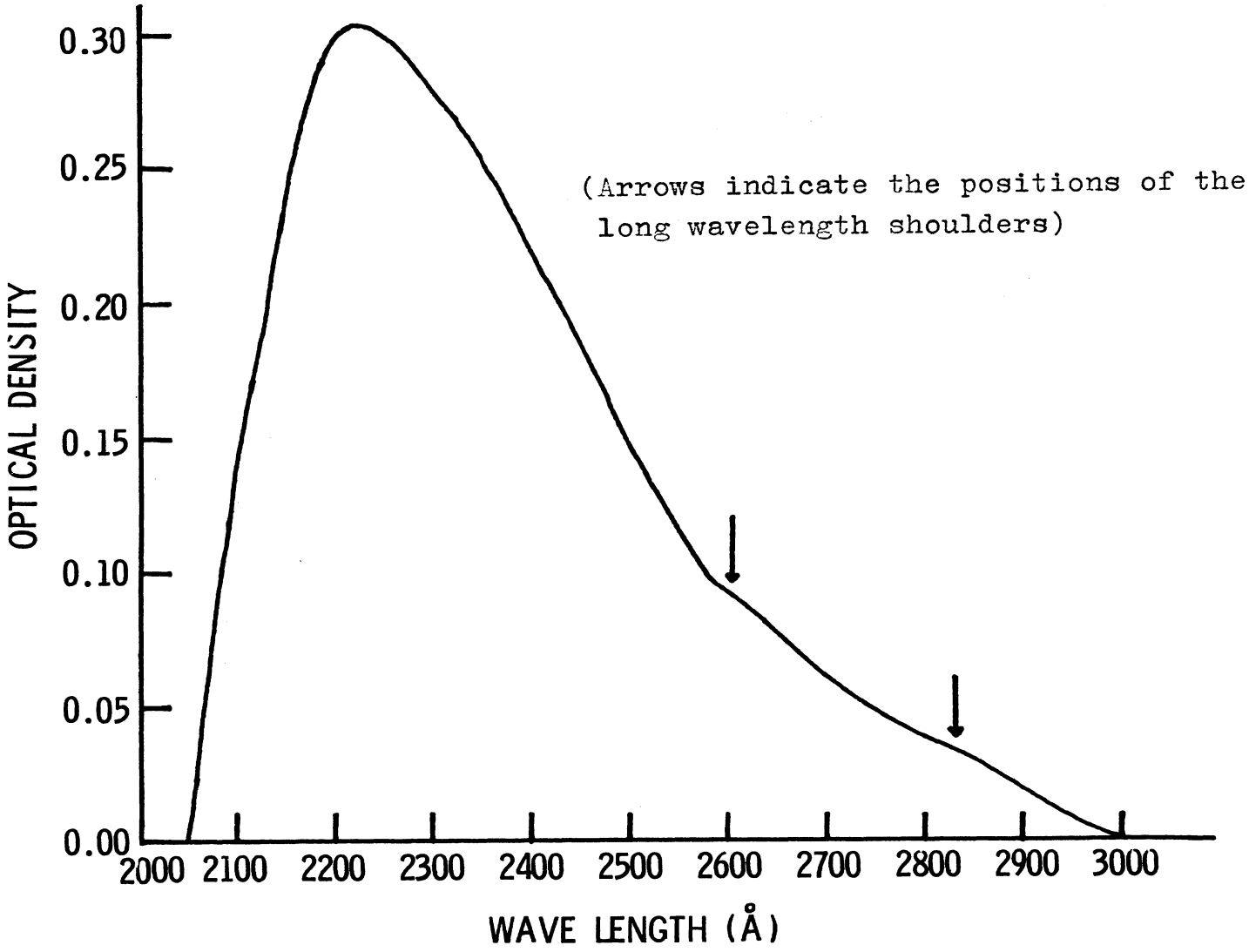

Figure 31. Ultraviolet Absorption Spectrum of UO_2SO_4 in H_2SO_4 Solution (versus wavelength).

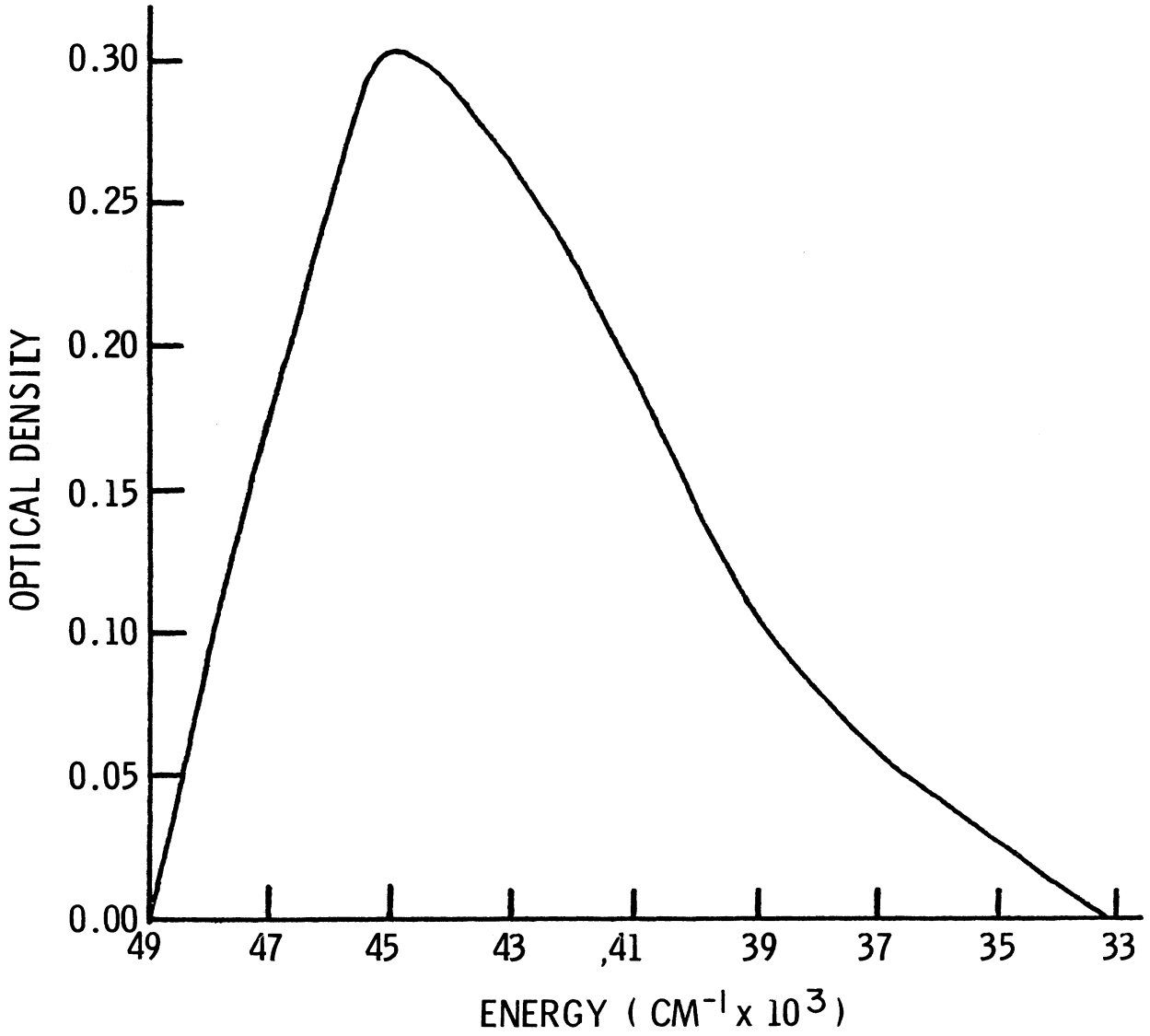

Figure 32. Ultraviolet Absorption Spectrum of UO_2SO_4 in H_2SO_4 Solution (versus energy).

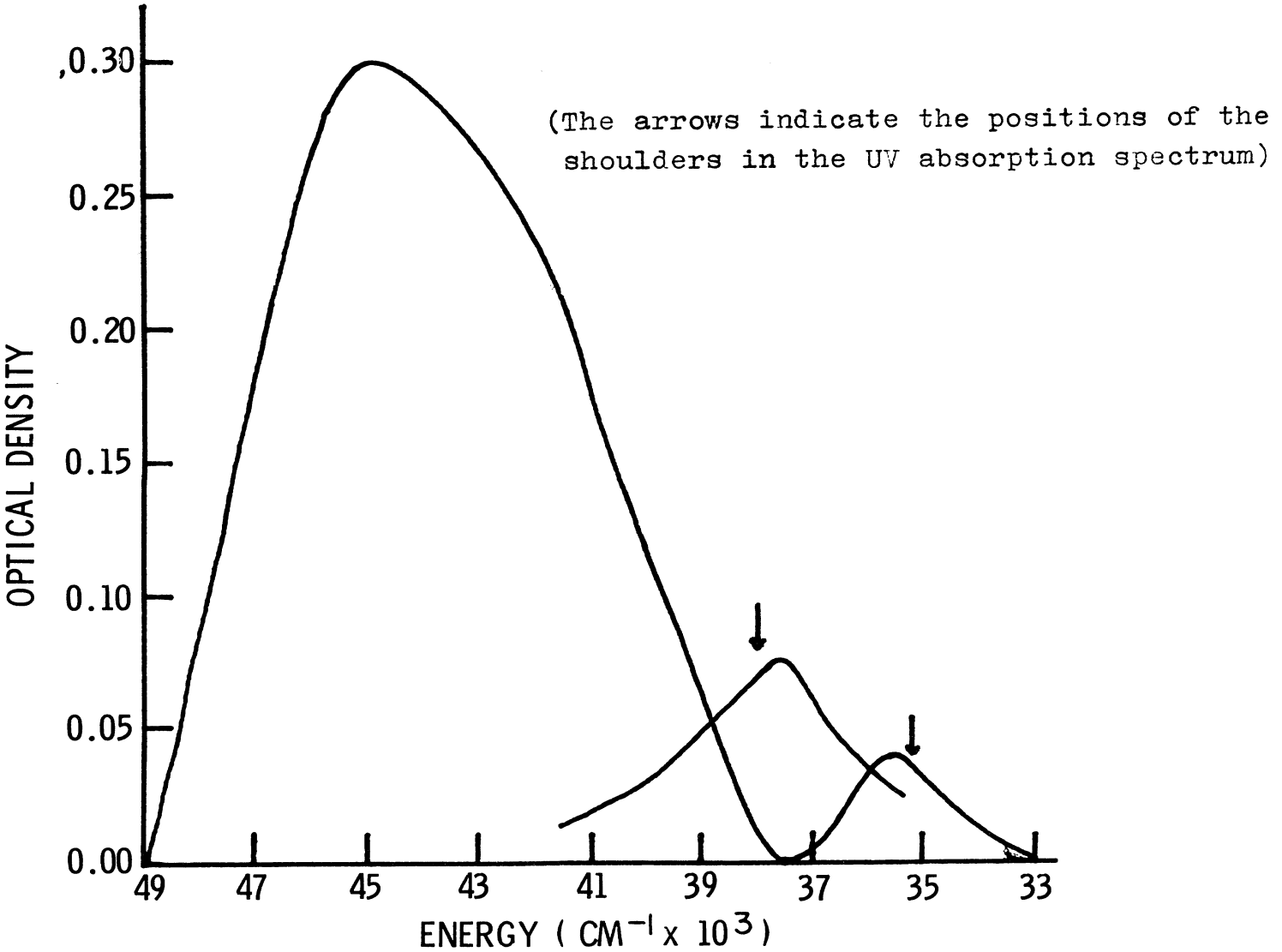

Figure 33. Resolution of the Ultraviolet Absorption Spectrum of UO_2SO_4 in H_2SO_4 Solution by Subtraction of the Induced Absorption Contour.

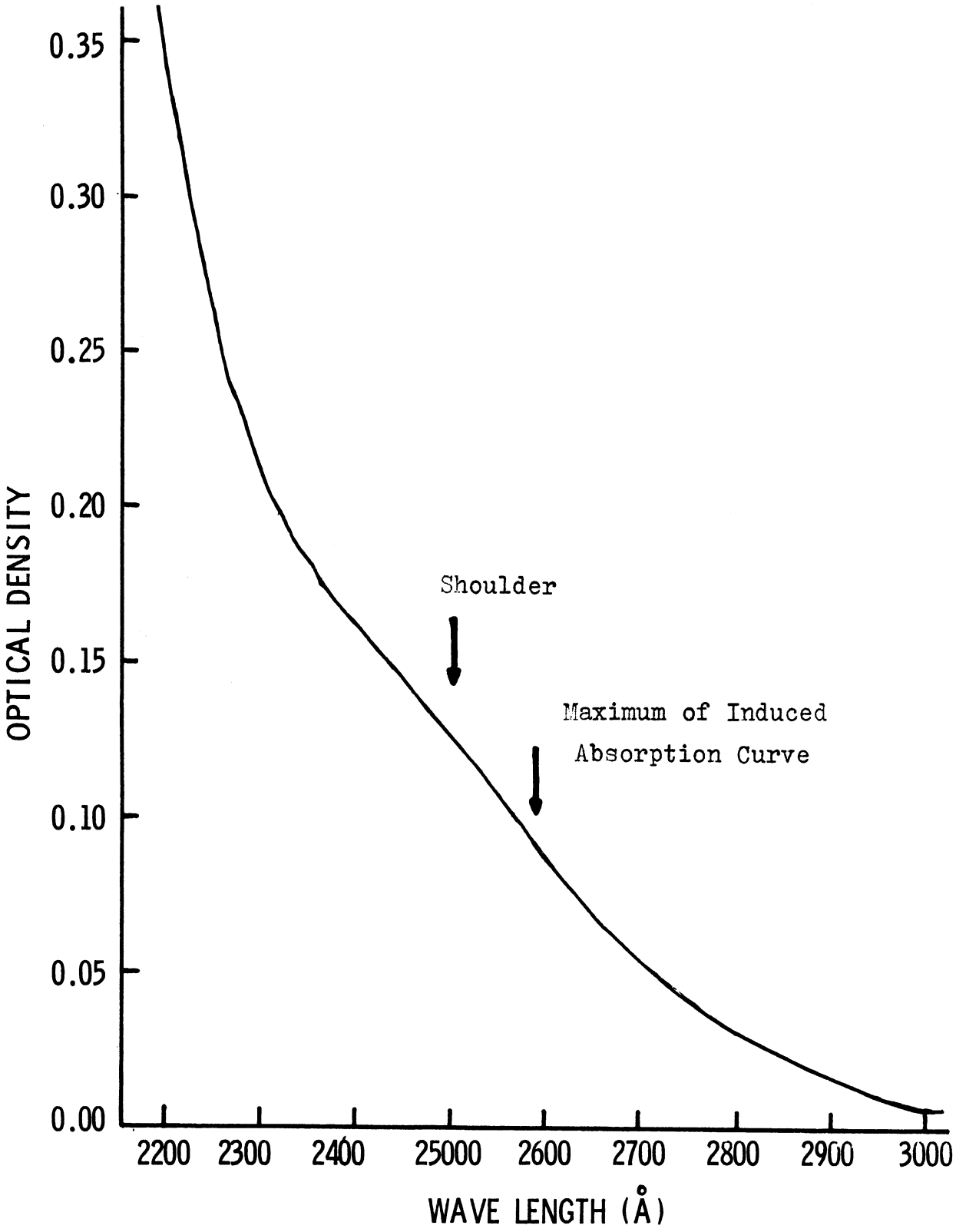

Figure 34. Ultraviolet Absorption Spectrum of UO_2HPO_4 in H_3PO_4 Solution Showing the Relationship Between the Long Wavelength Shoulder and the Induced Absorption Maximum.

TABLE IX

ULTRAVIOLET ABSORPTION BANDS OF URANYL SULFATE AND PHOSPHATE SOLUTIONS

	Uranyl Sulfate		Uranyl Phosphate	
λ(Å)	ϵ	σ(cm^2 x 10^{-23})	ϵ	σ(cm^2 x 10^{-23})
2200	500	82.5		
2600	146	24.1		
2830	48	7.9		
2500			117	18.8

same as the ground state, the mean intrinsic lifetime for relaxation from the UV system to the ground state is 4.2×10^{-8} seconds, in contrast with the previous authors' value of 1.63×10^{-8} seconds.

If the initial state of the fluorescence is the initial state of the induced absorption, as the close correspondence between the decay rates of the fluorescence in uranyl glass and uranyl sulfate solution and the decay rates of the induced absorption in the corresponding media seems to indicate, then the sum of the resonance fluorescence energy and the energy of the peak of the induced absorption band should give the energy separation of the higher excited state from the ground state of the uranyl ion. In the case of the uranyl sulfate, the resonance energy is 20,320 cm^{-1} and the peak of the induced absorption is at 17,240 cm^{-1} (5800 Å) so the energy sum is 37,560 cm^{-1}, i.e., there may be an absorption at 2660 Å. In the case of the uranyl phosphate, the resonance energy is 19,860 cm^{-1} and the peak of the induced absorption is at about 17,540 cm^{-1} (5700 Å) so the energy sum is 37,400 cm^{-1} and the expected absorption should occur at 2670 Å.

The agreement between the calculated positions of the previous bands and the positions of the shoulders in the ultraviolet absorption spectrum is quite satisfactory. It indicates that the transition probabilities for transitions from the first excited electronic state to the UV states must be quite different from those for transitions from the ground state to the UV states since the profile of the induced absorption does not all follow the profile of the upper band as given by the ordinary absorption spectrum. The induced absorption "eats a hole" in the UV band profile in the case of the sulfate and shows that the UV band must indeed be resolved into three bands as the shoulders would indicate. This is illustrated in Figure 33 which was obtained by adding 20, 230 cm^{-1} to all the frequencies of the induced absorption profile, normalizing the curve thus obtained to agree with that of the ultraviolet absorption curve at 37,470 cm^{-1} (the maximum of the curve), and then subtracting the

resulting curve from the ultraviolet absorption curve. This method of analysis assumes, of course, that the Frank-Condon profile of the UV level appears the same whether the transition to it occurs from the ground state or from the resonance level, i.e., that there is no great shift in the internuclear distance between the minimum of the potential curve in the first excited state and the minimum of the potential curve in the ground state and that these two have the same shape. This assumption is not too ill-founded on experimental evidence. The ordinary absorption spectrum shows that there must be some expansion of the uranyl molecule in the first excited electronic state since the $0 \leftarrow 0$ band is less intense than the $1 \leftarrow 0$ or $2 \leftarrow 0$ bands. The $2 \leftarrow 0$ band is more intense than the following bands (of the same electronic state) indicating that the minima of the two potential curves cannot be too different. It is therefore reasonable to assume that the maxima of the absorption curves obtained may be slightly different but not enough to cause confusion as on which of the three UV levels the induced transition terminates. The remaining portion of the UV bands of wavelengths longer than 2700 Å is resolved into a band whose peak agrees with the shoulder seen in the ultraviolet absorption curve at 2830 Å while the profile of the band to shorter wavelengths remains nearly the same but assumes a more symmetric shape. A few photoelectric measurements were conducted on uranyl sulfate solution at wavelengths shorter than 3700 Å to see if there was any indication of a higher induced absorption band but the results were entirely negative. Experiments conducted elsewhere[15] have shown that no absorption exists at the neodymium laser wavelength in uranyl glass which would correspond to a ground state to excited state separation 27,360 cm^{-1} or an ultraviolet absorption at 3650 Å which adds additional confirmation to this assignment.

Thus it seems well established that, unless by some coincidence there is another level at 38,000 cm^{-1} which is not detectable from the ground state, the induced absorption has as its initial level the resonance level and as its terminal level the middle one of the three ultraviolet levels. Figure 35 shows the relative positions and oscillator strengths of the transitions discussed here.

The oscillator strengths of the three main transitions shown in Figure 35, coupled with previous results on the absorption and fluorescence spectra of uranyl compounds, permit some conclusions to be drawn concerning the nature of the states involved. The ground state of the uranyl ion is almost certainly $^1\Sigma_g^+$ (see Appendix I) and the agreement between the fluorescence and absorption resonance line frequency measurements (Dieke and Duncan[3]) precludes the possibility of the transition from the ground state to the first excited electronic state being vibronically induced so that the transition is Laporte-allowed and the first electronic state must be ungerade. The intensity of this transition, however, is so low that it must be forbidden on some grounds, the most likely possibility being that the state is a triplet and the transition is spin-forbidden. Accordingly, the first excited electronic state may be designated ^3X_u, where X = Π, Δ, Φ, Γ as no low-lying $^3\Sigma$ states are to be expected. (See Appendix I.)

The oscillator strength of the transition from the ground state to the center UV level is three orders of magnitude higher than that of the first electronic transition so it is unlikely that it is forbidden overall, i.e., electronic x vibrational, on either spin or Laporte grounds. However, the oscillator strength is still not high enough to correspond to a fully allowed electronic transition. One explanation for this situation would be that the transition is vibronically allowed, and "borrows" intensity from a $^1\Pi_u$ lying some 7000 cm^{-1} above it. The electronic state is presumed to be a singlet and gerade, the only low-lying possibilities for these being the $^1\Sigma_g$, $^1\Pi_g$, and $^1\Delta_g$ derived from the configuration $(1\pi)^3$ $(1\delta_g)^1$. Each of these states, coupled with the proper vibration of the uranyl ion, can give rise to a vibronic level whose symmetry is $^1\Pi_u$: all of them coupled with a π_u vibration and only the $^1\Pi_g$ coupled with the σ_u vibration.

Since the first excited electronic state is assumed to be an ungerade triplet (or a component of one), a transition from it to a $^1\Pi_u$ vibronic state would be forbidden on the basis of both the Laporte rule and spin selection rule. Accordingly, it would be extremely weak. However, if the induced absorption transition terminates on the presumed pure electronic level, then the transition is ^3X_u (or one component of it)$\rightarrow Y_g$ and is forbidden only on spin grounds and would be of comparable intensity to the transition from the ground state to the first excited electronic state. This agrees with the experimental result. There should, accordingly, be a shift in the apparent position of this center level depending on whether the transition to it occurs from the ground state or from the resonance level. The measurements made in this study are not

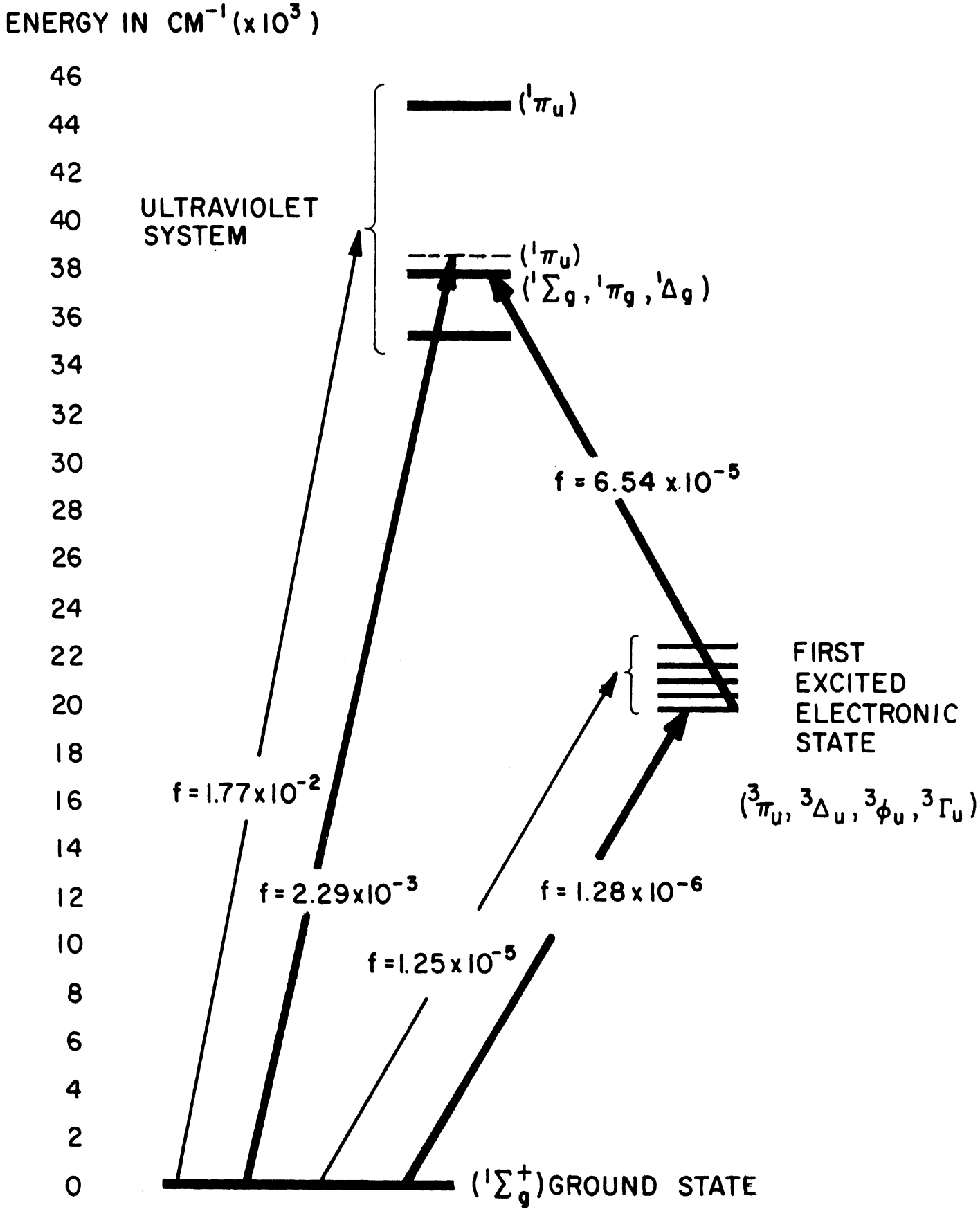

Figure 35. Principle Transitions Observed for the Uranyl Ion.

accurate enough to establish this difference but it should be possible to test these assignments with crystal spectra. As mentioned by McGlyan and Smith[13] (see Appendix I), the lowest excited electronic level shows no Zeeman splitting and probably corresponds to a $^3\Delta_1$ state.

APPENDIX I

DISCUSSION OF THE MOLECULAR ORBITAL REPRESENTATIONS FOR THE URANYL ION AND THE ASSIGNMENT OF TERM LEVEL DESIGNATIONS TO THE LOWER URANYL ION LEVELS

The symmetry of the uranyl ion, ignoring the presence of the secondary ligands, is $D_{\infty h}$ with the two oxygen nuclei and the uranium nucleus colinear and the oxygen nuclei equally displaced from the uranium nucleus. This configuration has been verified by x-ray diffraction in several salts.[16,17] The symmetry operations of the molecule are E (the identity), C_φ (rotation around the internuclear axis through an angle φ), σ_v (reflection through any plane containing the internuclear axis), i (inversion through the uranium nucleus), iC_φ (any improper rotation around the internuclear axis), and $i\sigma_v = C_2$ (rotation through the angle π about any axis perpendicular to the internuclear axis and intersecting it at the uranium nucleus). The character table for this symmetry group is given in Table X. Because of the symmetry about the internuclear axis, the projection of the angular momentum along this axis is a good quantum number, designated Ω, and, in the absence of spin-orbit coupling, so are the projections of the orbital angular momentum, designated Λ, and the spin, designated Σ. Such a state is specified in the spectroscopic notation as $^{2\Sigma+1}\Lambda_{\Omega,u \text{ or } g}$ and it is useful to find the correspondence between these states and the representations listed in Table X. Such a correspondence has been given by Rabinowitch and Belford[14] but there is some confusion in their table regarding the assignments of the $^3\Sigma$ states and the $^3\Pi_0$ and $^3\Pi_2$, $^3\Delta_1$, and $^3\Delta_3$, etc., which they list in the form $^3\Pi_{0,2}$ under one representation and as $^3\Pi_{2,0}$ under another.

TABLE X

THE CHARACTER TABLE FOR $D_{\infty h}$

(After 14)

$D_{\infty h}$	E	C_φ	σ_v	i	iC_φ	C_2	
$A_{1g}(\sigma_g^+)$	1	1	1	1	1	1	z^2, $x^2 + y^2$
$A_{1u}(\sigma_u^-)$	1	1	1	-1	-1	-1	
$A_{2g}(\sigma_g^-)$	1	1	-1	1	1	-1	I_z
$A_{2u}(\sigma_u^+)$	1	1	-1	-1	-1	1	z
$E_{1g}(\pi_g)$	2	$2\cos\varphi$	0	2	$2\cos\varphi$	0	xz,yz,I_x,I_y
$E_{1u}(\pi_u)$	2	$2\cos\varphi$	0	-2	$-2\cos\varphi$	0	x,y
$E_{2g}(\delta_g)$	2	$2\cos2\varphi$	0	2	$2\cos2\varphi$	0	x^2-y^2, xy
$E_{2u}(\delta_u)$	2	$2\cos2\varphi$	0	-2	$-2\cos2\varphi$	0	
$E_{3g}(\varphi_g)$	2	$2\cos3\varphi$	0	2	$2\cos3\varphi$	0	
$E_{3u}(\varphi_u)$	2	$2\cos3\varphi$	0	-2	$-2\cos3\varphi$	0	

The assignment of spectroscopic terms to the representations is very easy since the representations are already characterized by Ω. For instance, the representations $A_{1g} \cdots A_{2u}$ which have constant characters under C_φ must correspond to terms with $\Omega = 0$ and these can only be $^1\Sigma$, $^3\Pi_0$ or $^3\Sigma_0$. Similarly, the E_1 representations must have $\Omega = 1$ and therefore correspond to $^3\Sigma_1$, $^3\Pi_1$, or $^3\Delta_1$. Table XI gives the representations and the spectroscopic terms which are appropriate to them. The assignment of the triplets to the representations can be made more rigorous by observing that the direct product space of a singlet with that representation which transforms like a rotation about the z-axis is reducible to the representations of the corresponding triplet state and the same value of Ω. Similarly, the product space of the direct product of the singlet representation with the representation which transforms like a rotation about the x- or y-axis is reducible into the representations of the triplet state whose Ω value is 1 removed from the Ω value of the singlet state. From Table X, these representations are A_{2g} and E_{1g}, respectively. For example, the $\Omega = 0$ component is corresponding to the $^1\Sigma_g^+$ obtained by the direct product $A_{2g} \times A_{1g}$ which is, of course, A_{2g} so that the term $^3\Sigma_{0g}^+$ is assigned to A_{2g}.

TABLE XI

ASSIGNMENT OF TERMS FOR A MOLECULE OF SYMMETRY $D_{\infty h}$

Representation	Singlets	Triplets
A_{1g}	$^1\Sigma_g^+$	$^3\Pi_{0g}$ $^3\Sigma_{0g}^-$
A_{2g}	$^1\Sigma_u^-$	$^3\Pi_{0u}^-$ $^3\Sigma_{0u}^+$
A_{2g}	$^1\Sigma_g^-$	$^3\Pi_{0g}^-$ $^3\Sigma_{0g}^+$
A_{2u}	$^1\Sigma_u^+$	$^3\Pi_{0u}^+$ $^3\Sigma_{0u}^-$
E_{1g}	$^1\Pi_g$	$^3\Pi_{1g}$ $^3\Sigma_{1g}$ $^3\Delta_{1g}$
E_{1u}	$^1\Pi_u$	$^3\Pi_{1u}$ $^3\Sigma_{1u}$ $^3\Delta_{1u}$
E_{2g}	$^1\Delta_g$	$^3\Pi_{2g}$ $^3\Delta_{2g}$ $^3\Phi_{2g}$
E_{2u}	$^1\Delta_u$	$^3\Pi_{2u}$ $^3\Delta_{2u}$ $^3\Phi_{2u}$
E_{3g}	$^1\Phi_g$	$^3\Delta_{3g}$ $^3\Phi_{3g}$
E_{3u}	$^1\Phi_u$	$^3\Delta_{3u}$ $^3\Phi_{3u}$

A complete discussion of the attempts to explain the visible and ultraviolet absorption and the visible fluorescence spectra for the uranyl ion is given by Rabinowitch and Belford (op. cit.) and only a brief review of their work will be given here. The molecular orbitals are to be constructed from linear combinations of the unoccupied 5f, 6d, and 7s orbitals of the uranium and the occupied 2s and 2p orbitals of the oxygens. The representations to which these orbitals belong are listed in Table XII where it is assumed that the z-axis of the atomic wave functions is coincident with the internuclear axis.

TABLE XII

ASSIGNMENT OF THE URANIUM AND OXYGEN ORBITALS TO THE REPRESENTATIONS OF THE $D_{\infty h}$ GROUP

Representation	Uranium Orbitals	Oxygen Orbitals
$A_{1g}(\sigma_g^+)$	$7s$, $6d_0$	$2s$
$A_{1u}(\sigma_u^-)$	$5f_0$	$2p_0$
$A_{2g}(\sigma_g^-)$		
$A_{2u}(\sigma_u^+)$		
$E_{1g}(\pi_g)$	$6d_1$, $6d_{-1}$	
$E_{1u}(\pi_u)$	$5f_1$, $5f_{-1}$	$2p_1$, $2p_{-1}$
$E_{2g}(\delta_g)$	$6d_1$, $6d_{-1}$	
$E_{2u}(\delta_u)$	$5f_1$, $5f_{-1}$	
$E_{3g}(\varphi_g)$		
$E_{3u}(\varphi_u)$	$5f_3$, $5f_{-3}$	

The symmetry for the oxygen nuclei alone is also $D_{\infty h}$ so the only linear combinations of these which preserve this symmetry are permissable. These are listed in Table XIII. The designation $2p_0 + 2p_0$ means a $2p_0$ orbital centered on oxygen nucleus (1) and one centered on oxygen nucleus (2) and the sense of the z-axis of these two wave functions being the same along the internuclear axis. The designation $2p_0 - 2p_0$ means that the senses of the two z-axis are reversed (or, in the case where the wave functions are gerade, the sign of one of the wave functions has been reversed).

TABLE XIII

ASSIGNMENT OF THE OXYGEN LINEAR COMBINATIONS TO THE REPRESENTATIONS OF THE $D_{\infty h}$ GROUP

Representation	Oxygen Linear Combinations
$A_{1g}(\sigma_g^+)$	$2s + 2s,\ 2p_0 - 2p_0$
$A_{1u}(\sigma_u^-)$	$2s - 2s,\ 2p_0 + 2p_0$
$A_{2g}(\sigma_g^-)$	
$A_{2u}(\sigma_u^+)$	
$E_{1g}(\pi_g)$	$2p_1 - 2p_1,\ 2p_{-1}-2p_{-1}$
$E_{1u}(\pi_u)$	$2p_1 + 2p_1,\ 2p_{-1}+2p_{-1}$

There are, accordingly, $4\sigma_g^+$ states possible, constructed of linear combinations of 7s, $6d_0$, 2s + 2s, and $2p_0 - 2p_0$, $3\sigma_u^-$ states constructed of linear combinations of $5f_0$, 2s - 2s, $2p_0 + 2p_0$, $2\pi_g$ states constructed of linear combinations of $6d_1$ and $2p_1 - 2p_1$ or $6d_{-1}$ and $2p_{-1}-2p_{-1}$, and $2\pi_u$ states constructed of linear combinations of $5f_1$ and $2p_1 + 2p_1$ or $5f_{-1}$ and $2p_{-1}+2p_{-1}$.

To construct the molecular ion $(OUO)^{+2}$, 16 electrons must be put into the above one-electron orbitals and Rabinowitch and Belford give the ground state configuration as:

$$(\sigma_u)^2(\sigma_g)^2(\pi_u)^4(\pi_g)^4 .$$

This does, of course, account for only 12 electrons, not 16, but they have implicitely assumed by the use of hybrid sp orbitals that there are two occupied σ orbitals below all of the ones above. (These can be obtained by taking the symmetric and antisymmetric linear combinations of the orbitals which these authors designate as sp(I) and sp(II).) The complete configuration is:

$$(1\sigma_u)^2(1\sigma_g)^2(2\sigma_u)^2(2\sigma_g)^2(1\pi_u)^4(1\pi_g)^4 .$$

This configuration gives a $^1\Sigma_g^+$ state as the ground state which agrees with the apparent diamagnetism of the ground state. The excited configurations are assumed by these authors to rank in energy as:

$$(1\pi_g)^4 < (1\pi_g)^3(1\varphi_u)^1 \sim (1\pi_g)^3(1\delta_u)^1 < (1\pi_g)^3(1\delta_g)^1 .$$

The spectroscopic terms which can arise from each of these configurations are:

$$(1\pi_g)^4 \quad : \quad {}^1\Sigma_g^+$$

$$(1\pi_g)^3(1\varphi_u) \quad : \quad {}^3\Gamma(5,4,3,)u, {}^1\Gamma_{4u}, {}^3\Delta(3,2,1,)u, {}^1\Delta_{2u}$$

$$(1\pi_g)^3(1\delta_u)^1 \quad : \quad {}^3\Phi(4,3,2)u, {}^1\Phi_{3u}, {}^3\Pi(2,1,0)u, {}^1\Pi_{1u}$$

It is assumed by McGlynn and Smith[13] that the states giving rise to the absorption in the blue are either the components of the ${}^3\Delta_u$ or ${}^3\Pi_u$ since these are spin-forbidden transitions and would most likely have the low transition probabilities observed for these transitions from a ${}^1\Sigma$ ground state. The level which gives rise to the absorption in the ultraviolet is assumed to be ${}^1\Pi_u$ since a fully allowed transition must be present to give the large transition probability observed for this transition. There is, however, conflicting evidence for the nature of the lower levels since the Zeeman splittings do not agree with the lower levels being the three components of a single state. The splitting due to a magnetic field is given by $2|\Lambda + 2\Sigma|\beta\ \mu_o\ H_z$ and the 0, 1, and 2 components of a ${}^3\Pi$ state should split in the ration 1 : 1 : 3 while the 1, 2, and 3 components of a ${}^3\Delta$ state should exhibit no splitting for the 1 component, and a ratio of 1 : 2 for the 2 and 3 components. It has been experimentally observed that only the middle electronic state of the three which are assumed to make up the visible electronic absorption system splits. It is therefore clear that the assignments of these levels is far from complete.

It is of interest to examine the $D_{\infty h}$ double group, not because it applies to the uranyl ion, but because the next actinyl ion, neptunyl, and the second one after that, americyl, must belong to this group. The irreducible representations of this group, because it is infinite, cannot be derived in as simple a manner as those of the finite groups and it is necessary to return to first principles and the full rotation group. (A complete description of the method is given by Heine[18].) The symmetry operations of this double group will be the same as those of the single group with the addition of: $\bar{E}$ (rotation through 2π), $C_\varphi\bar{E}$, $\sigma_v\bar{E}$, $i\bar{E}$, and $iC_\varphi\bar{E}$. (Since C_2 is single-valued, $C_2\bar{E}$ and C_2 are in the same class.)

Consider first the representations having $\Omega = 1/2$. Heine gives as the matrix representing a rotation about the z-axis through an angle φ for a representation having $j = 1/2$ as:

$$D^{(1/2)}(\varphi,z) = \begin{bmatrix} e^{(i/2)\varphi} & 0 \\ 0 & e^{(-i/2)p} \end{bmatrix} \qquad \text{(I-1)}$$

and for a rotation about the y axis through an angle θ as:

$$D^{(1/2)}(\theta,y) = \begin{bmatrix} \cos 1/2\theta & \sin 1/2\theta \\ -\sin 1/2\theta & \cos 1/2\theta \end{bmatrix} \qquad \text{(I-2)}$$

Thus, according to (I-1), the representative for $j = 1/2$ of the rotation C_φ is:

$$\begin{bmatrix} e^{(i/2)\varphi} & 0 \\ 0 & e^{(-i/2)\varphi} \end{bmatrix}$$

and for the rotation $C_\varphi Q$ is:

$$\begin{bmatrix} e^{(i/2)\varphi + i\pi} & 0 \\ 0 & e^{(-i/2)\varphi - i\pi} \end{bmatrix}$$

The characters of these representatives are then:

$$\chi(C_\varphi) = e^{(i/2)\varphi} + e^{(-i/2)\varphi} = 2\cos(\varphi/2)$$

and

$$\chi(C_\varphi Q) = 2\cos(\varphi/2 + \pi) = -2\cos(\varphi/2) \ .$$

The character for $j = 1/2$ for C_2 can be found from (I-2) by observing that the character of C_2 must be independent of the axis about which the rotation is performed as long as it is in the x-y plane so that the y axis is perfectly general, not for the rotation matrix, but for the character. Accordingly, the representative is:

$$\begin{bmatrix} \cos(\pi/2) & \sin(\pi/2) \\ -\sin(\pi/2) & \cos(\pi/2) \end{bmatrix}$$

and

$$\chi(C_2) = 0 \ .$$

For the representation $D^{(3/2)}$, the step-up and step-down matrices are:

$$I_+ = \begin{bmatrix} 0 & 3 \\ 0 & 0 \end{bmatrix} \qquad I_- = \begin{bmatrix} 0 & 0 \\ 3 & 0 \end{bmatrix}$$

so the I_x and the I_y matrices are:

$$I_x = 3/2 \begin{bmatrix} 0 & 1 \\ 1 & 0 \end{bmatrix} \qquad I_y = 3/2i \begin{bmatrix} 0 & 1 \\ -1 & 0 \end{bmatrix}$$

and I_z is

$$I_z = 3/2 \begin{bmatrix} 1 & 0 \\ 0 & -1 \end{bmatrix}$$

Using Heine's equation for the rotation operator for a rotation through an angle α about an axis ξ:

$$\mathcal{G}(\alpha,\xi) = \underline{1} + i\alpha\, \underline{I}\xi + (i\alpha\, \underline{I}\, \xi)^2/2! + \ldots.$$

the representative for $D^{(3/2)}$ for $C\varphi$ may be derived from:

$$D^{(3/2)} = \underline{1} + \sum_{n=1} (i\varphi\, \underline{I}_z)^n/n! \qquad \text{(I-3)}$$

Since $\underline{I}_z^{\,2} = (9/4)\, \underline{1}$, where $\underline{1}$ is the unit matrix, (I-3) may be broken into a sum of even powers of $\underline{I}_z$ and a sum of odd powers:

$$D^{(3/2)} = \underline{1} + \underline{1} \sum_{n=1} ((3i/2)\varphi)^{2n}/(2n)!$$

$$+ \underline{I}_z \sum_{n=0} ((3i/2)\varphi)^{2n+1}/(2n+1)!$$

which reduces to:

$$D^{(3/2)}(\varphi,z) = \begin{bmatrix} e^{(3i/2)\varphi} & 0 \\ 0 & e^{(-3i/2)\varphi} \end{bmatrix} \qquad \text{(I-4)}$$

whose character is $2\cos(3/2)\varphi$. The character for $D^{(3/2)}(C_\varphi \bar{R})$ can similarly be shown to be $-2\cos(3/2)\varphi$ and that for $D^{(3/2)}(C_2)$ to be zero. The complete double group character table is given in Table XIV and the spectroscopic terms belonging to each of the representations in Table XV.

TABLE XIV

THE CHARACTER TABLE FOR THE $D_{\infty h}$ DOUBLE GROUP

$D_{\infty h}$	E	R	C_φ	RC_φ	∇_v	$R\nabla_v$	i	Ri	iC_φ	RiC_φ	C_2
A_{1g}	1	1	1	1	1	1	1	1	1	1	1
A_{1u}	1	1	1	1	1	1	-1	-1	-1	-1	-1
A_{2g}	1	1	1	1	-1	-1	1	1	1	1	-1
A_{2u}	1	1	1	1	-1	-1	-1	-1	-1	-1	-1
E'_{1g}	2	-2	$2\cos \varphi/2$	$-2\cos \varphi/2$	0	0	2	-2	$2\cos \varphi/2$	$-2\cos \varphi/2$	0
E'_{1u}	2	-2	$2\cos \varphi/2$	$-2\cos \varphi/2$	0	0	-2	2	$-2\cos \varphi/2$	$2\cos \varphi/2$	0
E_{1g}	2	2	$2\cos \varphi$	$2\cos \varphi$	0	0	2	2	$2\cos \varphi$	$2\cos \varphi$	0
E_{1u}	2	2	$2\cos \varphi$	$2\cos \varphi$	0	0	-2	-2	$-2\cos \varphi$	$-2\cos \varphi$	0
E'_{2g}	2	-2	$2\cos 3\varphi/2$	$-2\cos 3\varphi/2$	0	0	2	-2	$2\cos 3\varphi/2$	$-2\cos 3\varphi/2$	0
E'_{2u}	2	-2	$2\cos 3\varphi/2$	$-2\cos 3\varphi/2$	0	0	-2	2	$-2\cos 3\varphi/2$	$2\cos 3\varphi/2$	0
E_{2g}	2	2	$2\cos 2\varphi$	$2\cos 2\varphi$	0	0	2	2	$2\cos 2\varphi$	$2\cos 2\varphi$	0
E_{2u}	2	2	$2\cos 2\varphi$	$2\cos 2\varphi$	0	0	-2	-2	$-2\cos 2\varphi$	$-2\cos 2\varphi$	0
E'_{3g}	2	-2	$2\cos 5\varphi/2$	$-2\cos 5\varphi/2$	0	0	2	-2	$2\cos 5\varphi/2$	$-2\cos 5\varphi/2$	0
E'_{3u}	2	-2	$2\cos 5\varphi/2$	$-2\cos 5\varphi/2$	0	0	-2	2	$-2\cos 5\varphi/2$	$2\cos 5\varphi/2$	0
E_{3g}	2	2	$2\cos 3\varphi$	$2\cos 3\varphi$	0	0	2	2	$2\cos 3\varphi$	$2\cos 3\varphi$	0
E_{3u}	2	2	$2\cos 3\varphi$	$2\cos 3\varphi$	0	0	-2	-2	$-2\cos 3\varphi$	$-2\cos 3\varphi$	0

TABLE XV

ASSIGNMENT OF TERMS FOR A MOLECULE OF THE $D_{\infty h}$ DOUBLE GROUP

Rep.	Singlets	Doublets	Triplets			Quartets		
A_{1g}	$^1\Sigma_g^+$		$^3\Pi_{0g}^+$					
A_{1u}	$^1\Sigma_u^-$		$^3\Pi_{0u}^-$					
A_{2g}	$^1\Sigma_g^-$		$^3\Pi_{0g}^-$					
A_{2u}	$^1\Sigma_u^+$		$^3\Pi_{0u}^+$					
E_{1g}'		$^2\Pi_{1/2g}$ $^2\Sigma_{1/2g}$				$^4\Pi_{1/2g}$	$^4\Delta_{1/2g}$	
E_{1u}'		$^2\Pi_{1/2u}$ $^2\Sigma_{1/2u}$				$^4\Pi_{1/2u}$	$^4\Delta_{1/2u}$	
E_{1g}	$^1\Pi_g$		$^3\Pi_{1g}$	$^3\Sigma_{1g}$	$^3\Delta_{1g}$			
E_{1u}	$^1\Pi_u$		$^3\Pi_{1u}$	$^3\Sigma_u$	$^3\Delta_{1u}$			
E_{2g}'		$^2\Pi_{3/2g}$ $^2\Delta_{3/2g}$				$^4\Pi_{3/2g}$	$^4\Delta_{3/2g}$	$^4\Phi_{3/2g}$
E_{2u}'		$^2\Pi_{3/2u}$ $^2\Delta_{3/2u}$				$^4\Pi_{3/2u}$	$^4\Delta_{1/2u}$	$^4\Phi_{1/2u}$
E_{2g}	$^1\Delta_g$		$^3\Pi_{2g}$	$^3\Delta_{2g}$	$^3\Phi_{2g}$			
E_{2u}	$^1\Delta_u$		$^3\Pi_{2u}$	$^3\Delta_{2u}$	$^3\Phi_{2u}$			
E_{3g}'		$^2\Delta_{5/2g}$ $^2\Phi_{5/2g}$				$^4\Pi_{5/2g}$	$^4\Delta_{5/2g}$	$^4\Phi_{5/2}$ $^4\Gamma_{5/2g}$
E_{3u}'		$^2\Delta_{5/2u}$ $^2\Phi_{5/2u}$				$^4\Pi_{1/2u}$	$^4\Delta_{5/2u}$	$^4\Phi_{5/2u}$ $^4\Gamma_{5/2u}$
E_{3g}	$^1\Phi_g$			$^3\Delta_{3g}$	$^3\Phi_{3g}$ $^3\Gamma_{3g}$			
E_{3u}	$^1\Phi_u$			$^3\Delta_{3u}$	$^3\Phi_{3u}$ $^3\Gamma_{3u}$			

APPENDIX II

THE EXPERIMENTAL ARRANGEMENT AND ITS OPERATION

The problem of obtaining the absorption spectrum of a sample while it is exposed to a bright secondary illumination poses a major difficulty which is not encountered in ordinary absorption spectroscopy: that of isolating the signal light from that of the pumping light which excites the absorption. If the sample exhibits absorption in a region far different from that where it is pumped then this isolation is accomplished by the frequency difference between them. However, in the case of the uranyl ion, the pumping band extends from 3700 to 5000 Å and the induced absorption from 4600 to 7000 Å so there is a significant region where the two overlap. Having the pump and signal frequencies different is not sufficient, moreover, because if the sample fluoresces in the same region in which it absorbs, this also causes an error signal to be present. The uranyl ion fluorescence spectrum almost completely covers its induced absorption spectrum. Thus, it is not possible to set up such an experiment in the same manner as the conventional absorption spectrum would be taken: to image the source light on the surface of the sample and then to focus the transmitted light onto the entrance slit of the dispersive device. Since the exciting light is, in general, so much brighter than the source lamp, illuminating a sample set up in the preceeding manner would simply yield a spectrum consisting of the light scattered from the sample and its fluorescence.

The isolation between the signal and pump (or fluorescence) may be obtained in another manner: that of spatial (or optical) separation. This is accomplished in the following manner: (1) the source light is collimated and passed through the sample as a parallel beam; (2) the sample is contained in a flash head arranged so that the sample is illuminated in a direction perpendicular to the direction of the source beam; and (3) the source light is refocused and may be passed through a series of beam stops to eliminate as much scattered flash light as desired. This arrangement then has the following characteristics: (1) the flash light cannot enter directly into the path of the signal light but must be scattered through 90° to even be propagating in the same direction; and (2) as viewed from the lens following the flash head, the two sources of light have an infinite separation: the source is at infinity and the flash lamp scatter and sample fluorescence is at some small finite distance. Figure 36 illustrates the flash lamp and arc lamp setup.

There is still another method of obtaining isolation between the two signals: that of a difference in time. Suppose the exciting light is fired in such a manner that it cuts off very rapidly and that immediately following

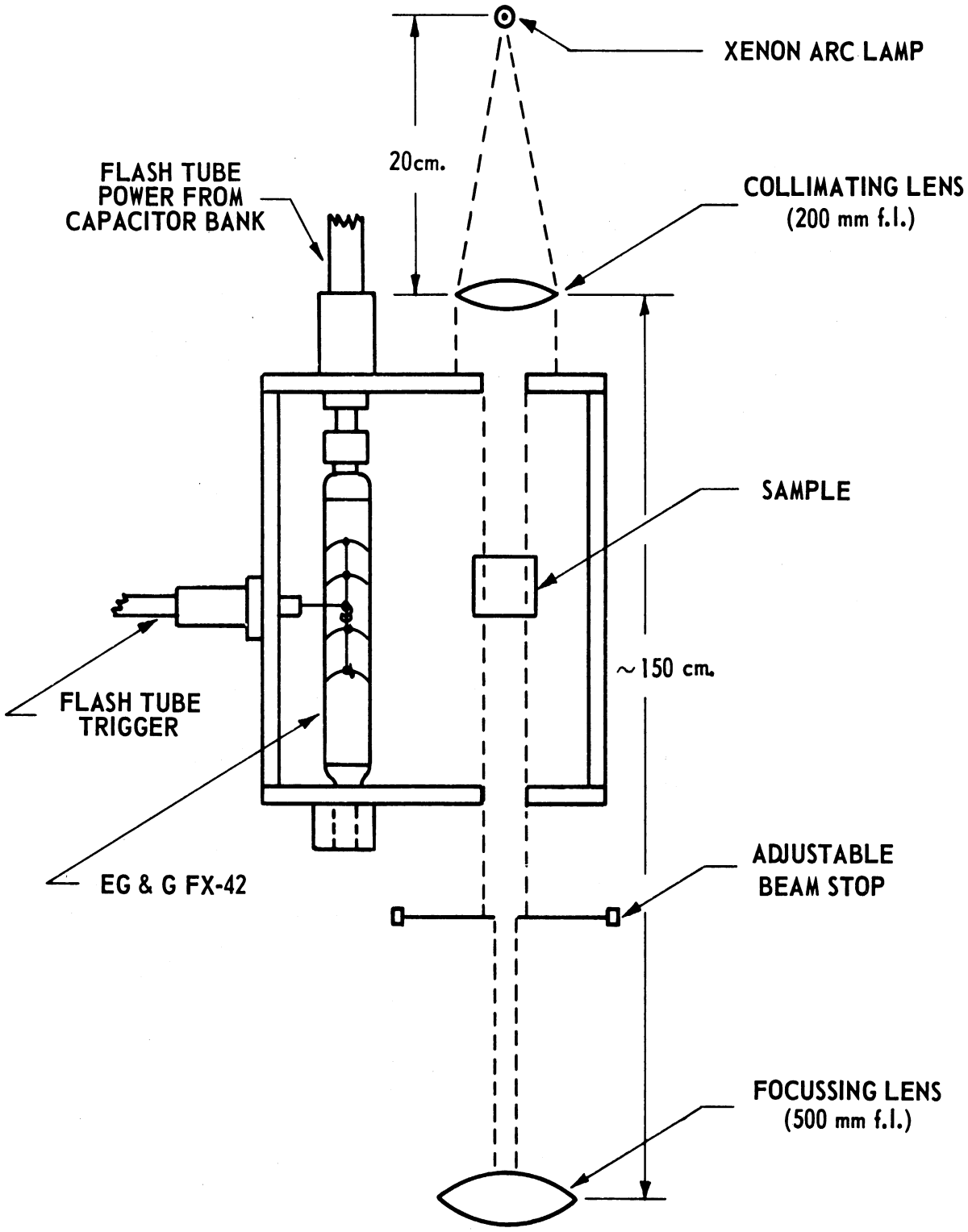

Figure 36. Flash Head and Arc Lamp Arrangement.

this, a signal flash lamp is fired that is of so short a duration that no appreciable decay of the absorption can occur in the time interval. Then the difference in time of these two signals will provide the isolation required. There are, however, disadvantages to this procedure which make it unsuitable under certain circumstances: the signal light must be much more intense than in the previous case since the same amount of light must get through in a much shorter time. Ordinarily this would make no difference but in the case of induced absorption it would at best be questionable to assume that no changes in energy level populations (and hence in absorption spectrum) would occur under the application of a high intensity signal light. If the fluorescence of the sample is located in the same region as the induced absorption, it can still give an error signal under these circumstances.

Figure 37 shows the arrangement of the xenon arc light source, the flash head, and the spectrographs.

The photographically recorded spectra were taken with the 1.5 meter Bausch & Lomb spectrograph in the following manner:

(1) the mirror which reflects the light beam onto the slit of the spectrograph had a thin plane glass (a photographic plate with the emulsion removed) attached to the front of it forming an angle of about 5° with the first surface of the mirror. This glass provided a secondary image of the arc source on the Exakta camera shutter about 1/2 inch to the right of the primary image from the mirror as viewed from the front of the camera. (Many secondary images were thrown to the left as well.) This is illustrated in Figure 38. When the camera shutter is triggered, the shutter sweeps open and permits the secondary image to pass through first, leading the main image by about 10 msec. A small 45° mirror mounted beside the slit reflected the secondary beam onto an RCA 922 photodiode. The purpose of this arrangement was to provide a precise reliable trigger by which the exact time the arc light would pass through the slit of the spectrograph could be established. By mounting an RCA 921 photodiode at the film holder of the spectrograph, measurements were made to check both the reproducibility of this trigger and the shape of the light pulse transmitted through the slit. It was found that the width of the light pulse was a strong function of the distance between the slit and the focal plane shutter, and when the shutter is placed as close to the slit as possible, the transmitted light pulse has the appearance of a Gaussian wave form with a half-width of 1.0 msec. The time variation between the trigger provided by the 922 photodiode and the light transmitted through the shutter was 50 μsec or less, a small fraction of the pulse duration. The camera shutter was wound and triggered by a mechanical timing network which cycled automatically. This process was limited by the time that was required to rewind the shutter and was ordinarily repeated every 15 seconds.

(2) The trigger pulse from the RCA 922 photodiode was fed into the input of a Fairchild Type 76-01A Single Trace amplifier using a Type 74-03A Time

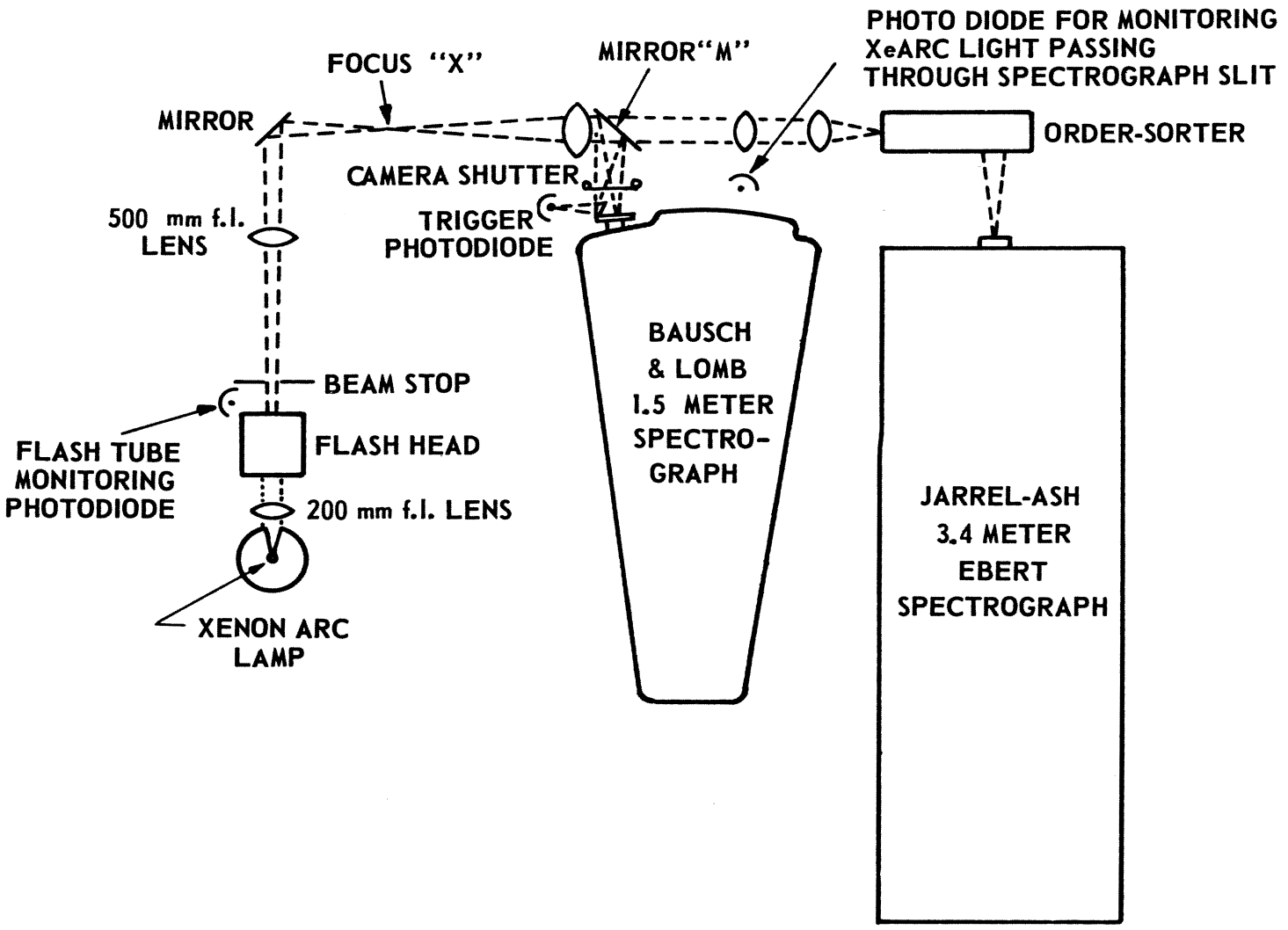

Figure 37. Optical Bench Arrangement for the Recording of Induced Absorption Spectra.

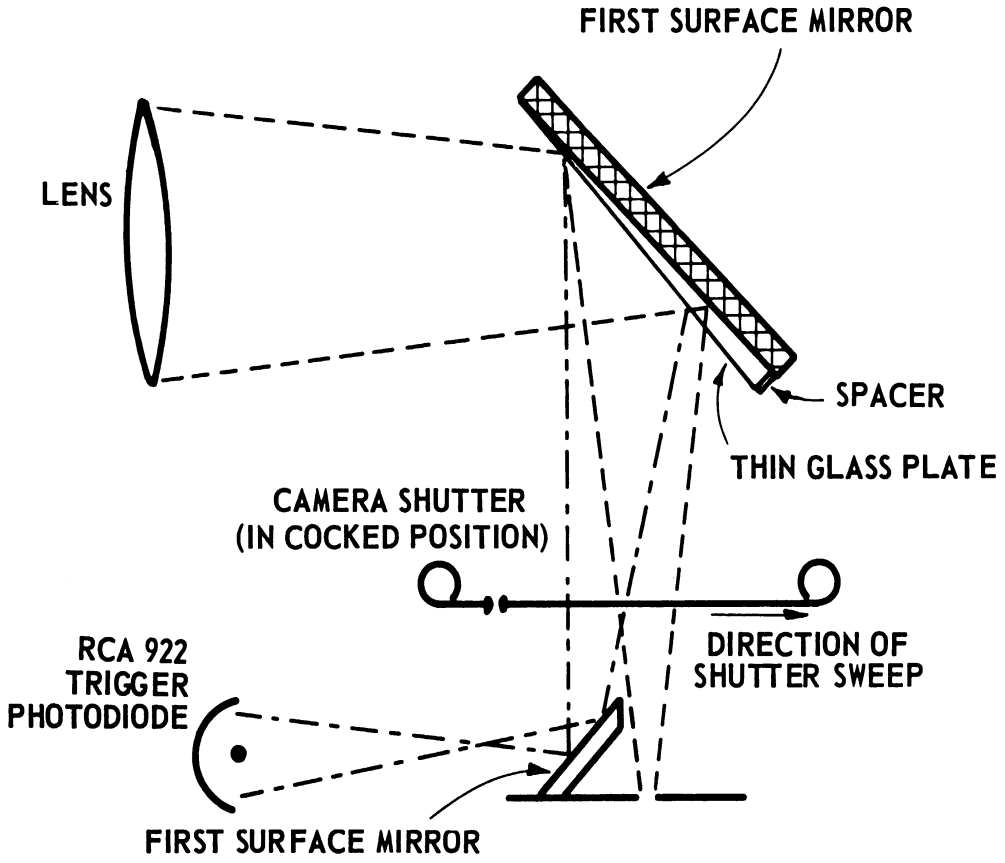

Figure 38. Camera Shutter, Mirror, and Trigger Photodiode Arrangement.

Base on the 777 Main Frame (dual beam). The time base was set to trigger from this input signal.

(3) The + gate from the Type 74-03A Time Base was then used to trigger a Tektronix Type 162 Waveform Generator, i.e., the oscilloscope in this application acts as an amplifier for the trigger pulse, and the correct delay such that the flash tube would trigger when the camera shutter was open was selected from a Tektronix Type 161 Pulse generator fed by the waveform generator. Both of the Tektronix units were powered by the same Type 160A power supply. Figure 39 shows the arrangement of this timing network.

The pulse duration of the flash tube was, unfortunately, only about 0.5 msec so the sample could not be irradiated throughout the time that the shutter was open. In the case of the uranyl sulfate solution, the decay of the induced absorption was known to be rapid so, in order to achieve a maximum absorption signal, the maximum of the flash tube discharge was adjusted to the maximum of the transmission through the spectrograph slit. In uranyl glass, however, the induced absorption decays more slowly and a larger signal on the film could be recorded if the flash tube maximum occurred 50-100 μsec before the transmission maximum. The solution to this problem, which unfortunately was not available at that time, would have been to lengthen the discharge of the flash lamp.

No camera shutter was employed in the recording of the fluorescence spectra on the 1.5 meter Bausch & Lomb spectrograph and the only change in the setup was to move the flash head from its position shown in Figure 37 to the focus point marked "X" in the same figure. This permitted the sample to be imaged on the slit of the spectrograph and the fluorescence spectrum to be taken.

The photoelectrically recorded fluorescence and induced absorption spectra were taken in a manner analogous to that above except, of course, the mirror "M" (Figure 37) was removed and there was no necessity for the use of a camera shutter. The output from the photodiode monitoring the flash tube light output (see Figure 37) and the output from the RCA 1P28 photomultiplier were fed into the inputs of the Fairchild Type 76-02A Dual Trace amplifier. The sweep was provided by a Fairchild Type 74-11A Delaying Sweep whose trigger was obtained by simply wrapping the innter conductor of a RG-58A/U coaxial cable several times around the trigger lead to the flash tube and leading the other end to the external trigger input of the sweep amplifier. The whole system was then activated by firing the flash tube.

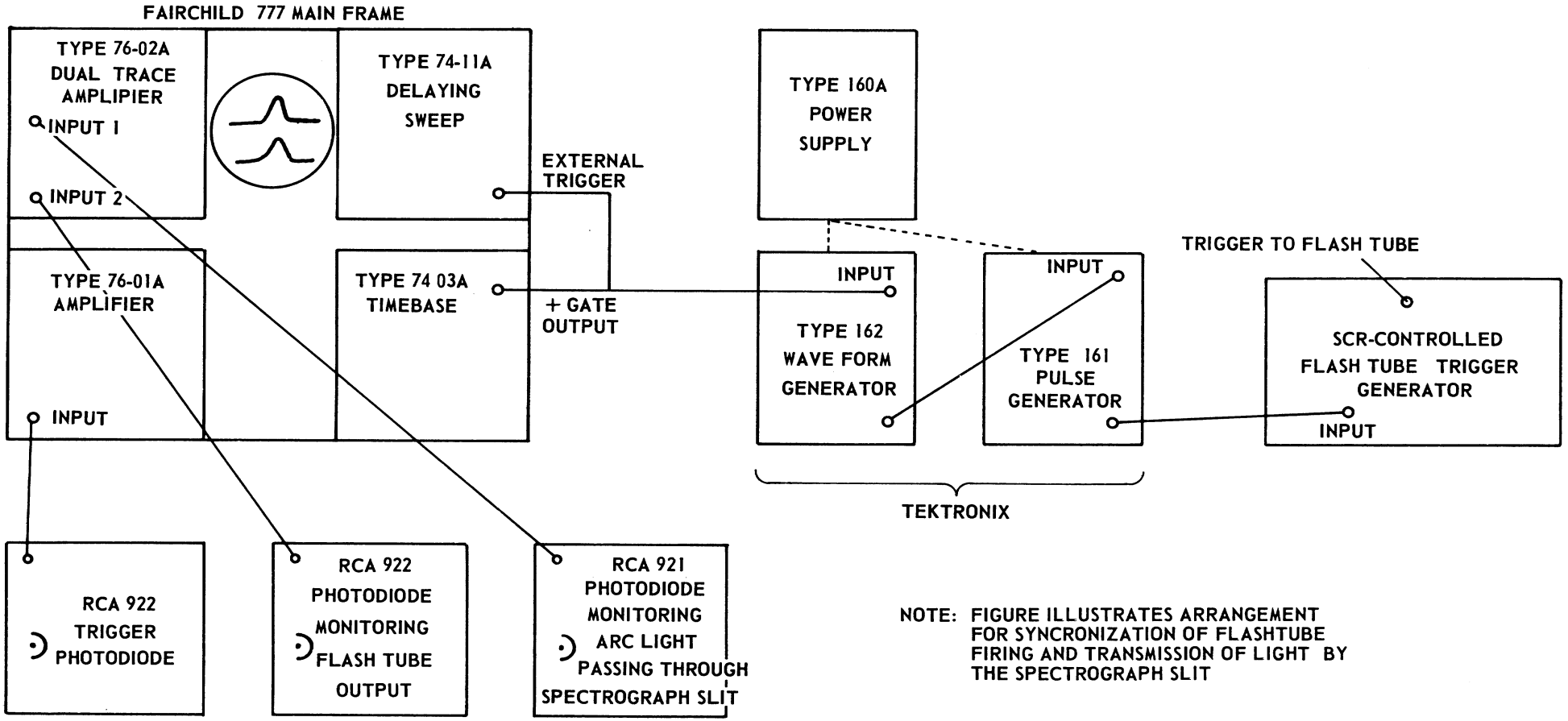

Figure 39. Oscilloscope and Delay Network Arrangement.

APPENDIX III

ATTEMPTS AT CRYSTAL GROWTH AND REMARKS ON SIZE AND CLARITY REQUIREMENTS

Following the procedure given by Dieke and Duncan,[3] many attempts to grow single crystals of cesium uranyl nitrate, $Cs_2UO_2(NO_3)_4$, from a concentrated nitric acid solution were made. This crystal was chosen because it, unlike the majority of uranyl single and double salts, has no water of hydration which must be avoided if the crystal is to withstand the high intensity light flash from the xenon flash lamp and because the spectrum has been analysed in some detail by previous workers (cf. Dieke and Duncan). (To test the stability of a crystal containing water of hydration, a large single crystal of manganous chloride, $MnCl_2 \cdot 2H_2O$, was placed in the flash head and the flash lamp fired. The crystal was very clear (but not without imperfections) and after two firings of the flash lamp had become frosted throughout. It is probably the momentary heating which causes the fracture.) Despite all precautions, which finally included placing the nitric acid solution in a dessicator suspended in a 30-gallon water tank to provide shock and thermal insulation and sweeping the solvent out with dry nitrogen, the crystals failed to grow large and clear enough for use in these experiments. The cesium uranyl nitrate, which is only moderately soluble in concentrated nitric acid, crystallizes in flat square plates having a width (and length) to thickness ratio of about 5:1. Although many seed crystals of about 2 mm cross-section were obtained which were without imperfections, these could not be grown to a larger size without developing a very characteristic pair of flaws: two lines of imperfections which run diagonally across the large square face of the crystal. As it is imperative to have samples which are extremely clear and of at least 5 mm diameter, attempts at the growth of crystals had to be abandoned.

Clarity, more than size, is of extreme importance in these experiments because of the need to isolate the xenon arc lamp signal, which provides the information concerning the induced absorption, from the light signal from the xenon flash lamp which excites the induced absorption. The light intensity from the flash lamp is so much higher than that of the arc lamp that if the sample scatters the flash lamp light, some of it, albeit a very small fraction, can register as the arc signal. Since the arc signal is expected to go down during the time of the flash but the flash signal would increase at the same time, the two effects oppose one another. The glass and solutions employed were without imperfection but even these gave a small scattering of the xenon light. It does not require much degradation of the optical quality from this high standard before the scattered light overwhelms the relatively small arc signal. For example, a crystal of fusion-grown

sodium fluoride containing a small amount of uranium trioxide* which showed no imperfections of any kind other than a slight amount of schlieren was tried but produced a signal-to-noise ratio at least five times worse than the uranyl glass. This is due to two causes: (1) a scattering of the flash lamp light into the optical path of the arc light, and (2) a loss in the arc light signal due to imperfections. It might be possible, by the use of repeated exposures and a subsequent mathematical analysis of the photoelectric signal, to analyse the spectrum of a material which scatters badly but it is unlikely that such a solution is available in the case of the spectrum recorded on photographic film.

There are two areas in which the size of the sample is important: (1) The number of exposures which would be required for the photographic record will increase as the sample is decreased. This is not of too much concern however, because with the existing setup only 50 exposures on Pan-X film are required to give a readable spectrum. This film is quite slow and with the faster films available a considerable reduction in sample size could probably be tolerated. (2) The aperture of the system is limited by the size of the sample since it is in a parallel beam of light and not at a point of focus. It was just possible to fill the aperture of the 3.4 meter Ebert spectrograph with a 5-mm diameter sample with the setup described here so any smaller sample would have vignetted the grating and spoiled its resolution. This problem was not encountered with the 1.5 meter B & L spectrograph which has approximately the same aperture as the Jarrell-Ash. (This was due to the difference in lens arrangement.) However, it would be possible, with a different physical arrangement, to use a smaller aperture.

*Provided by Ojars Risgin, WRRL, University of Michigan.

APPENDIX IV

FILM ERRORS, THEIR EFFECTS ON THE SPECTRA, AND THEIR CORRECTION

Figure 40 shows the tracings obtained when the induced absorption spectrum of uranyl sulfate solution was recorded for the first time. There are two features which are particularly evident and whose cause needed to be investigated: (1) the pumped sample apparently transmitted more light in the region with wavelength longer than 5800 Å; and (2) the strong emission lines of the xenon lamp appear to be preferentially absorbed more than the continuum around them, i.e., the heights of the peaks are greatly reduced.

The first of these anamolies was discovered to have been caused by a malfunction in the camera shutter. Being a focal plane shutter, the two "leaves" of the shutter are drawn back together when the camera is recocked but a failure in the shutter permitted a small gap between the leaves to form during this process so that light could leak through during the recocking process. Thus, there was more light passing through the slit of the spectrograph when the pumped exposure was made and the first of these errors was disposed of. (The pumped exposure was made after the unpumped one and the failure in the shutter must have occurred at the end of one run or the beginning of the other.)

The second one, however, required more analysis of the behavior of the photographic film. Ideally, the optical density of an exposed film is a linear function of the logarithm of the exposure the film has received. In practice, this condition is met for a large number of films over a large range of optical density.

There are three main deviations from this ideal behavior, the first two of which do not appear in the results here. These are: (1) reciprocity failure, (2) the intermittancy effect, and (3) the curvature of the optical density versus log (exposure) curve at low log (exposure) values. The real optical density versus log (exposure) curve has an "S" shape, the slope of the curve being smaller close to the origin than further out. The apparent overabsorption of the xenon lines can then be interpreted according to this curve. In the pumped tracing, the general light level is lower due to absorption by the sample so the portion of the curve whose shape is reflected in the tracing is close to the origin. There, the slope of the optical density versus log (exposure) curve is small so that differences in light level are compacted into small differences in optical density. In the unpumped tracing, however, the small increase in light level has caused a greater amplification of the differences in light intensity. This process is illustrated in Figure 41.

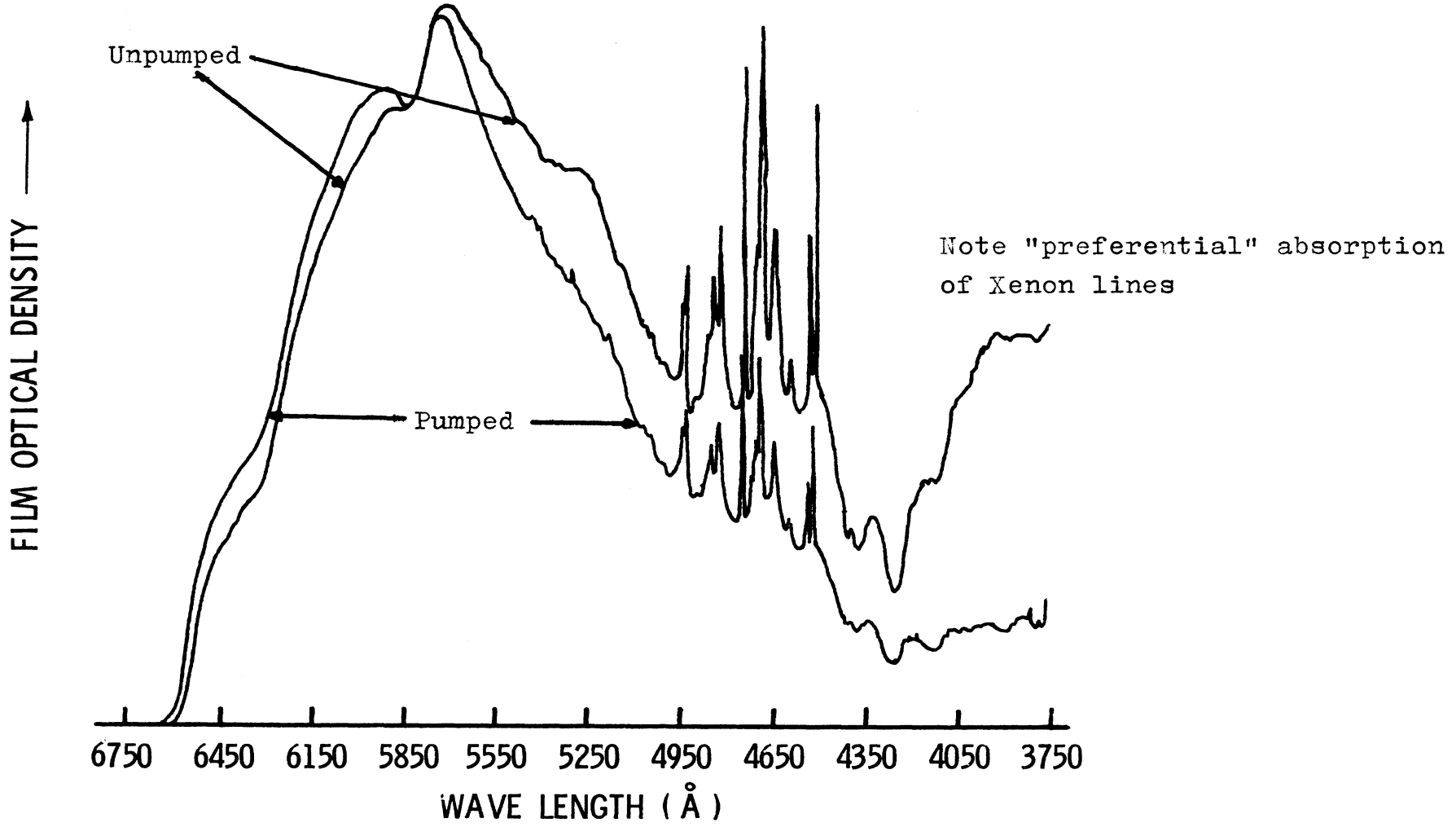

Figure 40. Induced Absorption Tracings for UO_2SO_4 Solution Illustrating Film Error.

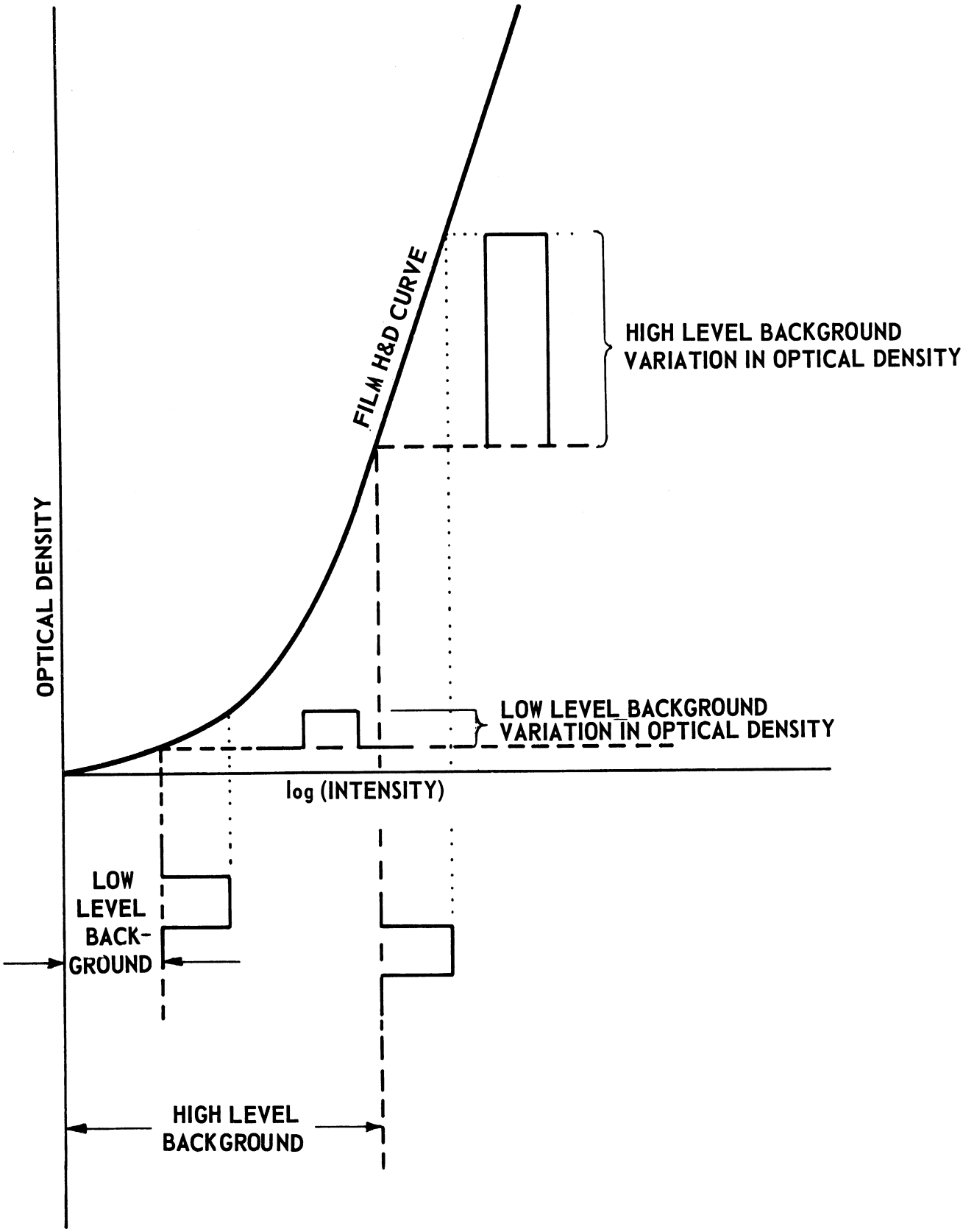

Figure 41. Intensity "Amplification" by Film H & D Curve.

To test the validity of the above conclusion, and optical density versus $\log_{10}$ (exposure) curve was constructed for Kodak Pan-X film, beginning with a background blackening of 0.3 optical density. The background was used to see if this would provide a sufficient pre-exposure to get the film over the "toe" of its response curve. The data points were obtained by the use of a tungsten lamp and five 0.5 optical density neutral filters to provide calibrated changes in exposure with the 1.5 meter B & L spectrograph to provide a wavelength dispersion. All of the data points thus obtained could be fit to a single curve regardless of wavelength indicating that the same background pre-exposure could be used to lift the film over the toe regardless of wavelength. This curve is shown in Figure 42. It will be noted that there is still some of the toe of the curve left even at such a pre-exposure and it is not until a total optical density of 0.6 is reached that the curve becomes linear for about 1.0 optical density. Accordingly, the spectra which were recorded on the 1.5 meter spectrograph were all given a pre-exposure of green light sufficient to blacken them to 0.6 optical density. The spectra thus taken are quite poor for viewing with the eye because of the lack of contrast but quite suitable for obtaining a microdensitometer tracing. Small deviations from linearity probably account for the unreal structure seen in the induced absorption spectrum of the uranyl sulfate solution (Figure 14).

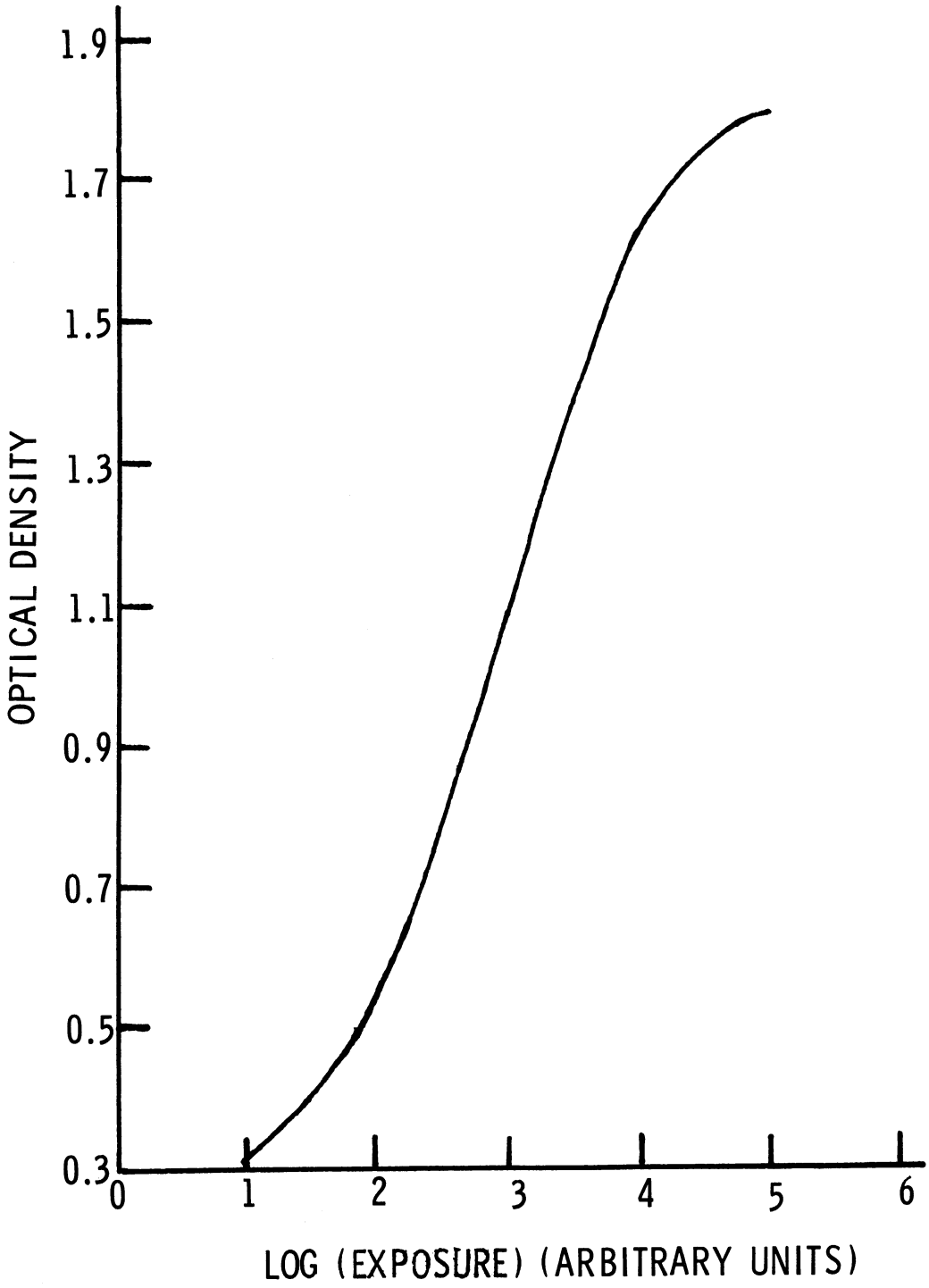

Figure 42. H & D Curve for Kodak Pan-X Film.

APPENDIX V

A DESCRIPTION OF THE SPECTROGRAPHS

The following is a brief description of the spectrographs employed in the recording of the induced absorption photographically and photoelectrically.

BAUSCH & LOMB 1.5 METER SPECTROGRAPH

This instrument, which was used to record the induced absorption spectrum photographically and also to record the fluorescence spectrum of uranyl sulfate trihydrate with DC and flash excitation, has an end-on Eagle mounting using a concave grating of 1.5 meter focal length with 450 lines/mm and a ruled area of 40 by 80 mm. In the first order the wavelength range covered is from 3750 to 7500 Å at a dispersion of 15 Å/mm and a theoretical resolution of 35,000 in the first order. This instrument is equipped with a fixed slit having widths of 10, 30, and 60 microns and was always run with the 10-micron slit. The instrument is rendered stigmatic by a cylindrical lens located between the slit and grating.

JARRELL-ASH 3.4 METER EBERT SPECTROGRAPH

This instrument, which was employed as a monochromator to record the time-resolved induced absorption and fluorescence spectra, is and over-and-under Ebert mount with a 4 inch x 8 inch interferometrically ruled plane grating. The grating has 300 rulings/mm and is blazed on one side at 59,000 Å in the first order and at 31,000 Å in the first order on the reverse side. Since high resolution was not required, the 31,000 Å blaze side was always employed because fewer orders have to be used to cover the visible region on this side. For the 39,000 Å blaze side, the orders for the visible region are fifth to eighth. On the 59,000 Å blaze side the same region is covered by the eighth to seventeenth. Table XVI gives the resolution, approximate dispersion, and wavelength region for each of the orders used to cover the visible region on the 39,000 Å blaze side. Had it been necessary, the 59,000 Å blaze side of the grating would have been employed. Table XVII lists the resolution, approximate dispersion, and wavelength region for this side of the grating. The resolution has been experimentally verified by the observation of the Iodine (I_2) absorption spectrum which showed that at least 90% of theoretical resolving power is being obtained.

Because of the large dispersion of the spectrograph and the large bandwidth of the spectrum being observed, the photomultiplier was operated with

TABLE XVI

RESOLUTION, DISPERSION, AND WAVELENGTH RANGE FOR
THE 31,000 Å BLAZE SIDE OF 3.4 METER EBERT SPECTROGRAPH

Order	Wavelength Range (Å)	Resolution	Approximate Dispersion (Å/mm)
5	5700-7000	305,000	1.68
6	4970-5690	366,000	1.40
7	4140-4960	427,000	1.20
8	3650-4130	488,000	1.05

TABLE XVII

RESOLUTION, DISPERSION, AND WAVELENGTH RANGES FOR
THE 59,000 Å BLAZE SIDE OF THE 3.4 METER EBERT SPECTROGRAPH

Order	Wavelength Range (Å)	Resolution	Approximate Dispersion (Å/mm)
7	6940-7000	427,000	.721
8	6210-6940	488,000	.631
9	5920-6210	549,000	.561
10	5130-5920	610,000	.505
11	4720-5130	671,000	.459
12	4370-4720	732,000	.421
13	4068-4370	793,000	.388
14	3806-4068	854,000	.361
15	3575-3806	915,000	.337
16	3371-3575	976,000	.316
17	-3371	1,037,000	.297

slits from 1 to 5 mm wide giving a bandwith of from 2 to 15 Å which is much below that of the vibrational spacings which were to be observed. The entrance slit of the spectrograph was opened to 400 microns.

Because of the small free spectral range of the spectrograph, a predispersion of the light before it enters the spectrograph is required. This was accomplished by the use of a small prism apparatus having a focal length of 23 cm constructed with a Pellin-Broca constant deviation prism. Figure 43 shows the arrangement for this predisperser (order-sorter).

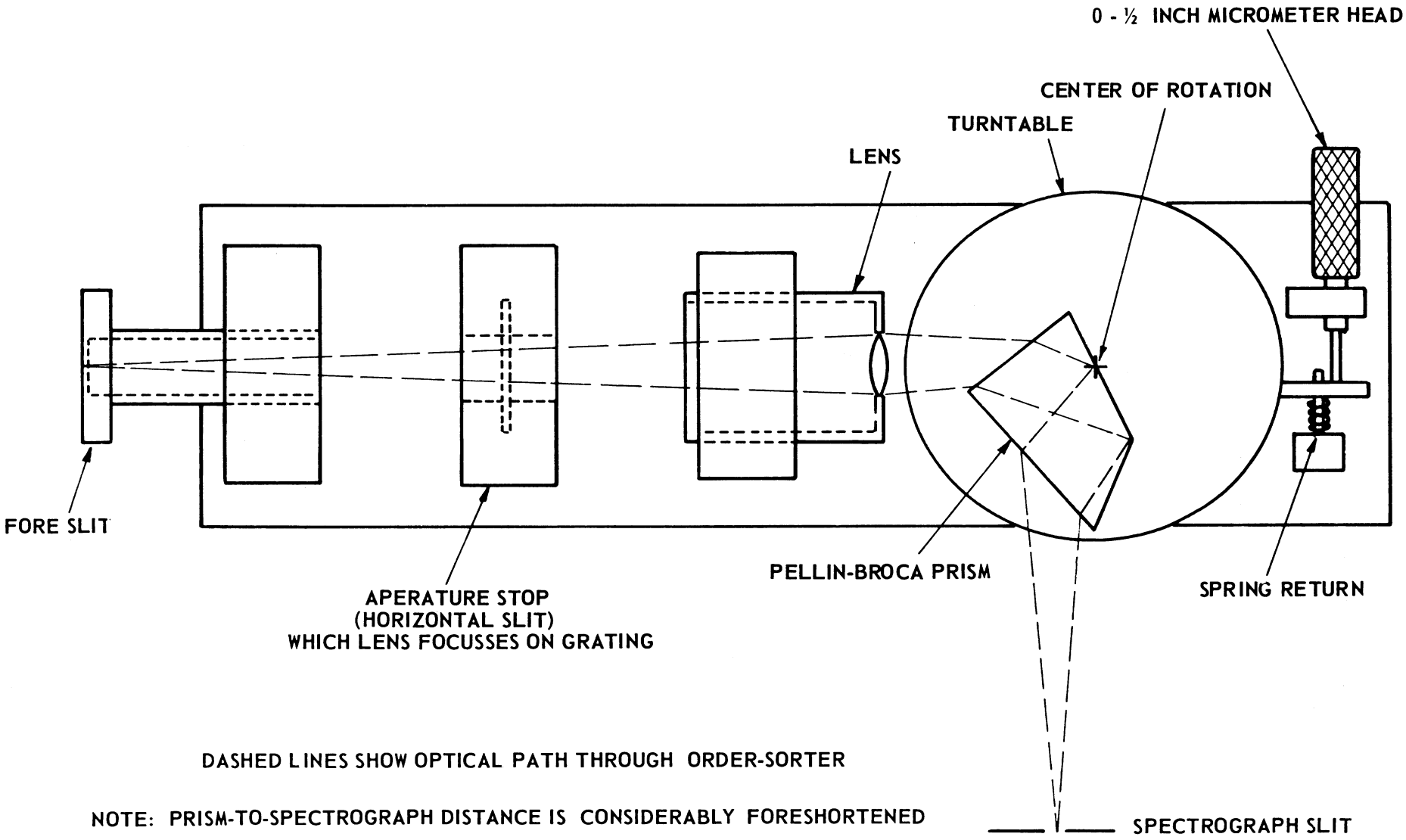

Figure 43. Order Sorter for 3.4 Meter Jarrell-Ash Spectrograph.

APPENDIX VI

AN ATTEMPT TO OBSERVE "BLEACHING" OF THE INDUCED ABSORPTION

As it was known that the light from a ruby Q-switched laser is capable of "bleaching" the uranyl glass induced absorption and to cause it to become transparent again, even though a flash lamp may be exciting the sample, an experiment was tried in which an attempt to observe this bleaching directly was made. To accomplish this end, two sources of pumping light are required, one to induce the absorption and the second to bleach the absorption in the same manner that the laser light does, by pumping the sample with light of a frequency which will not pump the uranyl ions from the ground state but which can be absorbed by the sample once the induced absorption is present. To accomplish this double pumping, the sample of uranyl glass was placed in a flash head so constructed that it would hold two linear flash tubes each at the focus of a different ellipse but whose other foci were coincident at which the sample was placed. The flash tube used to induce the absorption was an FX-100* dissipating only 67.5 joules (1500 VDC at 60 mfd). The other flash tube, an FX-42*, had a 2-mm thick section of Jena OG-2 filter glass located between it and the sample. This glass is a sharp-cut red filter which transmits about 90% of the light of wavelength longer than 5800 Å and whose transmission has dropped to zero before the uranyl glass absorption bands have begun. Although the input energy to this second flash tube was 700 joules (2000 VDC at 350 mfd) it was impossible for it to provide any radiation which would induce the absorption but could only cause transitions between the resonance level and the middle level of the ultraviolet system. The small flash tube was fired by itself and the induced absorption recorded. The large flash tube was then fired by itself and it was verified that no induced absorption was observed. Both the flash tubes were then fired at the same time (the larger one lagging because of the longer time constant of its circuit) with the hope of observing that the induced absorption would diminish due to the depumping provided by the larger flash lamp. The oscilloscope traces for this experiment are shown in Figure 44.

The failure of the secondary pump lamp to produce any change in the absorption induced by the primary one can probably be ascribed to the fact that the relaxation time from the middle level of the ultraviolet system to the resonance level must be considerably shorter than 10^{-7} seconds, a process with which the flash tube illumination cannot compete, only a light source as intense as the laser can show any changes in the population of these levels.

---

*Edgerton, Germeshausen, & Grier, Boston, Mass.

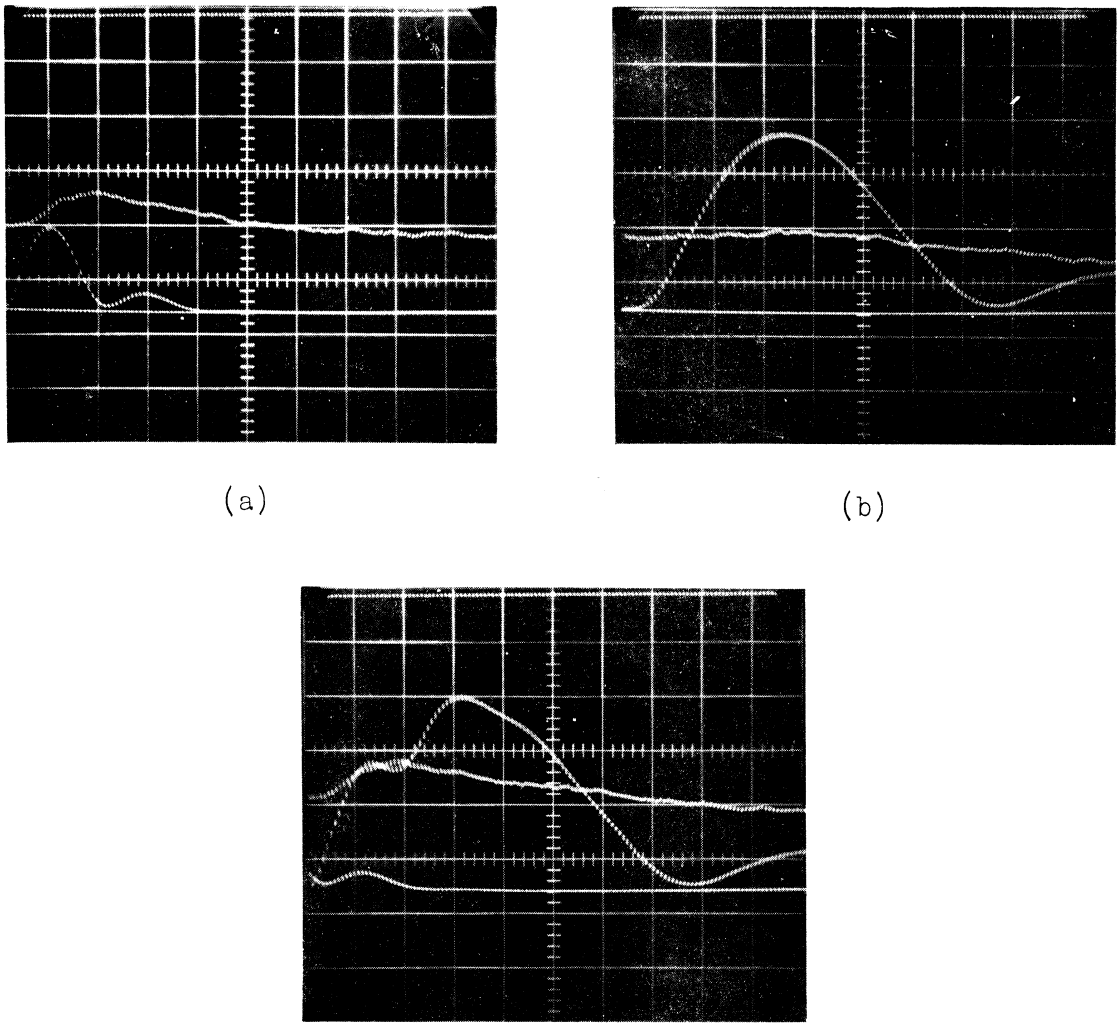

Figure 44. An Attempt to Observe Quenching of the Induced Absorption in Uranyl Sulfate Solution.

(a) Small pumping flash tube only firing.
(b) Large "depumping" flash tube only firing.
(c) Both flash tubes firing.

BIBLIOGRAPHY

1. L. A. Cross, and L. G. Cross, IEEE Conference, Cincinnati, Ohio, April 7, 1964 (1st paper).

2. L. G. Cross, and L. A. Cross, IEEE Conference, Cincinnati, Ohio, April 7, 1964 (2nd paper).

3. G. H. Dieke, and A.B.F. Duncan, "Spectroscopic Properties of Uranium Compounds," National Nuclear Energy Series, Div III, 2, McGraw-Hill, New York, 1949.

4. H. Morton, and H. C. Bolton, Chem. News, 28: 47, 113, 164, 233, 244, 257, 268 (1873).

5. H. Kayser, "Handbuch der Spectroskopie," S. Herzel, Leipzig, 1905.

6. R. S. Mulliken, J. Chem. Phys., 7: 14 (1939).

7. B. E. Gordon, Dokl. Akad. Nauk SSSR, 74: 913 (1950).

8. D. D. Pant, J. Sci. Research Benares Hindu Univ., 3: 27 (1952).

9. V. L. Levshin, and G. D. Sheremetjev, Zhur. Eksptl. Theoret. Fiz., 17: 209 (1947).

10. C. Billington, Phys. Rev., 120: 710 (1960).

11. V. Henri, and M. Landau, Compt. Rend., 158: 1511, 1688 (1914).

12. S. Ahrland, Acta. Chem. Scand., 5: 1151 (1951).

13. S. P. McGlynn, and J. K. Smith, J. Mol. Spec., 6: 164, 188 (1961).

14. E. Rabinowitch, and R. L. Belford, "Spectroscopy and Photochemistry of Uranyl Compounds," MacMillan Co., New York, 1964.

15. L. G. Cross (private communication).

16. W. H. Zachariasen, Acta. Cryst., 1: 288 (1948).

17. W. H. Zachariasen, Acta. Cryst., 7: 783 (1954).

18. V. Heine, "Group Theory in Quantum Mechanics," Pergamon Press, New York, 1960.